CONSENSUS BASED POWER CONTROL ALGORITHMS FOR HETEROGENEOUS NETWORKS

by

Kamil Şenel

B.S., Electrical and Electronics Engineering, Boğaziçi University, 2006

M.S., Electrical and Electronics Engineering, Boğaziçi University, 2010

Submitted to the Institute for Graduate Studies in
Science and Engineering in partial fulfillment of
the requirements for the degree of
Doctor of Philosophy

Graduate Program in Electrical and Electronics Engineering

Boğaziçi University

2016

CONSENSUS BASED POWER CONTROL ALGORITHMS FOR HETEROGENEOUS NETWORKS

APPROVED BY:

Prof. Mehmet Akar (Thesis Supervisor)	.....
Prof. Emin Anarım	.....
Prof. Şirin Tekinay	.....
Assoc. Prof. Mutlu Koca	.....
Assist. Prof. Onur Cihan	.....

DATE OF APPROVAL: 31.10.2016

ACKNOWLEDGEMENTS

Firstly, I would like to express my sincere gratitude to my advisor Prof. Mehmet Akar for his support, patience, motivation and immense knowledge. During the writing of this thesis and in all the time of research, his guidance helped me to grow as a researcher. I could not have imagined having a better advisor for my Ph. D study.

Besides my advisor, I would like to thank my thesis committee: Prof. Şirin Tekinay, Assoc. Prof. Mutlu Koca, for their insightful comments and encouragement, but also for the challenging question which encouraged me to widen my research from various perspectives.

My sincere thanks goes to Prof. Emin Anarım who has always helped me in times of need. I am grateful for his support which goes beyond my Ph. D. studies.

I gratefully acknowledge the funding I have received from TÜBİTAK Project 115E397.

Finally, a special thanks goes to my family and I cannot express how grateful I am to my beloved wife. Without their endless support and love, none of this would be possible.

ABSTRACT

CONSENSUS BASED POWER CONTROL ALGORITHMS FOR HETEROGENEOUS NETWORKS

The resource allocation problem is crucial for unveiling the potential of heterogeneous networks. The demand for higher data rates from an increasing number of devices compels the operators to look for solutions beyond the traditional network architecture. Heterogeneous network architecture is a promising solution to provide data rates required by the emerging applications and high-speed multimedia services. In this dissertation, we focus on the interference management for heterogeneous networks which is a major problem to be resolved and propose solutions based on power control techniques. We utilize the inherent advantages of consensus algorithms such as non-essentially of objective functions and fairness to design power control algorithms suitable for the task of resource allocation in heterogeneous networks.

In this dissertation, several novel, distributed and self optimized power adjustment algorithms are proposed. Contrary to the approaches in the literature, the instantaneous or statistical measurements on channel gains are not required during the power adjustment process. The convergence analyses reveal that the proposed algorithms achieve optimum solution for the power allocation problem with fairness constraints, even under a setup with imperfect communication links. Furthermore, the theoretical analyses show that the convergence properties of the proposed algorithms are preserved under different spectrum allocation schemes. The numerical analyses are in agreement with the theoretical analyses and demonstrate significant improvement in terms of overall network performance.

ÖZET

HETEROJEN AĞLARDA ONAYLAŞIM TABANLI GÜÇ ATAMA ALGORİTMALARI

Kaynak atama problemi, heterojen ağların potansiyelini ortaya çıkarmak için büyük bir öneme sahiptir. Sürekli artan yüksek veri hız taleplerinden dolayı, operatörler geleneksel ağ yapısının ötesinde çözümler aramaya başlamıştır. Heterojen ağlar, multimedya servislerinin ve uygulamalarının gerektirdiği yüksek veri hızlarını sağlama potansiyeline sahiptir. Bu tezde, heterojen ağlar için çok önemli bir problem olan girişim problemi ele alınmaktadır ve güç kontrolü tekniklerine dayalı çözümler önerilmektedir. Onaylaşım algoritmalarının doğal olarak sahip olduğu, amaç işlevinden bağımsız çalışabilme, adillik gibi avantajları kullanarak, heterojen ağlarda kullanılmak üzere güç atama algoritmaları tasarlanmıştır. Bu tez içerisinde, üç tane özgün, dağıtık ve özdüzenleyen güç kontrol algoritması sunulmaktadır. Literatürdeki yaklaşımların aksine, kanal kazançları üzerine anlık veya istatistiksel ölçümler güç ataması sırasında gerekmemektedir. Yakınsama analizleri, önerilen algoritmaların adillik kısıtlamasının göz önünde bulundurulduğu durumlarda, kusurlu kanal yapısı altında bile optimal sonuçlara ulaştığını göstermektedir. Ayrıca, gerçekleştirilen kuramsal analizler, önerilen algoritmaların kararlılık özelliklerinin farklı spektrum atama durumlarında korunduğunu göstermektedir. Kapsamlı benzetim çalışmaları, kuramsal analizleri desteklemektedir ve önerilen algoritmaların genel ağ performansını önemli ölçüde iyileştirdiğini göstermektedir.

TABLE OF CONTENTS

ACKNOWLEDGEMENTS iii
ABSTRACT iv
ÖZET v
LIST OF FIGURES viii
LIST OF TABLES xi
LIST OF SYMBOLS xii
LIST OF ACRONYMS/ABBREVIATIONS xvi
1. INTRODUCTION 1
1.1. Power Control Literature 4
1.2. Motivation of the Thesis 10
1.3. The Contributions of the Thesis 11
1.4. The Organization of the Thesis 11
2. POWER CONTROL IN HETEROGENEOUS NETWORKS 13
2.1. Power Control Problem 13
2.1.1. QoS Based Performance Metric 17
2.2. Consensus Problem 18
2.3. Graph Representation 21
2.4. Mathematical Preliminaries 23
2.5. Chapter Summary 24
3. CONSENSUS BASED POWER CONTROL ALGORITHMS 25
3.1. Power Control Algorithm-I (PCA-I) 25
3.1.1. Connection Weights 27
3.1.2. Creating the Underlying Communication Graph 30
3.2. Power Control Algorithm-II (PCA-II) 31
3.2.1. Discrete Time Form of Power Control Algorithm-II 32
3.3. Power Control Algorithm-III (PCA-III) 33
3.3.1. Discrete Time Form of Power Control Algorithm-III 34
3.4. Convergence Analysis For the Proposed Power Control Algorithms . . . 34

3.4.1. Convergence Analysis of PCA-I 37
3.4.1.1. Convergence Rate Analysis 41
3.4.2. Convergence Analysis of PCA-II 43
3.4.3. Convergence Analysis of PCA-III 46
3.5. Chapter Summary 48
4. IMPERFECT CHANNEL SETUP AND OPTIMALITY ANALYSIS 49
4.1. Imperfect Connection Setup 49
4.2. Convergence Analysis Under Imperfect Connection Setup 51
4.3. Optimality Analysis 58
4.4. Chapter Summary 62
5. RESOURCE ALLOCATION IN HETEROGENEOUS NETWORKS 63
5.1. Joint User Association and Power Allocation 63
5.2. Joint Frequency-Power Allocation Problem 67
5.3. Chapter Summary 69
6. EXPERIMENTS AND RESULTS 70
6.1. Channel Models 71
6.2. Fairness Metrics 75
6.3. Simulation Results 76
6.3.1. Numerical Analysis for PCA-I 76
6.3.2. Numerical Analysis for PCA-II 85
6.3.3. Comparison of PCA-I and PCA-II 92
6.3.4. Numerical Analysis for PCA-III 93
6.3.5. Numerical Analysis on Transmission Powers 97
6.4. Chapter Summary 100
7. CONCLUSION 101
REFERENCES 102

LIST OF FIGURES

Figure 1.1. An example network setup. 2

Figure 1.2. A heterogeneous cellular network example. 6

Figure 2.1. An example consensus algorithm. 20

Figure 2.2. Graph representation examples with different number of nodes. . . 22

Figure 3.1. Two connected underlying communication graph examples. 30

Figure 4.1. Approximation of unit step function with sigmoid function. 55

Figure 6.1. An example simulation setup with grid distribution 70

Figure 6.2. An example simulation setup with random distribution 71

Figure 6.3. Power update algorithm example 72

Figure 6.4. An example of SINR change under split spectrum setup 76

Figure 6.5. Comparison of the PCA-I with the SOCC algorithm 77

Figure 6.6. Self-organization of femtocells under split spectrum setup. 78

Figure 6.7. Simulation results with imperfect connections: Shared spectrum setup. 79

Figure 6.8. Shared spectrum example setup with 3 tiers of BSs. 80

Figure 6.9. Fairness analysis of the PCA-I using Jain's Fairness Index. 81

Figure 6.10. Evaluation of fairness based on Atkinson Index ($\epsilon = 1$). 82

Figure 6.11. Evaluation of fairness based on Atkinson Index ($\epsilon = 0.5$). 83

Figure 6.12. The effect of N_{max}. 84

Figure 6.13. The effect of D_{max}. 85

Figure 6.14. SINR change under new femtocell deployment for the PCA-II. . . 86

Figure 6.15. Comparison of the PCA-II with SOCC. 87

Figure 6.16. Comparison of the PCA-II with the LQP. 88

Figure 6.17. Comparison of the PCA-II with the ASMA and PWFA. 88

Figure 6.18. Evaluation of fairness based on Jain's Index. 90

Figure 6.19. Evaluation of fairness based on Atkinson Index ($\epsilon = 1$). 91

Figure 6.20. Evaluation of fairness based on Atkinson Index ($\epsilon = 0.5$). 91

Figure 6.21. Comparison of PCA-I and PCA-II. 92

Figure 6.22. SINR adjustment example for the PCA-3 under a 2-tier setup. . . 93

Figure 6.23. Error change example for the PCA-3 under a 2-tier setup. 94

Figure 6.24. SINR change example for the PCA-3 under a 2-tier setup with imperfect communication links. 95

Figure 6.25. Optimum solution and error change for an infeasible example. . . 95

Figure 6.26. Optimum solution and error change example with dynamic desired SINR values. 96

Figure 6.27. Fairness analysis based on relative QoS values using Jain's Fairness Index. 97

Figure 6.28. Empirical CDF of the transmission powers for the PCA-I and PCA-II. 98

Figure 6.29. Histogram of the transmission powers for the PCA-I and PCA-II along with the initial power levels. 99

Figure 6.30. Histogram of the resulting Jain's Fairness Index values for the PCA-I and PCA-II. 100

LIST OF TABLES

Table 6.1. System Parameters for Setup-1 73

Table 6.2. System Parameters for Setup-2 74

LIST OF SYMBOLS

$\mathbf{A}^T$	Transpose of matrix $\mathbf{A}$
$\mathbf{A}^{-1}$	Inverse of matrix $\mathbf{A}$
$\mathbf{B}$	Diagonal matrix with algorithm speed parameters
c_{ij}	Entry of the matrix $\mathbf{C}$ at row i, column j
$\mathbf{C}$	Sum of the connection matrix with its transpose
d_i	Base station that user i is associated with
$\mathbf{d}$	Base station-user allocation vector
D_{max}	Maximum distance value for neighborhood
D_{ref}	Reference distance
e^*	Optimal relative error
$e_{i,ref}$	Reference error value for user i
$e_i(\mathbf{p}, t)$	Weighted error for user i at time t for a given $\mathbf{p}$
$\mathbf{e}$	Relative error vector
E	Set of edges for a graph
f_c	Carrier frequency
f_{ij}	Connection weight between base stations i and j
g_{ij}	Channel gain between the ith user and the jth transmitter
$\underline{g}$	Minimum channel gain
$\overline{g}$	Maximum channel gain
$\mathcal{G}$	Interval set for channel gains
G	A graph
$G(\mathbf{A})$	A directed graph of matrix $\mathbf{A}$
h_{ij}	Normalized channel gain between user i and transmitter j
$H_{X,Y}$	Rayleigh fading between locations X and Y
$\mathbf{H}$	Normalized channel gain matrix
$\mathcal{I}$	Set of base stations
I_i	Interference experienced by user i
I_{max}	Maximum interference experienced by a user

$I(T)$	Interval completion of T
$\mathbf{I}$	Identity Matrix
$\mathbf{I}_d$	Diagonal matrix with normalized interference values
K	Number of subchannels
K_c	Fixed cellular transmission loss
K_{f_i}	Fixed indoor transmission loss
K_{f_o}	Fixed indoor to outdoor transmission loss
$\mathcal{K}$	Set of subchannels
l_{ij}	Entry of Laplacian matrix at row i, column j
$L_{X,Y}$	Path loss between locations X and Y
$\mathbf{L}$	Connection matrix
$\mathbb{L}$	Set of connection matrices
N	Number of base stations
N_f	Number of femtocell base stations
N_i	Neighbor set of user i
N_{max}	Maximum number of neighbors
$\mathbb{N}$	Set of natural numbers
o_{ik}	Decision variable for allocation of subchannel k to user i
$\mathbf{O}$	Subchannel allocation matrix
p_i	Transmission power of ith base station
p_{max}	Maximum transmission power
p_{min}	Minimum transmission power
$P_{f,max}$	Maximum transmit power of femtocells
$P_{m,max}$	Maximum transmit power of macrocell
P_X	Transmission power from location X.
$P_{1_{max}}$	Maximum transmit power for tier-1
$P_{2_{max}}$	Maximum transmit power for tier-2
$P_{3_{max}}$	Maximum transmit power for tier-3
$\mathbf{p}(t)$	Transmission power vector at time t
$\mathbf{p}^*$	Optimal power vector
$\mathbf{P}$	Permutation matrix

$q_i(\mathbf{p}, t)$	Relative quality of service for user i at time t for a given $\mathbf{p}$
$q*$	Optimal relative QoS
$\mathbf{q}$	Relative quality vector
$\mathbf{Q}$	Diagonal matrix with relative quality values at diagonals
r_i	Data rate of user i
R_c	Macrocell Radius
R_f	Femtocell Radius
$\mathbf{R}$	Diagonal Matrix with desired SINR values at diagonals
$\mathbb{R}$	Set of real numbers
S	A switching sequence
S_X	Shadowing term at location X
$\mathbb{S}$	Set of switching sequences
t	Time
T	A strictly increasing sequence of time
T_s	Sampling Period
u_i	Input of user i
$U(.)$	Utility function
v_i	Thermal noise experienced by user i
V	Set of nodes for a graph
W_i	Set of BS user i is allowed to associate with
x_i	State of node i
$\mathbf{x}$	State vector
$\mathbf{x}^*$	Optimal state vector
$\mathcal{X}$	Interval set for desired SINR values
Y	Bandwidth constant
z_i	Initial state of user i
z_{ij}	Entry of the matrix $\mathbf{Z}$ at row i, column j
$\mathbf{Z}$	Normalized channel gain matrix with ones at diagonals
α	Path loss exponent
α_c	Path loss exponent for cellular transmission

α_{f_o}	Path loss exponent for outdoor transmission
α_i	Path loss exponent for indoor transmission
β_i	Algorithm speed control parameter for base station i
β_{max}	Maximum algorithm speed control parameter
β_{min}	Minimum algorithm speed control parameter
γ_i	The desired(target) SINR of user i
γ_{max}	Maximum desired SINR value for macrocell user
γ^*	Optimal max-min SINR solution
$\underline{\gamma}$	Minimum desired SINR value
$\overline{\gamma}$	Maximum desired SINR value
$\Gamma_{i,des}$	Desired SINR value for user i
$\Gamma_{i,ref}$	Reference SINR value for user i
$\Gamma_i(\mathbf{p}, t)$	SINR value of user i at time t for a given $\mathbf{p}$
Γ_{th}	Threshold SINR value for the SOCC algorithm
Γ_0	SINR value at the minimum power that provides coverage
Γ_Δ	Additional threshold SINR without leakage
$\mathbf{\Gamma}$	SINR value vector
Δp	Step size for the SOCC algorithm
ϵ	Atkinson Index sensitivity parameter
η	Normalized noise vector
θ	Proportionality constraint
λ_2	Fiedler Value
μ	Average value
$\rho(.)$	Spectral Radius Function
σ	Lognormal standart deviation
$\sigma_2(\mathbf{A})$	Second largest eigenvalue of matrix $\mathbf{A}$
ϕ	Wall penetration loss
$\varphi(\mathbf{x})$	Disagreement function of $\mathbf{x}$
$\nabla f(.)$	Gradient of function f

LIST OF ACRONYMS/ABBREVIATIONS

4G	Fourth Generation
AI	Atkinson's Index
ASMA	Adaptive Spectral Mask Algorithm
AWGN	Additive White Gaussian Noise
BS	Base Station
CDF	Cumulative Distribution Function
CoMP	Cooperative Multi Point
dB	Decibel
D2D	Device to Device
FM	Foschini Miljanic
Gb	Gigabyte
JFI	Jain's Fairness Index
LQP	Link Quality Protection
LTE	Long Term Evolution
MBS	Macrocell Base Station
MHz	Mega Hertz
MIMO	Multiple Input Multiple Output
OFDMA	Orthogonal Frequency Division Multiple Access
PCA-I	Power Control Algorithm one
PCA-II	Power Control Algorithm two
PCA-III	Power Control Algorithm three
PSO	Particle Swarm Optimization
PWFA	Priced Water Filling Algorithm
QoS	Quality of Service
SINR	Signal to Interference plus Noise Ratio
SOCC	Self Organized Coverage Coordination
SoS	Sum of Squares

1. INTRODUCTION

Mobile data traffic, mainly fueled by the high-speed multimedia services, is predicted to grow exponentially in the foreseeable future [1]. Especially emerging new technologies such as augmented reality, mobile-broadband substitution are expected to increase the load on mobile networks. In order to handle this increasing load, current cellular structures require a massive network deployment which is neither economically nor ecologically viable using current cellular architectures [2]. Furthermore, radio link improvement is approaching the theoretical limit and the spectrum available to operators is limited which compels a paradigm shift in wireless communication networks.

The most promising solution is the densification of the existing networks with smaller base stations. These smaller cells range from residential femtocells, which have size of a regular router to microcells which can provide service in hotspots such as airports, shopping malls and train stations. Some types of small cells such as picocells and microcells are small base stations deployed by the operator and they are not quite suitable for small businesses and home users due to their cost and difficult setup process. On the other hand, femtocells are low-powered wireless access points that are designed to operate in the licensed spectrum, and are suitable for small businesses or home users [3].

Next generation wireless networks are predicted to have an increased number of base stations (BS) as a result of the increased viability of small cells both technically and financially [4]. The number of BSs is increasing at such a pace that, some predictions go as far as to suggest that the number of BSs will be higher than the number of cellular users in the near future [5]. The pivotal benefit of such an approach can be briefly summarized as reducing the penetration loss along with the distance between transmitter and receiver. The advantages of smaller cells become more apparent considering 90% of data communications is taking place indoors. Providing indoor coverage with outdoor base stations is not only inefficient but also quite expensive from

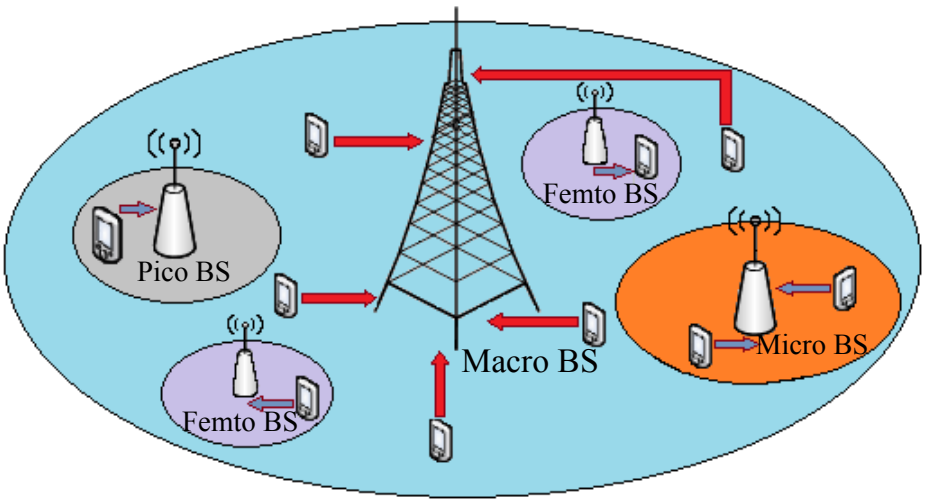

Figure 1.1. An example network setup.

the operators' perspective. Furthermore, future mobile communication standards (e.g., 4G and beyond) have strict regulations on maximum transmission power. There are also other technological advances that have improved the capacity of wireless communication systems such as coding and modulation schemes, however the dominant ingredient is utilizing smaller cells and universal frequency reuse. Hence, in the long-term, data rates such as Gb/s are not possible without integrating smaller cells to the existing networks.

The densification of cellular networks will result in a heterogeneous network configuration consisting of base stations with different power levels and coverage areas. Despite their potential for providing the required capacity leap, heterogeneous cellular networks bring a variety of problems to be considered such as cell association, self-organization, interference management, etc. These problems are more challenging compared to the single-tier networks. To give a clear example, an interference management technique in heterogeneous networks must consider inter-tier interference along with intra-tier interference. Especially, under a closed access scheme where users have restrictions on base station associations, there may be a significant increase in the interference experienced by macrocell users due to small cells [6].

A heterogeneous cellular network example with four tiers is illustrated in Figure 1.1. Each tier of base stations has a different coverage area and maximum transmission power. Unlike traditional single tier networks, a user may choose to connect with any of the base stations based on different metrics such as signal strength, distance, load of the base station, etc. Another important difference from the single tier networks is that there is inter-tier interference between different tiers of base stations during both downlink and uplink transmissions.

The main challenges for the emerging heterogeneous networks can be summarized as follows [7, 8]:

(i) Interference Management: Deployment of smaller cells into the existing networks will introduce interference between different tiers of the network. The problem becomes more complex as the operators have no control on the location of the small cells.

(ii) Distributed Interference Coordination: The small cells with little to no coordination, require an interference technique based on local measurements. Access to the unlicensed spectrum and the amount of overhead required for cooperation intensify the necessity of an effective distributed interference coordination technique.

(iii) Medium Access Control: In dense small cell deployment areas, high throughputs may not be possible. Especially, under a distributed medium access, optimum usage of available channels is a challenging problem.

(iv) Device to Device (D2D) Communication: Coordinating the link setup in a non-network assisted scheme may be difficult, especially when the number of devices is large. Furthermore, maintaining multiple D2D communication links which utilizes the same frequency may not be possible without network assistance.

(v) BackHaul Capacity: The coordination between base stations utilizes the backhaul networks which may not have the capacity to provide delay resiliency for a large number of base stations. The congestion on the backhaul networks may limit the effectiveness of coordinated approaches.

(vi) Handoff/Handover Management: Handoffs require synchronization between base stations which may be a complicated task without centralized coordination.

In this thesis, we focus on the interference management problem and propose distributed interference coordination techniques based on power control for heterogeneous networks. The proposed algorithms are inspired by consensus algorithms which utilize inherent advantages of consensus algorithms such as fairness and ability to operate without objective functions.

1.1. Power Control Literature

In wireless networks resource allocation problem can be summarized as utilizing system resources to provide acceptable signal quality to users. Power control based early approaches to this problem, aim to provide a centralized solution [3, 9]. The drawback of these early approaches is that they assume all of the information on the network can be collected and processed in a centralized unit, which is impossible in practice. Semi-distributed solutions with some modifications on the centralized methods for the interference limited systems are proposed in [10, 11]. Despite being fully distributed is usually a desired property, there are also some approaches which consider the possibility of information exchange between base stations in a traditional network architecture [12, 13].

A fully decentralized power control algorithm which also considers the thermal noise, is proposed by Foshini and Mijanic [14]. A key contribution of [14] is to introduce the conditions on feasibility of the power allocation problem based on the channel gains. Inspired by this work, different decentralized power control algorithms are proposed [15]. A very important drawback of these algorithms is that they did not consider the possibility of handover/handoff or the user association problem. The approaches mentioned so far have only considered a single base station setup. Some of the first approaches which consider the user-base station association problem along with power control problem, are presented in [16,17]. In these works, a decentralized power control

algorithm is utilized to minimize the total transmission power which is employed after user base station association is carried out. The approaches mentioned so far are designed for the traditional network architecture which utilizes only macrocell base stations for providing service to users.

Adjusting transmission powers of base stations is a crucial problem to be resolved before unveiling the potential of heterogeneous network architecture. Heterogeneous networks are designed to give better performance than the traditional wireless networks. However, the limits of this improvement are unknown. For a wireless system, utilizing a heterogeneous network with multiple tiers may improve the spectrum efficiency of the system, but this improvement is shown to be limited in the absence of a power control algorithm [18].

A power control algorithm in heterogeneous networks must overcome a more complex problem compared to single tier networks. For a network consisting of different tiers of base stations, an uncontrolled power transmission may result in inferior link quality for some of the users. Macrocell users are especially vulnerable to the interference caused by small cells as users connected to the small cell base stations are usually in close proximity of their base stations. Furthermore, small cells are usually deployed indoors which gives them an advantage in terms of penetration loss compared to macrocell base stations. The unknown small cell locations, due to deployment by end users which renders centralized planning impossible, add more complication to the already difficult power control problem. Therefore, approaches developed for power adjustment in single-tier networks such as [19], [20] are not suitable for heterogeneous networks.

In Figure 1.2, an example heterogeneous network is illustrated [21]. The multi-tier structure introduces the inter-tier interference along with intra-tier interference and effective interference management is required to enhance the capacity and performance of the cellular system. In this thesis, we focus on interference management techniques based on power control. Apart from power control, there are also different approaches

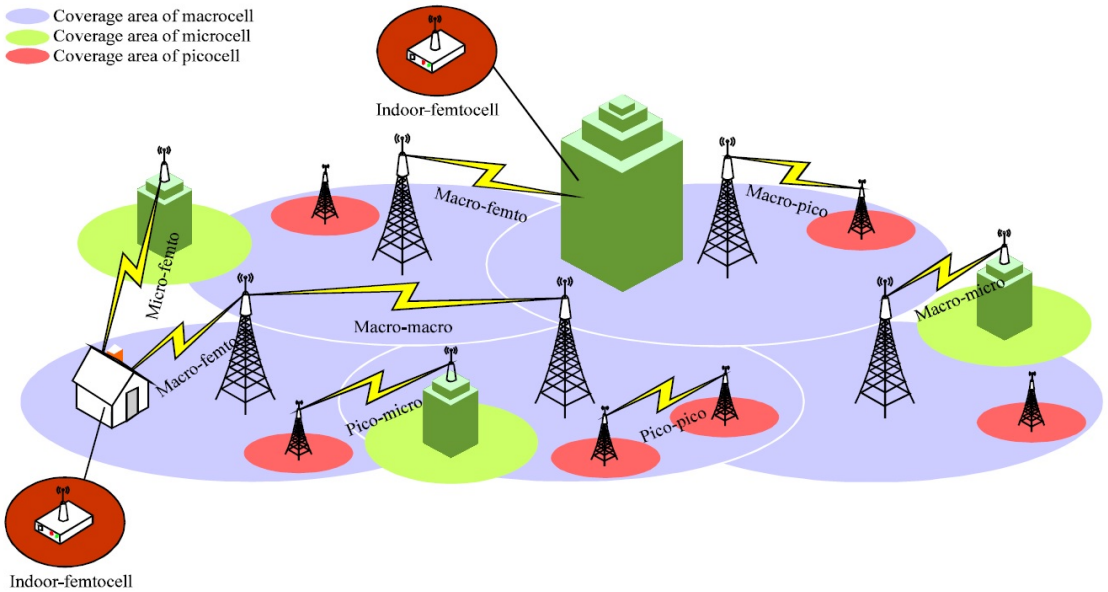

Figure 1.2. A heterogeneous cellular network example.

to the interference management problem based on multiuser detection [22], feedback control [23], game theory and pricing [24], cognitive approaches [25], multiple input multiple output (MIMO) techniques [26, 27], coordinated multipoint (CoMP) [28, 29], successive interference cancellation [30,31] and spectrum allocation [32–35]. An advantage of heterogeneous networks is that during the power adjustment, base stations are able to exchange information with each other. This exchange of information may help in power allocation process, however excessive messaging may lead to a performance decrease in terms of overall system capacity.

The inter-tier interference may be avoided by allocating orthogonal channels to different tiers of BSs by utilizing detection and spectral sensing techniques. However, such an approach comes at the expense of deficient spectral efficiency [36]. Furthermore, due to out-of-band radiation a split spectrum allocation scheme may not completely prevent inter-tier interference for dense deployments of small cells [37]. Along with interference management issues, utilizing a split spectrum setup requires accurate spectrum sensing techniques and makes inter-frequency handover a challenging task. A shared spectrum setup, where the available spectrum can be accessed by every tier

is preferable from an operator's perspective as it leads to a more efficient utilization of spectrum resources [38]. However, this requires careful interference management.

The interference created by femtocells, especially for macrocell users, can be lowered by assigning a lower transmission power. At a first glance, this approach may seem to reduce the number of handover events in an open access setup where users can connect to any BS, whether macro or small cells such as micro, pico, femto. An outdoor user will experience less interference and therefore will less likely change the serving BS. However, from an indoor user's perspective the signal quality may be inferior and an indoor user may switch the serving BS to achieve the required signal quality. Hence, a power control algorithm must account for users in all tiers of network. We consider both shared and split spectrum setups in this thesis. However, power control problem is considered for a given spectrum allocation. In other words, we apply power control after channels are allocated to users by a preceding process.

One of the main concerns of utilizing heterogeneous networks is protecting the signal quality of the macrocell users which may be degraded due to the interference originating from the small cells. There are various interference management approaches which relies on the feedback reports created by macrocell base station (MBS) to manage the inter-tier interference. A non-cooperative game model for femtocell networks where MBS adjusts the price of the interference created by femtocell users is given in [39]. A similar study which proposes two different power adjustment algorithms utilizing the interference reports created by MBS, is presented in [40]; The first algorithm adjusts the transmission power price for femtocell BSs whereas the second one imposes a constraint on the maximum transmission powers of the femtocell BSs based on the reports. Another approach where femtocell users iteratively decrease their target signal to interference plus noise ratio (SINR) values based on the reports created by MBS is presented in [41]. In [42], a modified approach which also allows femtocell BSs to create reports with a low privilege along with MBS is provided. However, these approaches require knowledge of channel gains between a user and its interfering BSs. This information can only be obtained by additional communication between BSs and

it introduces overhead to the system which is not desirable. Furthermore, the impact of delays and time-outs during the transmission of the interference reports is not fully investigated.

Coordination of multi point is another interference management technique which relies on coordination among BSs. Two main CoMP approaches are joint transmission which coordinates BSs in a way to jointly serve users [43] and coordinated beamforming which utilizes the coordination among BSs to control the interference [44]. CoMP techniques are shown to provide spectral efficiency and improve capacity especially for cell edge users [28]. However, the coordination of BSs requires a considerable amount of information exchange between BSs via backhaul. P. Xia *et al.* [45], analyzes the performance of the CoMP approaches with a non-ideal backhaul (a backhaul with limited bandwidth and delays) setup and show that CoMP techniques may result in performance degradation in terms of normalized throughput and coverage.

Interference alignment, first proposed in [46], is another cooperative technique which provides an interference free subspace for the desired signal by aligning the interfering signals to a reduced dimensional subspace [47]. A drawback of interference alignment techniques is that they require strict coordination between BSs along with perfect channel state information. The performance analyses of various interference alignment approaches are presented in [48].

The power control in heterogeneous networks is an optimization problem, in the sense that the goal is to minimize total consumption of the system resources under some constraints such as minimum SINR, data rate, outage probability, etc. Combining constraints with a goal to create fitness functions is an extensively used method in optimization techniques, especially for heuristic methods. Due to the nature of the joint channel allocation and power control problem where individual transmission power levels in channels are to be decided, the problem is inherently suitable for algorithms such as particle swarm optimization (PSO) or genetic algorithms. Note that, in the most general case, one have to consider the channel allocation problem along with

user association and power control problems. The resource allocation problem in its core is a joint optimization problem. However, in power control algorithms joint problem is usually avoided and it is assumed that either channel allocations and/or user base station associations are given. The joint problems, power-channel allocation and user association-power allocation, are known to be NP-hard [49, 50] which along with inherent compatibility of the resource allocation problem, prompted many researches to use heuristic methods. An example PSO algorithm is given in [51] which aims to improve the throughput and outage probability of macrocell users with little impact on femtocell users. A genetic algorithm which uses differential evolution is provided in [52] which aims to maximize the throughput of the macrocell user while employing a fitness function consisting of both a penalty and reward term for femtocells. In a different approach, a genetic algorithm is employed to decide channel allocation for femtocells [53] which allows channel borrowing from neighboring cells.

Game theoretic approaches are also widely utilized for the resource allocation problem in heterogeneous networks. A Stackelberg game is used to formulate the interference management and resource allocation problem in a two tier wireless network in [54], where incomplete channel state information is utilized in an interference limited environment. Another game theoretic approach which uses a three stage Stackelberg game model is given in [55]. The proposed approach in [55] considers electricity price decision along with power allocation and interference management to reduce the operational expenditures. A cooperative bargaining game theoretic approach for uplink subchannel and power allocation problem is proposed in [56], which investigates minimum outage probability, cross-tier interference mitigation and fairness under imperfect channel state information. A non-cooperative Stackelberg game setup where each user aims to maximize its own capacity is introduced in [57]. A self organizing algorithm for small cells in heterogeneous networks based on evolutionary game theory is proposed in [58].

In [59], a joint subchannel and power allocation algorithm which tries to maximize the number of users of small cells while simultaneously minimizing the bandwidth

usage of small cells, is introduced for downlink transmission in a two-tier network. The joint subchannel and power allocation problem is also considered in [60], where protection of macrocell users is prioritized along with fair sharing of resources. Another approach given in [61] aims to maximize the throughput of users via assigning the subchannels to users based on the SINR values and iteratively adjusting the transmission powers. B. Han *et al.* [62] divide the joint optimization problem into three subproblems in order to maximize the sum rate of users. A technique proposed in [63] relies on protecting victims, users with inferior signal quality, from their aggressors, the most dominant interfering source for a particular user, via limiting the aggressors' access to the network resources (subchannels or component carriers). A coverage management and power control approach to maximize the expected throughput of the system is introduced in [64]. Under an open access scheme, a base station association and power control problem is investigated in [65]. A subchannel and power allocation algorithm where users are classified based on the service they receive is introduced in [66]. The cooperative setup introduced in [67] focuses on resource allocation for femtocell base stations in a split-spectrum setup.

1.2. Motivation of the Thesis

The approaches mentioned in Section 1.1, rely on assumptions which may not always be satisfied in real systems. Among these assumptions are: 1) The communication exchange between BS utilizes an ideal communication link; 2) The channel state information is available perfectly or with low uncertainties. An interference management technique which relies on intensive message exchange between BSs, may not always improve the system performance of a multi-tier network architecture [48]. Furthermore, this underlying communication network which allows BSs to communicate with each other, is susceptible to delays and timeouts. In addition, the perfect channel state information may not always be available to a BS due to noisy channel conditions which may lead to channel outage and/or delayed feedback [68]. Even in ideal conditions accurate channel state information may only be acquired with an overwhelming signaling overhead.

1.3. The Contributions of the Thesis

The major contributions of this thesis are summarized as follows:

- Three novel power control algorithms for heterogeneous networks are proposed. The proposed power update algorithms are inspired by consensus algorithms. The proposed algorithms accomplish power allocation without utilizing channel state information.
- An imperfect communication link setup is introduced to model the information exchange between base stations. The model assumes non-ideal links and considers time-outs during communications. The convergence properties of the proposed algorithms are investigated under this non-ideal model.
- The proposed algorithms are shown to achieve the optimum solution for the max-min SINR and Quality of Service (QoS) problems with fairness constraint in a distributed manner.
- The fairness performances of the power control algorithms are investigated using two different metrics, namely Jain's and Atkinson's fairness indices. The algorithms are shown to achieve perfect fairness independent of the number of users or spectrum allocation setups.
- The self-organization properties of the power control algorithms are analyzed theoretically by using time varying connection matrices. The results are further verified by numerical simulations which illustrate the performance of the power control algorithms under dynamic system conditions.
- The results provided by the theoretical analysis are verified by extensive numerical analysis.

1.4. The Organization of the Thesis

The rest of this thesis is organized as follows: In Chapter 2, the power control problem in heterogeneous networks is defined along with example power control algorithms. The consensus problem and graph representation is briefly introduced. Then,

the mathematical preliminaries utilized throughout the thesis are presented.

In Chapter 3, the proposed power algorithms are introduced and their theoretical analyses are presented. The modified versions of the proposed algorithms and their stability properties are also investigated.

An imperfect connection setup which uses a non-ideal model for communication links is given and the theoretical analysis on the performance of the proposed algorithms under imperfect connection setup are provided in Chapter 4. Additionally, the optimality analysis for the solutions provided by the proposed power control algorithms are carried out.

In Chapter 5, the joint user association, frequency allocation and power control problem is introduced. Some of the approaches in the literature are presented along with some preliminary results. The joint problems will be considered as future research areas.

Chapter 6 contains the numerical analyses for the proposed algorithms. First, the channel models and system setup used for simulations are introduced. Next, performance metrics which are utilized to assess the fairness performance of the proposed algorithms, are presented. Then, the simulation results for the proposed algorithms are provided.

In Chapter 7, concluding remarks and outcomes of this thesis are given.

2. POWER CONTROL IN HETEROGENEOUS NETWORKS

In this chapter, we present the power control problem along with different power allocation approaches. Furthermore, consensus problem is briefly introduced, followed by the graph representation model for the information exchange between base stations. Finally, necessary mathematical preliminaries which are utilized throughout the thesis, are given.

2.1. Power Control Problem

The transmission power for the ith BS is denoted by p_i and $\mathcal{I} = \{1, \ldots, N\}$ represents the set of BSs. Given a power vector $\mathbf{p}(t) = [p_1(t), \ldots, p_N(t)]^T$, the Signal to Interference-Noise ratio of user i given $\mathbf{p}(t)$, $\Gamma_i(\mathbf{p}, t)$, can be computed as

$$\Gamma_i(\mathbf{p}, t) = \frac{g_{ii}(t)p_i(t)}{\sum\limits_{j \in \mathcal{I}, j \neq i} g_{ij}(t)p_j(t) + v_i(t)} \tag{2.1}$$

where g_{ij} represents the channel gain between the ith user and the jth transmitter; and v_i denotes the thermal noise experienced for user i. The term g_{ii} is assumed to contain post processing SINR gains (e.g. diversity reception, interference suppression, etc.). Note that, we assume the frequency allocation and user-base station association have been carried out by a preceding process. The power control problem is considered as a standalone problem in this chapter.

In traditional single-tier networks, power control algorithms aim to provide every user with minimum SINR requirement

$$\Gamma_i(\mathbf{p}, t) \geq \gamma_i, \quad \forall i \in \mathcal{I} \tag{2.2}$$

where γ_i is the minimum acceptable SINR for the ith user. The desired SINR values are assumed to be chosen from an interval set $\mathcal{X} = [\underline{\gamma}, \overline{\gamma}]$ based on the service or the application of the user. Combining (2.1) and (2.2) in vector notation we obtain

$$\mathbf{p} \geq \mathbf{RHp} + \eta, \tag{2.3}$$

where $\mathbf{R} = \text{diag}(\gamma_1, \ldots, \gamma_N)$, $\mathbf{H} = [h_{ij}]$ is the normalized channel gain matrix defined as

$$h_{ij} = \begin{cases} \frac{g_{ij}}{g_{ii}}, & j \neq i, \\ 0, & j = i, \end{cases} \tag{2.4}$$

and η is the normalized noise vector

$$\eta = \left[\gamma_1 \frac{v_1}{g_{11}}, \ldots, \gamma_N \frac{v_N}{g_{NN}} \right]^T. \tag{2.5}$$

The target SINR γ_i values are achievable with a non-negative power vector if the spectral radius of the matrix $\mathbf{RH}$ (denoted as $\rho(\mathbf{RH})$) is less than or equal to 1. When $\rho(\mathbf{RH}) = 1$, γ_i's are achievable only if there is no noise in the system ($\eta = 0$) [69].

For the case where the given SINR targets are achievable, the non-negative power vector that satisfies (2.2) with equality is given by

$$\mathbf{p}^* = (\mathbf{I} - \mathbf{RH})^{-1}\eta. \tag{2.6}$$

where $\mathbf{I}$ is the identity matrix with appropriate dimensions.

To achieve the optimal power vector given in (2.6), a well known algorithm is proposed by Foschini and Miljanic in [14]. The algorithm is

$$\dot{p}_i(t) = -\theta \left[1 - \frac{\gamma_i}{\Gamma_i(\mathbf{p}, t)} \right] p_i(t), \quad i \in \mathcal{I} \tag{2.7}$$

where θ is the proportionality constraint. The algorithm works as follows, every user compares its actual SINR value with its desired SINR value and adjusts its transmission power based on this comparison. The algorithm is shown to converge to the $\mathbf{p}^*$ value given in (2.6) if $\rho(\mathbf{RH}) < 1$. An important drawback of this algorithm is that the achievable target SINR values are not known beforehand, i.e., the users do not have the knowledge of feasible target SINR values. For the cases where the target values are not feasible, this algorithm is known to diverge.

A modified version of Foschini-Miljanic (FM) algorithm is introduced in [41] which utilizes feedbacks from macrocell to protect the macrocell user. These feedbacks reduce the desired SINR value of the femtocell users based on the interference they create on the macrocell users. This approach achieves two things simultaneously: Macrocell user's signal quality is protected and the feasibility problem is avoided by iteratively reducing the desired SINR value for femtocell users.

Two power control algorithms called priced water filling algorithm (PWFA) and adaptive spectral mask algorithm (ASMA) are proposed in [40]. PWFA utilizes a power update rule which penalizes femtocell BS based on the interference they create on macrocell user. On the other hand ASMA adjusts the maximum power transmission level for femtocell BSs based on feedback.

The algorithms proposed in [40, 41] assume the knowledge on channel gains for macrocell user, i.e., g_{ij} values between macrocell user and femtocell BSs, are available. Furthermore, there are predefined target values to attain (maximum interference tolerable for ASMA and PWFA, target SINR value in [41]).

The self-optimized coverage coordination algorithm (SOCC) given in [70], adjusts the power levels according to

$$p_i[k+1] = \begin{cases} \min\left(p_i[k] + \Delta p, p_{max}\right), & \text{for } \ \Gamma_i \leq \Gamma_{th}, \\ \max\left(p_i[k] - \Delta p, p_{min}\right), & \text{otherwise,} \end{cases}$$

where $\Gamma_{th} = \Gamma_0 + \Gamma_\Delta$; the statistical threshold Γ_0 is the SINR value corresponding to the minimum power at which the femtocell covers the building area; and Γ_Δ is an additional threshold that can be utilized without creating leakage. The SOCC algorithm does not rely on channel gains for power adjustment. The downside of the SOCC algorithm is that it utilizes a fixed target SINR value, similar to the Foschini-Miljanic algorithm (FM algorithm) given in (2.7). For the cases in which the target value is achievable, the algorithm converges to the optimal power vector. However, similar to the FM algorithm, for an infeasible case the algorithm diverges. The power adjustment algorithms introduced in [40, 41, 70] are utilized for comparison with the proposed power control algorithms.

An interesting problem arises when fairness constraint is imposed along with the max-min SINR objective. The problem can be expressed as adjusting the transmission powers such that the minimum SINR value in the system is maximized under the fairness constraint, i.e., determine $\mathbf{p}^*(t)$ where

$$\Gamma(\mathbf{p}^*, t) = \max_{i \in \mathcal{I}} \min \ \Gamma_i(\mathbf{p}, t) \tag{2.8}$$

such that

$$\max_{i \in \mathcal{I}} \ \Gamma_i(\mathbf{p}^*, t) = \min_{i \in \mathcal{I}} \ \Gamma_i(\mathbf{p}^*, t). \tag{2.9}$$

Therefore, the objective of this power allocation problem is to provide users with equal signal quality while maximizing the minimum SINR value among the users (max-min fairness [60]). Note that a constant on maximum power can be incorporated to the problem in (2.8)-(2.9) as follows:

$$p_i \leq p_{max}, \quad \forall i \in \mathcal{I}. \tag{2.10}$$

There exists a positive power vector which is the solution of the problem presented by the equations (2.8)-(2.9) and it is given by

$$\mathbf{p}^* = (\mathbf{I} - \gamma^* \mathbf{H})^{-1} \eta \tag{2.11}$$

where γ^* is the max-min SINR value solution [41]. The max-min SINR value can be computed using

$$\gamma^* = \frac{1}{\rho(\mathbf{H})} \tag{2.12}$$

where $\rho(\mathbf{H})$ is the spectral radius of $\mathbf{H}$. To compute the $\mathbf{p}^*$ by utilizing equation (2.11), a centralized algorithm along with knowledge on channel gain matrix $\mathbf{H}$ is required. Such an approach is impossible in a practical system, as the amount of overhead required to compute the channel gains is insurmountable.

2.1.1. QoS Based Performance Metric

Another approach is to use quality of service (QoS) as a performance metric and maximize the minimum QoS of the users. Let the relative QoS for user i defined by

$$q_i(\mathbf{p}, t) = \frac{\Gamma_i(\mathbf{p}, t)}{\gamma_i}. \tag{2.13}$$

Then, the weighted error for user i, $e_i(\mathbf{p}, t)$, given a power vector $\mathbf{p}$ can be defined as

$$e_i(\mathbf{p}, t) = \frac{\gamma_i - \Gamma_i(\mathbf{p}, t)}{\gamma_i} \tag{2.14}$$

$$= 1 - q_i(\mathbf{p}, t) \tag{2.15}$$

The emerging applications and services have heterogeneous QoS requirements. Furthermore, applications such as video streaming, file transfer, etc., have the ability to operate at various bit rates which makes the traditional approach of satisfying the minimum QoS requirement obsolete. With that motivation in mind, we use the rela-

tive error and the relative QoS as performance measures. Our goal is to minimize the maximum weighted error of the users, while providing fairness among users. Thus, the problem considered can be expressed mathematically as determining $\mathbf{p}^*$ from

$$e(\mathbf{p}^*, t) = \min_{i \in \mathcal{I},\ \mathbf{p} \geq 0} \max\ e_i(\mathbf{p}, t) \tag{2.16}$$

with the fairness constraint

$$\max_{i \in \mathcal{I}}\ e_i(\mathbf{p}^*, t) = \min_{i \in \mathcal{I}}\ e_i(\mathbf{p}^*, t). \tag{2.17}$$

To find $\mathbf{p}^*$, we propose a distributed power adjustment algorithm that can be employed in heterogeneous networks. Note that, this problem is different from the one introduced by (2.8)-(2.9) as the performance metric is not based on the SINR value of the users, but the weighted errors.

2.2. Consensus Problem

Consensus problem dates back to 1960s when it was introduced as a management science and statistics problem [71]. In a multi-agent dynamic system, consensus is the state of having an identical value for a certain feature which depends on the state of all agents. The interaction between the agents in the system is described by a consensus algorithm which depends on the information exchange between agents.

A framework for identifying and solving consensus problems is presented in [72], which is later expanded by [73, 74]. An important feature of consensus problems is that without utilizing a fitness function, the agents are capable of reaching an agreement. In other words, even though the agents have no notion of how well they are doing during the process, they can still achieve consensus.

Let $G = (V, E)$ denote a graph which represents a communication network of agents. Here, $V = \{1, 2, \ldots, n\}$ and $E \subseteq V \times V$ denotes the set of nodes and edges of

the graph respectively. The neighbors of a node i is usually defined as the set of nodes that shares information with node i, and is denoted by $N_i = \{j \in V : (i,j) \in E\}$. A simple consensus algorithm for a system with node dynamics $\dot{x}_i = u_i$ is given in [73] as follows:

$$\begin{aligned} \dot{x}_i &= \sum_{j \in N_i} (x_j(t) - x_i(t)), \\ x_i(0) &= z_i \in \mathbb{R}, \quad \forall i \in V, \end{aligned} \tag{2.18}$$

which can be represented in matrix form as

$$\dot{\mathbf{x}} = -\mathbf{L}\mathbf{x} \tag{2.19}$$

where $\mathbf{L} = [l_{ij}]$ denotes the graph Laplacian of the networks and its elements are defined as follows:

$$l_{ij} = \begin{cases} -1, & j \in N_i, \\ |N_i|, & j = i. \end{cases}$$

where $|N_i|$ denotes the cardinality of set N_i. The Laplacian matrix is a singular M-matrix with important properties that are useful for analytical analysis of a consensus algorithm [74]. All of the row sums of $\mathbf{L}$ are zero, therefore $\mathbf{L}$ matrix always has a zero eigenvalue with a corresponding eigenvector $\mathbf{1} = (1, \ldots, 1)^T$. An equilibrium of the system 2.19 is given as $\mathbf{x}^* = (\alpha, \ldots, \alpha)^T = \alpha\mathbf{1}$. This equilibrium point can be shown to be the unique equilibrium point where all nodes agree [75].

For undirected graphs the Laplacian satisfies the sum-of-squares(SoS) property,

$$\mathbf{x}^T\mathbf{L}\mathbf{x} = \frac{1}{2} \sum_{(i,j) \in E} (x_j - x_i)^2. \tag{2.20}$$

If we define a quadratic *disagreement function* as

$$\varphi(\mathbf{x}) = \frac{1}{2}\mathbf{x}^T\mathbf{L}\mathbf{x} \tag{2.21}$$

then, algorithm given in (2.19) can be defined as

$$\dot{\mathbf{x}} = -\nabla\varphi(\mathbf{x}) \tag{2.22}$$

which is the gradient descent algorithm for (2.21).

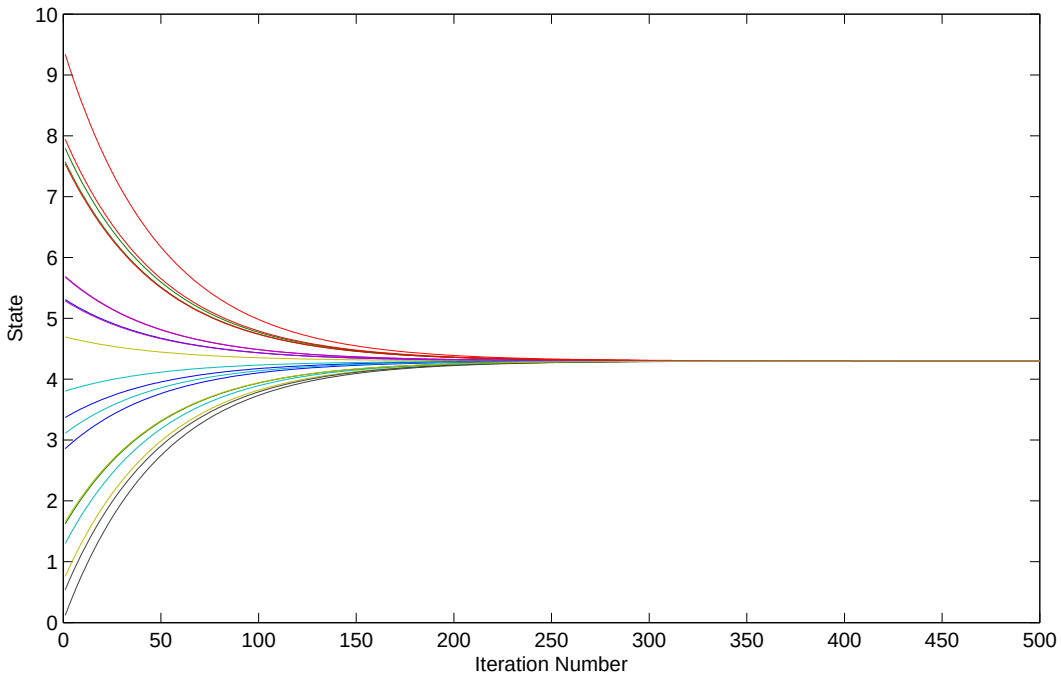

Figure 2.1. An example consensus algorithm.

Figure 2.1 depicts the state changes for 20 agents utilizing the consensus algorithm defined in 2.19. The agents start from a random initial state and adjust their state values based on the information received from other agents to achieve consensus.

2.3. Graph Representation

A communication network, where BSs communicate with each other can be modeled using a graph representation as follows; BSs are the nodes and the communication links are the edges of the graph. Recall that an advantage of heterogeneous networks which should be utilized in resource allocation process is that base stations are capable of exchanging information with each other. The information exchange allows semi-distributed algorithms to be employed. This exchange of information is assumed to be carried out via using Internet and/or a backhaul. The content of the information relayed is specific to the algorithm employed and is irrelevant for the graph representation introduced in this section.

Let $G = (V, E)$ denote a graph, with set of edges and nodes given by E and V. There exists a communication link between BSs i and j if information is exchanged between them, which corresponds to existence of an edge between node i and j in the graph. We will refer to this graph as the underlying information exchange graph.

The underlying graph is modeled as a time varying graph due to the dynamic nature of cellular systems. There are many reasons for this erratic behavior such as user mobility, fading, users connecting/disconnecting to system and even change on weather conditions. Under such a hectic system, assuming static communication links between users is unrealistic. Furthermore, in a practical system the communication links are susceptible to delays and time-outs. Most of the approaches in the literature considers a setup with ideal communication links. However, the performance of the aforementioned approaches under a non-ideal communication link setup, which considers delays and timeouts, is usually not analyzed. Under such a setup with imperfect connections, some power control techniques are known to exhibit poor performances [45]. For the algorithms proposed, both theoretical and numerical analysis are carried out under the imperfect connection setup, where the connections are susceptible to time-outs at all times during adjustment.

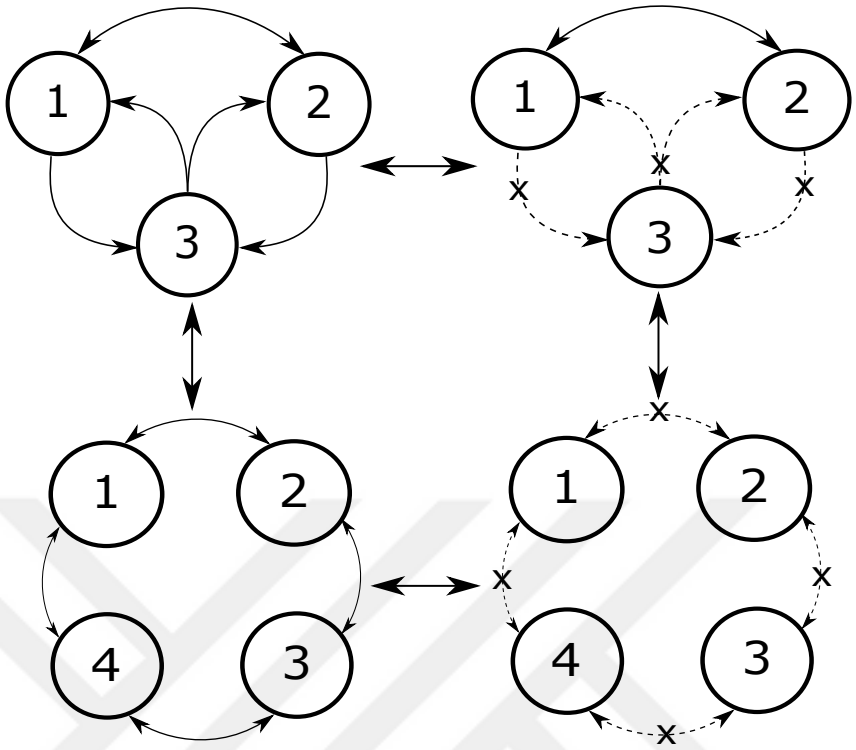

Figure 2.2. Graph representation examples with different number of nodes.

For illustrative purposes, an example graph representation is given in Figure 2.2, which shows communication links for different number of users. In the example shown on top left subfigure, three nodes can receive and send information to every other node corresponding to a complete graph, which is equivalent to each BS being able to communicate with every other BS in a cellular network. On the top right-side of Figure 2.2, another graph representation is shown in which node 3 is isolated and is not able to send or receive information from nodes 1 and 2. Another dynamic of the communication systems is the number of users in the system. In the bottom left sub figure, the communication graph contains four nodes with different connections and finally, the sub figure on the bottom right shows an isolated graph where each of the four nodes are unable to send or receive information. A successful resource allocation algorithm should not only consider the ideal communication links in which information is perfectly shared between every node in the system. We consider a setup in which the cases shown in the Figure 2.2 are possible and may change from one to another.

2.4. Mathematical Preliminaries

A matrix with non-positive off-diagonals is called Z-matrix. A Z-matrix with positive principal minors is called M-matrix. M-matrices, first introduced by Ostrowski in 1937 [76], occur in different areas such as power control, growth models in economics and Markov processes [77].

Definition 1. *An $N \times N$ matrix $\mathbf{A} = [a_{ij}]$ is called a non-singular M-matrix if $a_{ij} \leq 0,\ \forall i \neq j$ and all principal minors of $\mathbf{A}$ are positive [78].*

More details on non-singular M-matrices can be found in [77], [78], [79], [80]. The following theorems on singular M-matrices are required for stability analysis.

Lemma 2.1 (Theorem 3.1 in [78])**.** *Let $\mathbf{A} = [a_{ij}]$ be an $N \times N$ matrix with non-negative diagonals and non-positive off-diagonals, i.e. $a_{ii} \geq 0,\ \forall i$ and $a_{ij} \leq 0$ whenever $i \neq j$. Then the following statements are equivalent:*

(a) $\mathbf{A} = s\mathbf{I} - \mathbf{B}$ *for a non-negative matrix* $\mathbf{B}$ *and* $s \geq \rho(\mathbf{B})$*, where* $\rho(\mathbf{B})$ *is the spectral radius of* $\mathbf{B}$*.*

(b) The real part of each nonzero eigenvalue of $\mathbf{A}$ *is positive.*

(c) All principal minors of $\mathbf{A}$ *are nonnegative.*

During the analysis, we require the following definition of a graph for a given matrix.

Definition 2. *The* directed graph *of an $N \times N$ matrix $\mathbf{A} = [a_{ij}]$ is the directed graph $G(\mathbf{A})$, such that there exists a directed arc in $G(\mathbf{A})$, from node i to node j if and only if $a_{ji} \neq 0$ [79].*

Definition 3. *Let G be a directed graph. If there exist a directed path of finite length between node i and j for every node pair of distinct nodes in G, then the directed graph G is* strongly connected.

A matrix $\mathbf{A}$ is *irreducible* (sometimes called *indecomposable*), if there exists no permutation matrix $\mathbf{P}$ such that

$$\mathbf{PAP}^T = \begin{bmatrix} \mathbf{B} & 0 \\ \mathbf{C} & \mathbf{D} \end{bmatrix} \tag{2.23}$$

where $\mathbf{B}, \mathbf{D}$ are square matrices [78].

Definition 4. *For a graph with N nodes, Laplacian matrix $\mathbf{L} = [l_{ij}] \in \mathbb{R}^{N\times N}$ is defined as $l_{ii} = \sum_{j\neq i} a_{ij}$ and $l_{ij} = -a_{ij}$, $\forall i \neq j$. a_{ij} is a non-negative number which represents the weight of the connection between node i and j [81].*

Laplacian matrix is a singular M-matrix by definition. If the graph is undirected, $\mathbf{L}$ is a symmetric matrix which is not necessarily the case for the directed graphs. The row sums of $\mathbf{L}$ are equal to 0, therefore $\mathbf{L}$ always has one zero eigenvalue with corresponding eigenvector $\mathbf{1} = [1, \ldots, 1]^T$. 0 is a simple eigenvalue of $\mathbf{L}$ if the undirected graph is connected and for the directed case if the graph is strongly connected [72], [82]. A weaker condition than being strongly connected for directed graphs is existence of a spanning tree.

Definition 5. *A directed graph has a* spanning tree *if there exists at least one node with a directed path to all of the other nodes.*

2.5. Chapter Summary

In this chapter, the power control problem in heterogeneous networks is described mathematically. The problems considered in this thesis, namely maximizing the minimum SINR and minimizing the maximum relative error along with fairness constraint, are introduced. The proposed algorithms presented in the next chapter are inspired by the consensus algorithms which are introduced briefly in this chapter with an example. Finally, mathematical preliminaries utilized in theoretical analysis, are provided.

3. CONSENSUS BASED POWER CONTROL ALGORITHMS

In this chapter, three different power control algorithms which are inspired by the consensus algorithms, are presented. The algorithms are specifically designed for the problems described by (2.8)-(2.9) and (2.16)-(2.17). The convergence properties of the proposed power control algorithms under ideal communication link assumption are also investigated. The analyses under non-ideal communication links are presented in the next chapter.

3.1. Power Control Algorithm-I (PCA-I)

The first proposed power control algorithm is presented in [83]. It is described by

$$\dot{p}_i(t) = -\beta_i \frac{\Gamma_i(t)}{p_i(t)} \left[f_{ii}(t)\Gamma_i(t) - \sum_{j \in N_i} f_{ij}(t)\Gamma_j(t) \right], \quad i \in \mathcal{I} \tag{3.1}$$

where β_i is a positive parameter that controls the speed of the update process for user i; N_i is the set of neighbors of user i with which it can exchange information on SINR values; and $f_{ij}(t)$ represent the connection weights. One of the main advantages of heterogeneous networks is the availability of information exchange between BSs which is utilized in the design of the proposed power control algorithms. The details on information exchange graph and connection weights are given in Sections 2.3 and 3.1.1, respectively.

Let the reference SINR value, $\Gamma_{i,ref}$ for user i be defined as

$$\Gamma_{i,ref}(t) = \sum_{j \in N_i} f_{ij}(t)\Gamma_j(t), \; i \in \mathcal{I}. \tag{3.2}$$

Then, the PCA-I becomes

$$\dot{p}_i(t) = -\beta_i \frac{\Gamma_i(t)}{p_i(t)} \left[f_{ii}(t)\Gamma_i(t) - \Gamma_{i,ref} \right], \quad i \in \mathcal{I}. \tag{3.3}$$

Note that BS i requires information only on p_i, Γ_i and $\Gamma_{i,ref}$, to update its power in (3.3). The values of p_i and Γ_i are readily available at the BS; the only additional information required is the SINR values from its neighbors (i.e., Γ_j, $j \in N_i$) which can be obtained via the operator backbone or Internet connection.

The algorithm described by (3.3) can be utilized at each tier of the network, under shared and split spectrum setups. The difference between different spectrum allocation schemes is determining the neighbor set of users. In shared spectrum setup, the neighbor set of a user may consist of users from every tier of the system whereas in split spectrum setup only neighbors from the same tier are allowed.

In (3.1), $\frac{\Gamma_i}{p_i} = \frac{1}{I_i}$ is a scaling term that slows the amount of power changes for users experiencing high interference whereas it has the opposite effect for users under low interference. In this sense, the algorithm allows the users that are less effected by interference to make larger amount of power changes. Since such users are more likely to have higher SINR values compared to other users, the algorithm tends to encourage faster decrease in total amount of interference created for all users.

In a heterogeneous network, a macrocell user may opt to use a predetermined threshold SINR value based on the application (e.g., voice, data, video) instead of relying on the SINR information obtained from the small cell users. Next, we show how to incorporate such a predetermined threshold by modifying the PCA-I. Assume that index 1 refers to the macrocell. In the modified algorithm, the power update is

$$\dot{p}_i(t) = \begin{cases} -\beta_1 \frac{\Gamma_1(t)}{p_1(t)} \left[\Gamma_1(t) - \Gamma_{1,des}(t) \right], & i = 1, \\ -\beta_i \frac{\Gamma_i(t)}{p_i(t)} \left[f_{ii}\Gamma_i(t) - \Gamma_{i,ref}(t) \right], & i \in \mathcal{I}, i \neq 1, \end{cases} \tag{3.4}$$

where $\Gamma_{1,des}(t) = \min(\gamma_1(t),\ \Gamma_{1,ref}(t))$ and the value $\gamma_1(t)$ is assumed to be chosen from a finite set, based on the service the macrocell user is receiving. Furthermore, we assume that $\dot{\gamma}_1(t)$ is finite for all time $t \geq 0$.

Remark 1. *The modified power control algorithm (3.4) is presented in a way that macrocell user utilizes a different update algorithm. However, the idea may be applied to any user and/or any tier in a straight-forward manner.*

3.1.1. Connection Weights

The connection weights or averaging coefficients f_{ij} are the weighted edge values of the underlying information exchange graph and these values are utilized to scale the effect of the received information on power update process. Recall that the information exchange between BSs is represented as a graph $G = (V, E)$ and the communication weights $f_{ij}(t)$ are the weighted entries of the connection matrix $\mathbf{L}$ whose components are given by

$$l_{ij} = \begin{cases} f_{ii}, & j = i, \\ -f_{ij}, & j \neq i. \end{cases} \tag{3.5}$$

To guarantee the convergence of the proposed algorithms, the connection matrix needs to be a Laplacian matrix. This constraint is satisfied via the following assumptions.

Assumption 1. *The connection weights satisfy the following conditions for all time $t \geq 0$:*

(i) *There exists a positive constant δ such that $f_{ij}(t) \geq \delta$ if $j \in N_i$; otherwise $f_{ij}(t) = 0,\ j \neq i,\ \forall i, j \in \mathcal{I}$*

(ii) $f_{ij}(t) = f_{ji}(t),\ \forall i, j \in \mathcal{I}$

(iii) $f_{ii}(t) = \sum_{j \in N_i} f_{ij}(t),\ \forall i \in \mathcal{I}.$

An example choice of parameters is

$$f_{ij}(t) = \begin{cases} \frac{|N_i|}{N_{max}}, & j = i, \\ \frac{1}{N_{max}}, & j \in N_i, \\ 0, & \text{otherwise}, \end{cases} \tag{3.6}$$

where $|N_i|$ denotes the cardinality of the set N_i and N_{max} is a bound on the maximum number of neighbors. For this set of parameters, (3.1) can be simplified as

$$\dot{p}_i(t) = -\beta_i \frac{\Gamma_i(t)}{p_i(t)} \frac{|N_i|}{N_{max}} \left[\Gamma_i(t) - \frac{1}{|N_i|} \sum_{j \in N_i} \Gamma_j(t) \right], \quad i \in \mathcal{I} \tag{3.7}$$

Recall that the set of neighbors for user i, N_i can be chosen to include the users closer to BS i than a threshold distance value D_{max} or by utilizing the user feedback reports which includes the interferer femtocell identifiers in LTE networks [67].

The conditions given in Assumption 1 is relaxed in one of our recent works [84]. The relaxed set of conditions on averaging coefficients are given below.

Assumption 2. *The averaging coefficients are assumed to satisfy the conditions given below for all time $t \geq 0$:*

(i) The information received from each user j in the neighbor set of user i is utilized in the power adjustment, i.e. $f_{ij}(t) > 0 \Leftrightarrow j \in N_i$.

(ii) The underlying information exchange graph is balanced, i.e., $\sum_{j \in \mathcal{I}} f_{ij}(t) = \sum_{j \in \mathcal{I}} f_{ji}(t), \ \forall i \in \mathcal{I}$

(iii) Power update for user i is accomplished based on the comparison of its SINR value with the weighted average of the received SINR values (SINR values of neighbors), i.e., $f_{ii}(t) = \sum_{j \in N_i} f_{ij}(t), \ \forall i \in \mathcal{I}$.

Assumption (i), requires that when an information on the SINR value of another user is received by a BS, it must be utilized. Hence, every information relayed is con-

sidered in the power update process. Assumption (ii) ensures that the total of the averaging coefficients used to scale the SINR information received by a user is equal to the total of the averaging coefficients used for scaling the SINR information that particular user is sending. This assumption leads to a balanced information exchange graph where every user affects other users as it is affected by them during the power update process. The final assumption is that every user compares its own SINR value with a scaled average of the received SINR values and adjusts its power based on this comparison.

An example choice of averaging coefficients which satisfies Assumption 2 is

$$f_{ij}(t) = \begin{cases} |N_i|, & j = i, \\ 1, & j \in N_i, \\ 0, & \text{otherwise}, \end{cases} \tag{3.8}$$

where $|N_i|$ denotes the number of users in the set N_i. For this set of parameters, (3.1) boils down to

$$\dot{p}_i(t) = -\beta_i \frac{\Gamma_i(t)}{p_i(t)} |N_i| \left[\Gamma_i(t) - \frac{1}{|N_i|} \sum_{j \in N_i} \Gamma_j(t) \right], i \in \mathcal{I} \tag{3.9}$$

The case where users are connected to the underlying communication graph for all t with a mutual information exchange condition (i.e., $f_{ij} = f_{ji}$), is investigated in [83]. The main difference is that Assumption 2 allows for a directed graph setting by relaxing the $f_{ij} = f_{ji}$ condition. Instead of using a mutual information exchange condition, a balanced graph is considered in [84] which is a more relaxed condition. Note that, mutual exchange condition satisfies the balanced graph assumption. The limits of relaxation on connection weights which guarantees the convergence of the algorithms, are not known. However, the conditions are further relaxed while considering the imperfect channel connection setup.

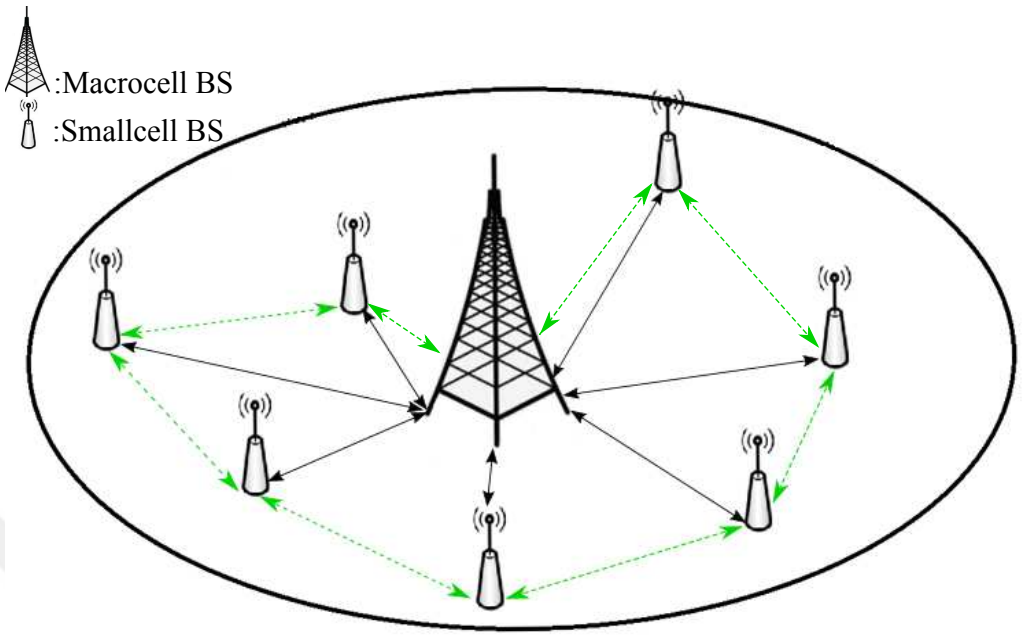

Figure 3.1. Two connected underlying communication graph examples.

For the convergence analysis, we assume that the connection weights takes finite values and continuous in the time varying case. These assumptions are given below

- $f_{ij}(t)$ is finite for all $i, j \in \mathcal{I}$ for all time $t \geq 0$.
- $\dot{f}_{ij}(t)$ exists and is finite for all $i, j \in \mathcal{I}$ and for all time $t \geq 0$.

We assume that these conditions for connections weights hold for the rest of the analyses.

3.1.2. Creating the Underlying Communication Graph

The proposed algorithms rely on the information exchange between base stations, however the set of rules for establishing connection between base stations are not discussed. In this section, we provide two simple approaches for creating the underlying communication graph.

Figure 3.1 illustrates two simple set of communication links that may be utilized for information exchange between BSs. In the first set of communication links, shown with black arrows, every BS exchanges information with only the macrocell BS. Such a setup may be desirable as macrocell BS is usually assumed to be communicating with small cell BSs in resource allocation approaches. Note that, the communication between BSs is accomplished via internet and/or backhaul. In the second set of communication links, shown with green arrows, the BSs create a ring topology. In this setup, every base station only exchanges information with the nearest two BSs. In both cases, the resulting communication graph is undirected and connected. In the subsequent analysis, we also consider an undirected graph setup with varying connection weights which results in the relaxation of design constraints.

An important contribution of this thesis is considering a setup in which the information exchange is carried out using non-ideal links. That is, the communication links are susceptible to time-outs which may result in failures during information exhange or even isolated BSs. The details of the model is given in Chapter 4. The content of the information utilized for the proposed algorithms is the SINR values for the PCA-I, PCA-II and the relative error values for PCA-III. Each BS exchanges only its current SINR value or relative error value with other BSs in its neighbor set.

3.2. Power Control Algorithm-II (PCA-II)

The second proposed power control algorithm is presented in [85]. It is described by

$$\dot{p}_i(t) = -\beta_i \Gamma_i(t) \left[f_{ii}(t)\Gamma_i(t) - \sum_{j \in N_i} f_{ij}(t)\Gamma_j(t) \right], \quad i \in \mathcal{I} \tag{3.10}$$

where the definition of parameters are analogous to the PCA-1 and the main difference is the scaling term of the power adjustment algorithm.

Next, we modify PCA-II to use a predetermined target SINR value similar to the modified PCA-I. A modified version of the power update (3.10) is given by

$$\dot{p}_i(t) = \begin{cases} -\beta_1 \Gamma_1(t) \left[\Gamma_1(t) - \Gamma_{1,des}(t)\right], & i = 1, \\ -\beta_i \Gamma_i(t) \left[\Gamma_i(t) - \Gamma_{i,ref}(t)\right], & i \in \mathcal{I}/1 \end{cases} \tag{3.11}$$

where $\Gamma_{1,des}(t) = \min(\gamma(t),\ \Gamma_{1,ref}(t))$. This setup gives the macrocell user two alternative options of utilizing the neighbor information or using a predetermined threshold SINR value based on the application.

3.2.1. Discrete Time Form of Power Control Algorithm-II

A discretized version of (3.10) can be obtained by approximating the derivative of $p(t)$ using the Euler's method as follows

$$\dot{p}(t) \approx \left. \frac{p(t+T_s) - p(t)}{T_s} \right|_{t=kT_s} \tag{3.12}$$

By letting $p_i[k] \triangleq p_i(kT_s)$ and using a sampling period $T_s = 1$, the resulting discrete–time algorithm is given by

$$p_i[k+1] = p_i[k] - \beta_i \Gamma_i[k] \left[f_{ii}[k]\Gamma_i[k] - \Gamma_{i,ref}[k]\right], \quad i \in \mathcal{I} \tag{3.13}$$

where the definition of parameters $\Gamma_i[k], \Gamma_{i,ref}[k]$ and β_i are similar to the continuous case. We assume that the connection weights of (3.13) also satisfy Assumption 1 given in Section 3.1.1.

Although the intuition given above in obtaining (3.13) relies on discretizing a continuous–time algorithm with $T_s = 1$, note that (3.13) can be considered as a stand–alone discrete time power adjustment algorithm independent of (3.10), i.e., (3.13) can be used as an iterative algorithm where $p_i[k]$ denotes the power level at the kth iteration and the sampling period T_s is chosen to meet the constraints of the network.

The discrete time extension of (3.13) given by

$$p_i[k+1] = \begin{cases} p_1[k] - \beta_1 \Gamma_1[k] \left[\Gamma_1[k] - \Gamma_{1,des}[k]\right], & i = 1, \\ p_i[k] - \beta_i \Gamma_i[k] \left[\Gamma_i[k] - \Gamma_{i,ref}[k]\right], & i \in \mathcal{I}/1 \end{cases} \tag{3.14}$$

where $\Gamma_{1,des}[k] = \min(\gamma[k], \Gamma_{1,ref}[k])$. Similar to the PCA-I case, the modified algorithm can be employed by any BS in the system.

3.3. Power Control Algorithm-III (PCA-III)

The proposed algorithm is presented in [86] and it is described by

$$\dot{p}_i(t) = \beta_i \frac{\Gamma_i(\mathbf{p}, t)}{\gamma_i} \left[e_i(t) - \frac{1}{|N_i|} \sum_{j \in N_i} e_j(t) \right], \quad i \in \mathcal{I} \tag{3.15}$$

where the adjustment speed for user i can be controlled by the positive parameter, β_i; and $|N_i|$ denotes the cardinality of the set N_i. Let $e_{i,ref}$ denote the reference error computed using the average error of BSs in N_i, i.e.

$$e_{i,ref}(t) = \frac{1}{|N_i|} \sum_{j \in N_i} e_j(t). \tag{3.16}$$

Then, the only information required by BS i for the update process is Γ_i and $e_{i,ref}$ values. The difference of PCA-III algorithm is that BSs uses the information on relative error values of other users.

The idea is achieving a power allocation such that every user achieves the same weighted error based on their desired SINR level. For the non-feasible case this results in every user achieving less than their target SINR value with same percentage. This is the main difference of the PCA-III algorithm from the previously presented algorithms. Such an approach allows the power adjustment process to consider the heterogeneous QoS requirements of users.

3.3.1. Discrete Time Form of Power Control Algorithm-III

In a practical system, a discrete time version of the proposed power control algorithm-III is required. Using the Euler's method for approximating the derivative of $p(t)$, we can obtain a discretized version of (3.15) as

$$p_i[k+1] = p_i[k] + \beta_i \frac{\Gamma_i(\mathbf{p}, k)}{\gamma_i} \left[e_i[k] - e_{i,ref}[k] \right], \quad i \in \mathcal{I}. \tag{3.17}$$

Similar to the previous algorithms, the discrete-time algorithm provided in (3.17) can be regarded as an independent power update algorithm with its sampling period adjusted to the problem at hand.

3.4. Convergence Analysis For the Proposed Power Control Algorithms

In this section, we present the convergence analysis for the proposed power control algorithms. The analyses are carried out using the following property:

Property 1. *Given a differentiable function $f(t)$, if $f(t)$ is lower bounded and non-increasing ($\dot{f}(t) \leq 0$), then it converges to a limit [87].*

We consider two different functions in the analyses. The utilized quadratic function is described by

$$V(\mathbf{p}) = \mathbf{p}^T \mathbf{B}^{-1} \mathbf{p} = \sum_{i=1}^{N} \frac{1}{\beta_i} p_i^2 \tag{3.18}$$

where $\mathbf{B}^{-1} = \text{diag}(\frac{1}{\beta_1}, \ldots, \frac{1}{\beta_N})$. With an abuse of notation, we drop the time dependency of variables in notation for simplicity when the context is clear. Another function utilized for convergence analysis is given below

$$V(\mathbf{p}) = \mathbf{1}^T \mathbf{B}^{-1} \mathbf{p} = \sum_{i=1}^{N} \frac{1}{\beta_i} p_i. \tag{3.19}$$

We assume that the channel conditions are finite, i.e., there exists a finite interval, $\mathcal{G} = [\underline{g}, \overline{g}]$, such that $g_{ij} \in \mathcal{G}$ for all (i, j) to exclude degenerate cases. Furthermore, we assume that there are finite number of users and BSs in the system.

We will use a step by step approach to show the convergence of the algorithms. In the first step, we will show that the functions given above converge to a limit. For this purpose, we need to show that (3.18) and (3.19) are lower bounded and non-increasing along system trajectories. Then, we will show that convergence to a limit value implies $\dot{V}(\mathbf{p}(t)) \to 0$ as $t \to \infty$. Finally, we will show that $\dot{V}(\mathbf{p}(t)) \to 0$ implies $\dot{\mathbf{p}}(t) \to 0$ and the equilibrium points are the solutions for the problems given by defined in Section 2.1.

First, we show that the given functions are lower bounded by using the following lemma.

Lemma 3.1. *For any positive power vector* $\mathbf{p}(t_0)$ *given to the proposed power control algorithms as an initial condition,* $\mathbf{p}(t) \geq 0$ *for all* $t \geq t_0$.

Proof. For any entry of power vector to be negative, there must exist a t_1 such that, $p_i(t_1) = 0$ and $\dot{p}_i(t_1) < 0$. We will investigate each algorithm separately. For PCA-I,

$$\begin{aligned} \dot{p}_i(t_1) &= -\beta_i \frac{1}{I_i(t_1)} \left[f_{ii}(t_1)\Gamma_i(t_1) - \sum_{j \in N_i} f_{ij}(t_1)\Gamma_j(t_1) \right] \\ &= \beta_i \frac{1}{I_i(t_1)} \left[\sum_{j \in N_i} f_{ij}(t_1)\Gamma_j(t_1) \right] \end{aligned}$$

which is non-negative and only equal to zero if $\sum_{j \in N_i} f_{ij}(t_1)\Gamma_j(t_1) = 0$, i.e., $p_j(t_1) = 0$ for all $j \in N_i$. This contradicts $\dot{p}_i(t_1) < 0$.

Next, we consider PCA-II,

$$\begin{aligned} \dot{p}_i(t_1) &= -\beta_i \Gamma_i(t_1) \left[f_{ii}(t_1)\Gamma_i(t_1) - \sum_{j \in N_i} f_{ij}(t_1)\Gamma_j(t_1) \right] \\ &= 0 \end{aligned}$$

which is also non-negative. Finally, for PCA-III, we have

$$\begin{aligned} \dot{p}_i(t_1) &= -\beta_i \frac{\Gamma_i(t_1)}{\gamma_i} \left[e_i(t_1) - \frac{1}{|N_i|} \sum_{j \in N_i} e_j(t_1) \right] \\ &= 0 \end{aligned}$$

hence, for any initial positive power vector $\mathbf{p}(t_0)$, the proposed power control algorithms have $\mathbf{p}(t) \geq 0$ for all $t \geq t_0$. □

The results given by the Lemma 3.1 are crucial for the subsequent analysis as it allows us to lower bound the function given by (3.19). Furthermore, it allows us to conclude that if the function (3.19) converges to a limit, then $\mathbf{p}(t)$ is bounded. Since, there is no analysis on $\dot{\mathbf{p}}(t)$, the convergence to a limit for $\mathbf{p}(t)$ values are not guaranteed. Another important advantage of Lemma 3.1 is that in real systems there are no negative power values. Hence, a dynamic system with negative values are not usable in real systems.

Unfortunately, showing the convergence of the functions given in (3.18) and (3.19) to a limit does not necessarily imply $\dot{V}(\mathbf{p}(t)) \rightarrow 0$. Consider the function, $f(t) = e^{-t}sin(e^{2t})$ which tends to zero as $t \rightarrow \infty$ [87]. However, not only $\dot{f}(t) \nrightarrow 0$, it is also unbounded. Hence, the convergence to a limit for the functions (3.18) and (3.19) does not allow us to draw any conclusions on the behavior of $\mathbf{p}(t)$. The next result known as Barbalat's Lemma allows us to investigate behavior of $\dot{V}(\mathbf{p}(t))$ asymptotically [87]. We require $\dot{V}(\mathbf{p}(t)) \rightarrow 0$ as $t \rightarrow \infty$ and show it using Barbalat's Lemma.

Lemma 3.2. *If the differentiable function $f(t)$ converges to a limit as $t \to \infty$ and $\ddot{f}(t)$ is bounded, then $\dot{f}(t) \to 0$ as $t \to \infty$.*

Lemma 3.2 allows us to show $\dot{V}(\mathbf{p}(t)) \to 0$ if we have functions that converges to a limit. Since the functions (3.18) and (3.19) are lower bounded, we need to show that $\ddot{V}(\mathbf{p}(t))$ is bounded and $\dot{V}(\mathbf{p}(t)) \leq 0$ along the system trajectories. For the rest of the analyses, we will investigate the convergence properties of each algorithm separately.

3.4.1. Convergence Analysis of PCA-I

In this part, the convergence analysis for PCA-I under Assumption 1 is provided. Then, the result is extended for a setup with Assumption 2. In vector notation, (3.1) can be described as

$$\dot{\mathbf{p}}(t) = -\mathbf{B}\mathbf{I}_d^{-1}(t)\mathbf{L}\boldsymbol{\Gamma}(t) \tag{3.20}$$

where $\boldsymbol{\Gamma} = [\Gamma_1, \ldots, \Gamma_N]^T$; $\mathbf{I}_d = \text{diag}(I_1, \ldots, I_N)$ is the diagonal matrix with normalized interference values, $I_i = p_i/\Gamma_i$ and $\mathbf{B} = \text{diag}(\beta_1, \ldots, \beta_N)$.

The equilibrium points of (3.20) are the points that satisfy $\mathbf{L}\boldsymbol{\Gamma}(t) = 0$, since β_i and $I_i(t)$, $i \in \mathcal{I}$ are positive. Furthermore, if 0 is a simple eigenvalue of $\mathbf{L}$, it can be shown that the set of equilibrium points satisfy $\Gamma_i = \Gamma_j$, $\forall i, j \in \mathcal{I}$, i.e., the update algorithm stops when every user has identical SINR values. This implies that the algorithm adjusts transmission powers for small cell BSs in a way that achieves fairness. This fairness is not in terms of the size of the area covered by BSs, but in the sense that each BS in the system can provide the same SINR value to its user, without the knowledge of a predefined target SINR value.

To account for time-varying communication infrastructure (i.e., the neighbor set of each user might be varying), the connection matrix $\mathbf{L}$ is assumed to be time-varying.

Theorem 3.3. *The power update algorithm given in (3.1) satisfying Assumption 1 converges to a fair coverage solution* $\Gamma_i = \Gamma_j,\ \forall i, j \in \mathcal{I}$, *if the underlaying communication graph is connected for all* t.

Proof. Consider the function defined by (3.18). $\dot{V}(\mathbf{p})$ is given by

$$\begin{aligned} \dot{V}(\mathbf{p}) &= \mathbf{p}^T\mathbf{B}^{-1}\dot{\mathbf{p}} + \dot{\mathbf{p}}^T\mathbf{B}^{-1}\mathbf{p} \\ &= -\mathbf{p}^T\mathbf{B}^{-1}\mathbf{B}\mathbf{I}_d^{-1}\mathbf{L}\mathbf{I}_d^{-1}\mathbf{p} - \mathbf{P}^T\mathbf{I}_d^{-1}\mathbf{L}^T\mathbf{I}_d^{-1}\mathbf{B}^{-1}\mathbf{B}\mathbf{P} \\ &= -\mathbf{p}^T\mathbf{I}_d^{-1}\mathbf{L}\mathbf{I}_d^{-1}\mathbf{P} - \mathbf{p}^T\mathbf{I}_d^{-1}\mathbf{L}^T\mathbf{I}_d^{-1}\mathbf{P} \\ &= -\mathbf{\Gamma}^T(\mathbf{L} + \mathbf{L}^T)\mathbf{\Gamma} \\ &= -2\mathbf{\Gamma}^T\mathbf{L}\mathbf{\Gamma} \end{aligned} \tag{3.21}$$

is negative for non–equilibrium points. Since $V(\mathbf{p})$ is lower bounded and $\dot{V}(\mathbf{p})$ is non-increasing, we can conclude that $V(\mathbf{p}(t))$ converges to a limit. This result allows us to conclude that $\mathbf{p}$ is bounded. Hence, $\mathbf{\Gamma}$ and $\mathbf{I}_d$ are also bounded. If we can show that $\ddot{V}(\mathbf{p})$ is bounded, Lemma 3.2 allows us to conclude $\dot{V}(\mathbf{p}(t)) \to 0$ as $t \to \infty$.

The Laplacian matrix of an undirected graph satisfies the sum of squares property. Hence, we can re-write the result of equation (3.21),

$$\dot{V}(\mathbf{p}) = -\sum_{(i,j)\in\mathcal{I}}^{N} f_{ij}(t)\left(\Gamma_i(t) - \Gamma_j(t)\right)^2 \tag{3.22}$$

which allows us to compute $\ddot{V}(\mathbf{p})$ as follows

$$\ddot{V}(\mathbf{p}) = -2\sum_{(i,j)\in\mathcal{I}}^{N} \left(\Gamma_i(t) - \Gamma_j(t)\right)^2 \left[\frac{f_{ij}(t)\left(\dot{\Gamma}_i(t) - \dot{\Gamma}_j(t)\right)}{\left(\Gamma_i(t) - \Gamma_j(t)\right)} + \frac{1}{2}\dot{f}_{ij}(t)\right] \tag{3.23}$$

and $\dot{\Gamma}_i(t)$ is given by

$$\frac{d\Gamma_i}{dt} = \frac{d}{dt}\left(\frac{p_i}{I_i}\right) = \frac{\dot{p}_i I_i - p_i \dot{I}_i}{I_i^2} \tag{3.24}$$

$$= -\frac{1}{I_i}\beta_i\left[\frac{\Gamma_i - \Gamma_{i,ref}}{I_i}\right] + \frac{\Gamma_i}{I_i}\sum_{\substack{j=1,\\ j\neq i}}^{N} h_{ij}\dot{p}_j \tag{3.25}$$

$$= -\frac{1}{I_i}\beta_i\left[\frac{\Gamma_i - \Gamma_{i,ref}}{I_i}\right] + \frac{\Gamma_i}{I_i}\sum_{\substack{j=1,\\ j\neq i}}^{N} h_{ij}\frac{1}{I_j}\beta_j(\Gamma_j - \Gamma_{j,ref}). \tag{3.26}$$

Since we know Γ_i, $\Gamma_{i,ref}$, I_i, β_i, p_i and h_{ij} are bounded for all $i, j \in \mathcal{I}$, we can conclude that $\dot{\Gamma}_i(t)$ is bounded. $\ddot{V}(\mathbf{p})$ given in (3.23) is bounded, since there are finite number of users, f_{ij}, $\dot{f}_{ij}$, $\dot{\Gamma}_i(t)$ and Γ_i are all bounded which allows us to deduce $\dot{V}(\mathbf{p}(t)) \to 0$ as $t \to \infty$. Next, we investigate the points which satisfy $\dot{V}(\mathbf{p}(t)) = 0$.

Note that under Assumption 1, $\mathbf{L}(t)$ is a symmetric singular M-matrix, and since the underlaying graph is connected for all t, 0 is a simple eigenvalue of for $\mathbf{L}(t)$ [74]. Therefore, $\dot{V}(\mathbf{p}(t))$ is negative for non–equilibrium points and is equal to zero for the cases where $\mathbf{\Gamma}$ is in the kernel of $\mathbf{L}$ which is independent of t and is given as span$\{\mathbf{1}\}$ corresponding to consensus.

Finally, we need to show that the points which satisfy $\dot{V}(\mathbf{p}) = 0$ are the points at which $\dot{\mathbf{p}}(t) = 0$. Since the equilibrium points of (3.20) are the points that satisfy $\mathbf{L\Gamma}(t) = 0$ which are exactly the equilibrium points which satisfy $\dot{V}(\mathbf{p}) = 0$. Hence, we can conclude that $\dot{V}(\mathbf{p}) \to 0$ implies $\dot{\mathbf{p}}(t) \to 0$. □

The proof shows the convergence properties of the PCA-I, which is independent of the initial power values and channel gains. This is a crucial advantage of the algorithm compared to the other approaches in the literature as there are no feasibility concerns for the proposed algorithm. Furthermore, we consider a case with time-varying connection matrix $\mathbf{L}$. A drawback of the algorithm proposed is the requirement of mutual information exchange, which results in a symmetric connection matrix $\mathbf{L}$. This condi-

tion is relaxed in the subsequent analysis. Next, we analyze the convergence properties of the modified PCA-I which allows macrocell user to utilize a predefined target SINR value.

This result is used in the subsequent analysis for the PCA-I and is not explicitly stated at each proof. For the rest of the convergence analysis for the PCA-I, we only show $\dot{V}(\mathbf{p}(t))$ is negative at non-equilibrium points and zero at equilibrium points. The rest of the proofs follows the same arguments given in the proof of Theorem 3.3. This result is used in the subsequent analysis for the PCA-I and is not explicitly stated at each proof.

Theorem 3.4. *The power update algorithm given in (3.4) converges to a fair solution* $\Gamma_i(t) = \Gamma_j(t),\ \forall i, j \in \mathcal{I}$, *if the underlaying communication graph satisfies Assumption 1 and is connected for all* t.

Proof. For the function given in (3.18), the case where $\Gamma_{1,des}(t) = \Gamma_{1,ref}(t)$, reduces to the proof of Theorem 3.3 and is therefore omitted. For the case where $\Gamma_{1,des}(t) = \gamma_1(t)$, an upper bound on $\dot{V}(\mathbf{p}(t))$ is

$$\begin{aligned}
\dot{V}(\mathbf{p}(t)) &= -2\Gamma_1(t)\left[\Gamma_1(t) - \Gamma_{1,des}(t)\right] + \sum_{i=2}^{N} \frac{2}{\beta_i}\dot{p}_i p_i \\
&\leq -2\Gamma_1(t)\left[\Gamma_1(t) - \gamma_{max}\right] + \sum_{i=2}^{N} \frac{2}{\beta_i}\dot{p}_i p_i \\
&\leq -2\Gamma_1(t)\left[\Gamma_1(t) - \Gamma_{max}(t)\right] + \sum_{i=2}^{N} \frac{2}{\beta_i}\dot{p}_i p_i \\
&= -\mathbf{\Gamma}^T(t)(\bar{\mathbf{L}}(t) + \bar{\mathbf{L}}^T(t))\mathbf{\Gamma}(t) \qquad (3.27)
\end{aligned}$$

where $\Gamma_{max}(t) = \max_{i \in \mathcal{I}/1} \Gamma_i(t)$ and without loss generality, we assume user N has the maximum SINR value. Notice that, we assume the desired SINR value of user 1 is chosen from a finite set with the maximum value γ_{max}.

The matrix $\bar{\mathbf{L}}(t)$ is given by

$$\bar{\mathbf{L}}(t) = \begin{bmatrix} 1 & 0 & \dots & -1 \\ -f_{21} & f_{22} & \dots & -f_{2N} \\ \vdots & & \ddots & \vdots \\ -f_{N1} & -f_{N2} & \dots & f_{NN} \end{bmatrix}. \tag{3.28}$$

Note that, unlike the previous case $\bar{\mathbf{L}}(t)$ is not necessarily symmetric. Under Assumption 1, $\bar{\mathbf{L}}(t) + \bar{\mathbf{L}}^T(t)$ is a symmetric singular Laplacian matrix with non-negative eigenvalues. Furthermore since the underlaying graph is connected for all t, 0 is a simple eigenvalue for all $\mathbf{L}(t) \in \mathbb{L}$. Hence $\dot{V}(\mathbf{p}(t))$ is negative for non–equilibrium points, and is equal to zero when consensus is achieved. To complete the proof we need to show $\ddot{V}(\mathbf{p}(t))$ is bounded. Let us re-write $\dot{V}(\mathbf{p}(t))$ as

$$\begin{aligned} \dot{V}(\mathbf{p}(t)) &= -2\Gamma_1(t)\left[\Gamma_1(t) - \min\left(\Gamma_{1,ref}, \gamma_1(t)\right)\right] + \sum_{i=2}^{N} \frac{2}{\beta_i} \dot{p}_i p_i \\ &= -2\Gamma_1(t)\left[\Gamma_1(t) - \min\left(\Gamma_{1,ref}, \gamma_1(t)\right)\right] - \sum_{i=2}^{N} 2\Gamma_i \left[\Gamma_1(t) - \Gamma_{i,ref}\right] \end{aligned} \tag{3.29}$$

The derivative of the summation term is shown to be bounded in the previous section. For the first term, since the minimum of two continuous functions is continuous and its derivative is finite and $\ddot{V}(\mathbf{p}(t))$ is bounded. Hence, $\dot{V}(\mathbf{p}(t)) \to 0$ as $t \to \infty$ □

3.4.1.1. Convergence Rate Analysis. The speed of convergence for a distributed power update algorithm in a wireless communication system is an important aspect. In such a highly dynamical system, a power adjustment algorithm should react to the changes instantly as adjusting powers after a user has already experienced inferior signal quality is not desirable. In this part, the convergence rate analysis of the PCA-I is presented. To this end, re–consider the function $V(\mathbf{p}(t))$ in (3.18) whose derivative

$$\dot{V}(\mathbf{p}(t)) = -2\mathbf{\Gamma}^T(t)\mathbf{L}(t)\mathbf{\Gamma}(t) \leq -2\lambda_2 \|\mathbf{\Gamma}(t)\|^2 \tag{3.30}$$

is bounded using $\lambda_2 = \min_{\mathbf{L}\in\mathbb{L}} \sigma_2(\mathbf{L})$, where $\sigma_2(\mathbf{L})$ denotes the second smallest eigenvalue of $\mathbf{L}$, known as Fiedler Value [88]. Let I_{max} denote the maximum interference experienced by a user. The lower and upper bounds on $V(\mathbf{p})$ is given by

$$\frac{1}{\beta_{max}}\|\mathbf{p}\|^2 \leq V(\mathbf{p}) = \mathbf{p}^T\mathbf{B}^{-1}\mathbf{p} \leq \frac{1}{\beta_{min}}\|\mathbf{p}\|^2 \tag{3.31}$$

where $\beta_{max} = \max_{i\in\mathcal{I}} \beta_i$ and $\beta_{min} = \min_{i\in\mathcal{I}} \beta_i$. As $V(\mathbf{p}(t))$ is shown to be bounded above, there exists a finite p_{max} which implies that I_{max} is finite. Note that $\Gamma_i \geq \frac{p_i}{I_{max}}$ and $\|\mathbf{\Gamma}\|^2 \geq \frac{\|\mathbf{p}\|^2}{I_{max}}$. From (3.31) and (3.30), we have

$$\dot{V}(\mathbf{p}(t)) \leq -2\frac{\lambda_2}{I_{max}}\|\mathbf{p}(t)\|^2 \leq -2\lambda_2\frac{\beta_{min}}{I_{max}}V(\mathbf{p}(t)) \tag{3.32}$$

whose solution leads to

$$V(\mathbf{p}(t)) \leq \exp\left(-2\lambda_2\frac{\beta_{min}}{I_{max}}t\right)V(\mathbf{p}(0)) \tag{3.33}$$

By exploiting the upper and lower bounds from (3.31), we finally obtain

$$\begin{aligned} V(t) &\leq \exp\left(-2\lambda_2\frac{\beta_{min}}{I_{max}}t\right)\frac{1}{\beta_{min}}\|\mathbf{p}(0)\|^2 \\ \frac{1}{\beta_{max}}\|\mathbf{p}(t)\|^2 &\leq \exp\left(-2\lambda_2\frac{\beta_{min}}{I_{max}}t\right)\frac{1}{\beta_{min}}\|\mathbf{p}(0)\|^2 \\ \|\mathbf{p}(t)\| &\leq \sqrt{\frac{\beta_{max}}{\beta_{min}}}\exp\left(-\lambda_2\frac{\beta_{min}}{I_{max}}t\right)\|\mathbf{p}(0)\| \end{aligned} \tag{3.34}$$

Hence, it can be concluded that convergence is exponential for (3.3).

Remark 2. *For the modified power control algorithm given in (3.4) the convergence rate analysis can be carried out using a similar approach.*

3.4.2. Convergence Analysis of PCA-II

The convergence analysis for the PCA-II is presented next. In vector notation, (3.10) is described by

$$\dot{\mathbf{p}}(t) = -\mathbf{B}\boldsymbol{\Gamma}_d(t)\mathbf{L}\boldsymbol{\Gamma}(t), \tag{3.35}$$

where $\boldsymbol{\Gamma}_d = \text{diag}(\Gamma_1, \ldots, \Gamma_N)$ is the diagonal matrix with SINR values; $\mathbf{L} = [l_{ij}]$ is the $N \times N$ connection matrix defined by (3.5).

Similar to the PCA-I, the equilibrium points of (3.35) are the points that satisfy $\mathbf{L}\boldsymbol{\Gamma}(t) = 0$, since β_i is positive and $\Gamma_i = 0$ implies $p_i = 0$, meaning that user i is not active. If 0 is a simple eigenvalue of $\mathbf{L}$, it can be shown that the set of equilibrium points satisfy $\Gamma_i = \Gamma_j,\ \forall i, j \in \mathcal{I}$, i.e., the update algorithm stops when every user has identical SINR. Similar to the PCA-I, this implies that the algorithm adjusts coverage areas in a way that achieves fairness in terms of SINR values.

Remark 3. *A similar analysis for (3.13) reveals that the set of equilibrium points satisfy $\Gamma_i[k] = \Gamma_j[k],\ \forall i, j \in \mathcal{I}$, if the network is connected.*

First, the stability analysis of the proposed algorithm for the case where the underlaying topology is fixed, i.e., the matrix $\mathbf{L}$ is constant, is presented which extended to the time-varying case. We now state the main result for the stability analysis under fixed information exchange topology.

Theorem 3.5. *The power update algorithm given in (3.10) satisfying Assumption 1 converges to a fair coverage solution $\Gamma_i = \Gamma_j,\ \forall i, j \in \mathcal{I}$, if the underlaying communication graph is connected for all t.*

Proof. Function given in (3.19), is used for the stability analysis of the proposed algorithm (3.10). To complete the proof, the derivative of $V(\mathbf{p})$ along system trajectories

is computed using (3.35) as follows:

$$\begin{aligned} \dot{V}(\mathbf{p}) &= \mathbf{1}^T\mathbf{B}^{-1}\dot{\mathbf{p}} \\ &= -\mathbf{1}^T\mathbf{B}^{-1}\mathbf{B}\mathbf{\Gamma_d}\mathbf{L}\mathbf{\Gamma} \\ &= -\mathbf{\Gamma}^T\mathbf{L}\mathbf{\Gamma} \end{aligned} \tag{3.36}$$

which is of quadratic form with a simple 0 eigenvalue of $\mathbf{L}$. Therefore, $\dot{V}(\mathbf{p})$ is always negative for non-equilibrium points. Similar to the PCA-I case, $\dot{V}(\mathbf{p}) \leq 0$ and $V(\mathbf{p})$ is lower bounded. Hence, we can conclude that $V(\mathbf{p})$ converges to a limit. This allows us to conclude that $p_i(t)$, $\Gamma_i(t)$, $I_i(t)$ are all bounded for all $i \in \mathcal{I}$ and time $t \geq 0$. Convergence to a limit implies that $\dot{V}(\mathbf{p}(t)) \to 0$ as $t \to \infty$ if $\ddot{V}(\mathbf{p})$ is bounded. $\ddot{V}(\mathbf{p})$ can be computed as

$$\ddot{V}(\mathbf{p}) = -\sum_{(i,j)\in\mathcal{I}}^{N} f_{ij}\left(\dot{\Gamma}_i(t) - \dot{\Gamma}_j(t)\right)\left(\Gamma_i(t) - \Gamma_j(t)\right) \tag{3.37}$$

and $\dot{\Gamma}_i(t)$ is given by

$$\frac{d\Gamma_i}{dt} = \frac{d}{dt}\left(\frac{p_i}{I_i}\right) = \frac{\dot{p}_i I_i - p_i \dot{I}_i}{I_i^2} \tag{3.38}$$

$$= -\Gamma_i\beta_i\left[\frac{\Gamma_i - \Gamma_{i,ref}}{I_i}\right] + \frac{\Gamma_i}{I_i}\sum_{\substack{j=1,\\ j\neq i}}^{N} h_{ij}\dot{p}_j \tag{3.39}$$

$$= -\Gamma_i\beta_i\left[\frac{\Gamma_i - \Gamma_{i,ref}}{I_i^2}\right] + \frac{\Gamma_i}{I_i}\sum_{\substack{j=1,\\ j\neq i}}^{N} h_{ij}\Gamma_j\beta_j(\Gamma_j - \Gamma_{j,ref}). \tag{3.40}$$

which is bounded. Hence, we can conclude $\ddot{V}(\mathbf{p})$ is bounded and $\dot{V}(\mathbf{p}(t)) \to 0$ as $t \to \infty$. Finally, the points which satisfy $\dot{V}(\mathbf{p}) = 0$ also satisfy $\dot{\mathbf{p}}(t) = 0$, hence $\dot{V}(\mathbf{p}) \to 0$ implies $\dot{\mathbf{p}}(t) \to 0$. It is important that the points which satisfy $\dot{V}(\mathbf{p}) = 0$ are exactly the points at which $\dot{\mathbf{p}}(t) = 0$. Because, $\dot{V}(\mathbf{p}) = 0$ does not necessarily imply the system is at its equilibrium points and at rest. □

We now extend the convergence results to time-varying communication topologies.

Theorem 3.6. *The power update algorithm given in (3.10) converges to a fair solution* $\Gamma_i(t) = \Gamma_j(t),\ \forall i, j \in \mathcal{I}$, *if the underlaying communication graph satisfies Assumption 1 and is connected for all time* $t \geq 0$.

Proof. Reconsider the function in (3.19) whose derivative can be computed as

$$\dot{V}(\mathbf{p}(t)) = -\mathbf{\Gamma}^T(t)\mathbf{L}(t)\mathbf{\Gamma}(t). \tag{3.41}$$

The intermediate steps to obtain (3.41) is the same as previous sections and is omitted. The difference for this case is that $\mathbf{L}(t)$ is time varying. However, the quadratic form is preserved and every possible $\mathbf{L}(t)$ is a symmetric singular Laplacian matrix with a single 0 eigenvalue. Furthermore, since $\dot{f}_{ij}(t)$ is assumed to be finite, $\ddot{V}(\mathbf{p}(t))$ is bounded. Hence, $\dot{V}(\mathbf{p}(t))$ is negative for non-equilibrium points and is equal to zero when consensus is achieved. □

The stability analysis of the proposed algorithm for the modified PCA-II algorithm given in (3.11) is presented next.

Theorem 3.7. *The power update algorithm given in (3.11) converges to a fair solution* $\Gamma_i(t) = \Gamma_j(t),\ \forall i, j \in \mathcal{I}$, *if the underlaying communication graph satisfies Assumptions 1 and is connected for all time* $t \geq 0$.

Proof. The derivative of the function $V(\mathbf{p})$ in (3.36), along system trajectories is

$$\begin{aligned} \dot{V}(\mathbf{p}(t)) &= \sum_{i=1}^{N} \frac{1}{\beta_i}\dot{p}_i \\ &= -\Gamma_1(t)\left[\Gamma_1(t) - \Gamma_{1,des}(t)\right] + \sum_{i=2}^{N} \frac{1}{\beta_i}\dot{p}_i \end{aligned} \tag{3.42}$$

The case where $\Gamma_{1,des}(t) = \Gamma_{1,ref}(t)$ reduces to Theorem 3.6 and is therefore omitted. For the case where $\Gamma_{1,des}(t) = \gamma(t)$, using (3.36), $\dot{V}(\mathbf{p}(t))$ is obtained as

$$\begin{aligned}
\dot{V}(\mathbf{p}(t)) &= \sum_{i=1}^{N} \frac{1}{\beta_i}\dot{p}_i \\
&= -\Gamma_1(t)\left[\Gamma_1(t) - \Gamma_{1,des}(t)\right] + \sum_{i=2}^{N} \frac{1}{\beta_i}\dot{p}_i \\
&\leq -\Gamma_1(t)\left[\Gamma_1(t) - \gamma_{max}\right] + \sum_{i=2}^{N} \frac{1}{\beta_i}\dot{p}_i \\
&\leq -\Gamma_1(t)\left[\Gamma_1(t) - \Gamma_{max}(t)\right] + \sum_{i=2}^{N} \frac{1}{\beta_i}\dot{p}_i \\
&= -\frac{1}{2}\mathbf{\Gamma}^T(t)(\bar{\mathbf{L}}(t) + \bar{\mathbf{L}}^T(t))\mathbf{\Gamma}(t)
\end{aligned} \tag{3.43}$$

where $\Gamma_{max}(t) = \max_{i \in \mathcal{I}/1} \Gamma_i(t)$ and $\bar{\mathbf{L}}(t)$ is defined as

$$\bar{\mathbf{L}}(t) = \begin{bmatrix} 1 & 0 & \dots & -1 \\ -f_{21} & 1 & \dots & -f_{2N} \\ \vdots & & \ddots & \vdots \\ -f_{N1} & -f_{N2} & \dots & 1 \end{bmatrix}. \tag{3.44}$$

The rest of the proof follows the arguments given in the proof of Theorem 3.4. □

3.4.3. Convergence Analysis of PCA-III

In this part, we present the convergence analyses results for the PCA-III. First, the main result for the PCA-III is stated as follows:

Theorem 3.8. *Suppose the underlying communication graph is connected for all time $t \geq 0$ and satisfies Assumption 1. Then, the proposed algorithm described by (3.15) converges to a positive power vector satisfying $e_i = e_j,\ \forall i, j \in \mathcal{I}$.*

Proof. Consider the function $V(\mathbf{p}(t))$ given by (3.19). For convergence, we need to show $\dot{V}(\mathbf{p})$ along system trajectories is non-positive. $\dot{V}(\mathbf{p})$ is

$$\begin{aligned}\dot{V}(\mathbf{p}(t)) &= \mathbf{1}^T\mathbf{B}^{-1}\dot{\mathbf{p}}(\mathbf{t}) \\ &= -\mathbf{1}^T\mathbf{B}^{-1}\mathbf{B}\mathbf{Q}(t)\mathbf{L}\mathbf{q}(t) \\ &= -\mathbf{q}^T(t)\mathbf{L}\mathbf{q}(t) \\ &= -\mathbf{e}^T(t)\mathbf{L}\mathbf{e}(t) \end{aligned} \tag{3.45}$$

which is non-negative for all t and since underlying graph is connected, 0 is a simple eigenvalue of the symmetric positive semidefinite matrix $\mathbf{L}$ with unique eigenvector $\mathbf{1}$. $\dot{V}(\mathbf{p})$ is only equal to zero when $e_i = e_j$, for all $(i,j) \in \mathcal{I}$. Similar to the PCA-I and PCA-II case, $\dot{V}(\mathbf{p}(t)) = 0$ implies $\dot{\mathbf{p}}(t) = 0$. Finally, we need to show $\ddot{V}(\mathbf{p}(t))$ is bounded.

$$\ddot{V}(\mathbf{p}) = -\sum_{(i,j)\in\mathcal{I}}^{N}\left[f_{ij}(t)\left(\dot{q}_i(t) - \dot{q}_j(t)\right)\left(q_i(t) - q_j(t)\right) + \dot{f}_{ij}(t)(q_i(t) - q_j(t))^2\right] \tag{3.46}$$

and $\dot{q}_i(t)$ is given by

$$\frac{dq_i}{dt} = \frac{d}{dt}\left(\frac{\Gamma_i}{\gamma_i}\right) = \frac{\dot{\Gamma}_i\gamma_i - \Gamma_i\dot{\gamma}_i}{\gamma_i^2} \tag{3.47}$$

where $\dot{\gamma}_i$ is bounded by definition and $\dot{\Gamma}_i$ is

$$\frac{d\Gamma_i}{dt} = \frac{d}{dt}\left(\frac{p_i}{I_i}\right) = \frac{\dot{p}_iI_i - p_i\dot{I}_i}{I_i^2} \tag{3.48}$$

$$= -q_i\beta_i\left[\frac{e_i - e_{i,ref}}{I_i}\right] + \frac{\Gamma_i}{I_i}\sum_{\substack{j=1,\\ j\neq i}}^{N} h_{ij}\dot{p}_j \tag{3.49}$$

$$= -q_i\beta_i\left[\frac{e_i - e_{i,ref}}{I_i}\right] + \frac{\Gamma_i}{I_i}\sum_{\substack{j=1,\\ j\neq i}}^{N} h_{ij}\beta_jq_j\left[e_j - e_{j,ref}\right] \tag{3.50}$$

and it is bounded which completes the proof. □

3.5. Chapter Summary

In this chapter, the proposed power control algorithms are introduced and their convergence properties are investigated. The analyses given in this chapter consider both time-varying and fixed information exchange topologies. However, the analysis relies on ideal communication links which assumes information between BSs are relayed over ideal communication links. Furthermore, the analyses in this section show the convergence of the proposed algorithms without any considerations for the quality of the solutions obtained. In the next chapter, we address these problems and investigate the performance of the proposed algorithms under an imperfect connection setup along with optimality analyses.

4. IMPERFECT CHANNEL SETUP AND OPTIMALITY ANALYSIS

The analyses provided in the previous chapters are carried out using the ideal communication links in which the information between BSs is assumed to be relayed perfectly without any delay or time-outs. In this chapter, we present an imperfect connection setup which uses a more realistic model for the communication links. Next, the convergence properties of the proposed algorithms are investigated under this setup. Moreover, the optimality of the solution obtained by the proposed algorithms is investigated.

4.1. Imperfect Connection Setup

Recall that the connection matrix $\mathbf{L}$ (Laplacian matrix of the underlying communication graph), is given by (3.5) and $\mathbb{L}$ denote the set of matrices that satisfies Assumption 2. Note that, the set $\mathbb{L}$ contains all possible connection matrices ranging from all zero matrix (corresponding to all of the users being isolated) to complete connection matrix (representing a complete graph). However, the analyses given previously consider only the cases where $\mathbf{L}$ represents the Laplacian of a connected graph. This constraint is relaxed in the following analyses.

In this section, the analysis is carried out based on Assumption 2 given in Section 3.1.1 as it is a relaxation of Assumption 1 and it is clear that the analysis presented for Assumption 2 is valid for Assumption 1. An advantage of utilizing Assumption 2 is that it allows for a directed graph due to not imposing a mutual information exchange constraint. That is to say, the resulting connection matrix may represent the Laplacian of a directed graph. For an undirected graph, the existence of a spanning tree is equivalent to being connected. However, for a directed graph being connected is a stronger condition and implies the existence of a spanning tree.

The imperfect connection setup which is a more realistic model compared to the ideal links model, is introduced next. The following assumption defines the imperfect connection setup considered.

Assumption 3. *The connection matrices are assumed to satisfy the following two conditions:*

(i) The dynamic underlying communication graph can be described using switching connection matrices such that $\mathbf{L}[t_i] \in \mathbb{L}$ *represents the connection matrix between the time intervals* $[t_i,\ t_{i+1})$ *for an infinite time sequence where* $t_{i+1} > t_i,\ i = 1, 2, \ldots$ *and* $t_1 = 0$.

(ii) There exists an infinite sequence of uniformly bounded, non-overlapping time intervals $[t_i,\ t_{i+l})$ *for some* $\tau > 0$ *such that the union of connection matrices across each interval has a spanning tree.*

Assumption 3(i) requires that the connections are updated at discrete time intervals which is not necessarily periodic. Note that BSs are in control of connections, hence it is suitable to assume that the process is updated at discrete time intervals. Moreover, this condition is inherently satisfied for a discrete time system. Assumption 3(ii) requires that no user is isolated at all times. The assumption is that users may be isolated for some finite time τ. However, every user either receives or sends information to the system after some finite τ. The conditions given in Assumption 3 can be expanded to include time-varying desired SINR values. This allows a more realistic setup in which users are allowed to change their target SINR value during the power adjustment process. For the PCA-I and PCA-II algorithm such a modification is irrelevant as there is no desired value definition in the power update algorithms. On the other hand, for the PCA-III allowing time-varying desired SINR values results in a more realistic scenario. The change on desired SINR values may be due to change of the service received by the user and the reason for the time-varying assumption is irrelevant for the convergence analysis.

For the analysis of the PCA-III, the following conditions are assumed regarding the desired SINR values.

(i) There are finite number of changes on $\gamma_i(t)$ in finite time.

(ii) $\gamma_i(t)$ can be described using switching connection matrices such that $\gamma_i(t_k) \in \mathcal{X}$ is the desired SINR value for user i between time intervals $[t_k,\ t_{k+1})$, for an infinite time sequence where $t_{k+1} > t_k,\ k = 1, 2, \ldots$ and $t_1 = 0$.

The conditions given above is already satisfied for a discrete time system. Hence, from a practical point of view these conditions does not impose a separate constraint on the system.

4.2. Convergence Analysis Under Imperfect Connection Setup

In this section, we provide the convergence analysis of the PCA-I and PCA-III under imperfect connection setup. The convergence analysis for the PCA-II can be carried out in a similar manner to the PCA-I case and will be considered as future work. Before considering the general case, we provide a simple extension to Theorem 3.3 which allows an initial adjustment phase for the PCA-I as follows.

Theorem 4.1. *Suppose Assumption 2 holds and there exists a t_0 such that underlying graph has a spanning tree for all time $t \geq t_0$. Then, the algorithm described by (3.1) achieves a fair solution $\Gamma_i = \Gamma_j$, for all $i, j \in \mathcal{I}$.*

Proof. Reconsider the function (3.18). The derivative of $V(\mathbf{p})$ along system trajectories is computed as follows:

$$\begin{aligned}
\dot{V}(\mathbf{p}) &= \mathbf{p}^T\mathbf{B}^{-1}\dot{\mathbf{p}} + \dot{\mathbf{p}}^T\mathbf{B}^{-1}\mathbf{p} \\
&= -\mathbf{p}^T\mathbf{B}^{-1}\mathbf{B}\mathbf{I}_d^{-1}\mathbf{L}\mathbf{I}_d^{-1}\mathbf{p} - \mathbf{P}^T\mathbf{I}_d^{-1}\mathbf{L}^T\mathbf{I}_d^{-1}\mathbf{B}^{-1}\mathbf{B}\mathbf{P} \\
&= -\mathbf{p}^T\mathbf{I}_d^{-1}\mathbf{L}\mathbf{I}_d^{-1}\mathbf{P} - \mathbf{p}^T\mathbf{I}_d^{-1}\mathbf{L}^T\mathbf{I}_d^{-1}\mathbf{P} \\
&= -\mathbf{\Gamma}^T(\mathbf{L} + \mathbf{L}^T)\mathbf{\Gamma} \qquad (4.1)
\end{aligned}$$

Note that, the matrix $\mathbf{L} + \mathbf{L}^T$ represents the Laplacian of an undirected graph and Assumption 2(iii) along with Gershgorin's circle theorem guarantees that the matrix

$\mathbf{L}+\mathbf{L}^T$ has non-negative eigenvalues [79]. Hence, $\mathbf{L}+\mathbf{L}^T$ is always positive semidefinite which implies $\dot{V}(\mathbf{p})$ is non-positive even at the worst case (the case where each BS is isolated). We can conclude that the algorithm (3.1) does not diverge for $t < t_0$. Next, we need to show the convergence of the algorithm for $t \geq t_0$. It is straight forward to show $\ddot{V}(\mathbf{p}(t))$ is bounded. Since $\mathbf{L}(t)$ has a spanning tree for all $t \geq t_0$, $\mathbf{L}(t) + \mathbf{L}^T(t)$ is the Laplacian of an undirected connected graph which has 0 as a simple eigenvalue. Hence, $\dot{V}(\mathbf{p}(t))$ is negative for all $\mathbf{L}(t)$ unless $\mathbf{\Gamma}$ lies in the null space of $\mathbf{L}(t) + \mathbf{L}^T(t)$ for $t \geq t_0$. Furthermore, the kernel of $\mathbf{L}(t) + \mathbf{L}^T(t)$ is given as span$\{\mathbf{1}\}$, corresponding to consensus. This implies that the algorithm converges. □

In Theorem 4.1, the underlaying graph is required to have a spanning tree for all time $t \geq t_0$ which is a relaxation of the connected graph requirement at all times given in Theorem 3.3. In practice, the power allocation algorithms need an initial adjustment period where connections are established. Theorem 4.1 shows that the convergence properties the algorithm (3.1) are preserved under such an adjustment period. On the other hand, the underlaying graph is still required to have a spanning tree for all time $t \geq t_0$ which may not be feasible in a real system. We relax this condition by considering the imperfect connection setup where the connections between BSs are susceptible to failures. Note that, an introduction of initial adjustment period t_0 is redundant for the imperfect connection case. The initial adjustment period $[0,\ t_0)$ can be considered as a time interval defined in Assumption 3(i). Therefore, the initial adjustment period is not considered explicitly in the subsequent analysis. With this setting, the convergence results under the imperfect communication setup are stated next.

Theorem 4.2. *Suppose Assumptions 2 and 3 hold. Then, the power values for the proposed algorithm described by (3.1) are bounded.*

Proof. Reconsider (3.18) whose derivative can be computed as

$$\begin{aligned} \dot{V}(\mathbf{p}(t)) &= -\mathbf{\Gamma}(t)(\mathbf{L}(t)+\mathbf{L}^T(t))\mathbf{\Gamma}(t) \\ &= -\frac{1}{2}\sum_{(i,j)\in\mathcal{I}}^{N} c_{ij}(t)\left(\Gamma_i(t)-\Gamma_j(t)\right)^2 \end{aligned} \tag{4.2}$$

where $\mathbf{L}(t)+\mathbf{L}^T(t)=\mathbf{C}(t)=[c_{ij}(t)]_{N\times N}$ is a singular symmetric M-matrix that represents the Laplacian of a connected undirected graph and satisfies sum-of-squares property [74]. Note that when user k is disconnected from the network, $c_{kj}=c_{jk}=0,\ \forall j\in\mathcal{I}$.

Let T be a strictly increasing sequence of times $T=t_0,t_1,\ldots,t_N,\ldots$, then the *interval completion* $I(T)$ is the set

$$\bigcup_{i\in\mathbb{N}}[t_i,t_{i+1}]. \tag{4.3}$$

Denote by S, a switching sequence with an initial state, $\mathbf{p}(0)$:

$$S=(i_0,t_{i_0}),(i_1,t_{i_1}),\ldots,(i_N,t_{i_N}),\ldots, \tag{4.4}$$

where the sequence is not necessarily finite. In the finite case, $t_{i_N}=\infty$ can be chosen. Note that S and (3.20) completely describes the trajectories as for $t_{i_k}\le t\le t_{i_{k+1}}$, the system becomes

$$\dot{\mathbf{p}}(t)=-\mathbf{B}\mathbf{I}_d^{-1}(t)\mathbf{L}[t_{i_k}]\mathbf{\Gamma}(t) \tag{4.5}$$

To complete the proof, we need to show that $\dot{V}(\mathbf{p}(t))\le 0$ for all $t\in I(T)$ and $V(\mathbf{p}(t))$ is monotonically non-increasing on T, for any $S\in\mathbb{S}$, where $\mathbb{S}$ is the set of all possible switching sequences [89]. The first condition clearly follows from (4.2) and is satisfied

for all t. For the second condition, consider the following equation:

$$\int_{t_i}^{t_{i+1}} \dot{V}(\mathbf{p}(\tau))\mathrm{d}\tau = V(\mathbf{p}(t_{i+1})) - V(\mathbf{p}(t_i))$$
$$= -\int_{t_i}^{t_{i+1}} \frac{1}{2} \sum_{(i,j)\in\mathcal{I}}^{N} c_{ij}(\tau)\left(\Gamma_i(\tau) - \Gamma_j(\tau)\right)^2 \mathrm{d}\tau$$

Hence, at every interval $[t_i, t_{i+1})$ the function $V(\mathbf{p})$ decreases which implies $V(\mathbf{p})$ is bounded. However, under this setup we are not able to conclude the convergence of $\dot{V}(\mathbf{p})$ since $\ddot{V}(\mathbf{P}(t))$ is not necessarily bounded due to the discontinuities of $\mathbf{L}(t)$. □

The convergence result for the PCA-III under imperfect connection setup is stated next. Note that, for PCA-III case, the desired SINR values are also assumed to be time-varying.

Theorem 4.3. *If Assumption 2 and 3 holds, then the power values for the proposed algorithm (3.15) are bounded.*

Proof. In vector notation (3.15) can be restated as

$$\dot{\mathbf{p}}(t) = -\mathbf{B}\mathbf{Q}(t)\mathbf{L}(t)\mathbf{q}(t) \tag{4.6}$$

Consider the function (3.19), its derivative with time-varying setup can be represented as

$$\begin{aligned}\dot{V}(\mathbf{p}(t)) &= -\mathbf{e}(t)\mathbf{L}(t)\mathbf{e}(t) \\ &= -\mathbf{q}(t)\mathbf{L}(t)\mathbf{q}(t).\end{aligned}$$

However, for the general case $\mathbf{L}(t)$ is not necessarily symmetric and we need to consider,

$$\dot{V}(\mathbf{p}(t)) = -\mathbf{q}(t)\mathbf{C}(t)\mathbf{q}(t). \tag{4.7}$$

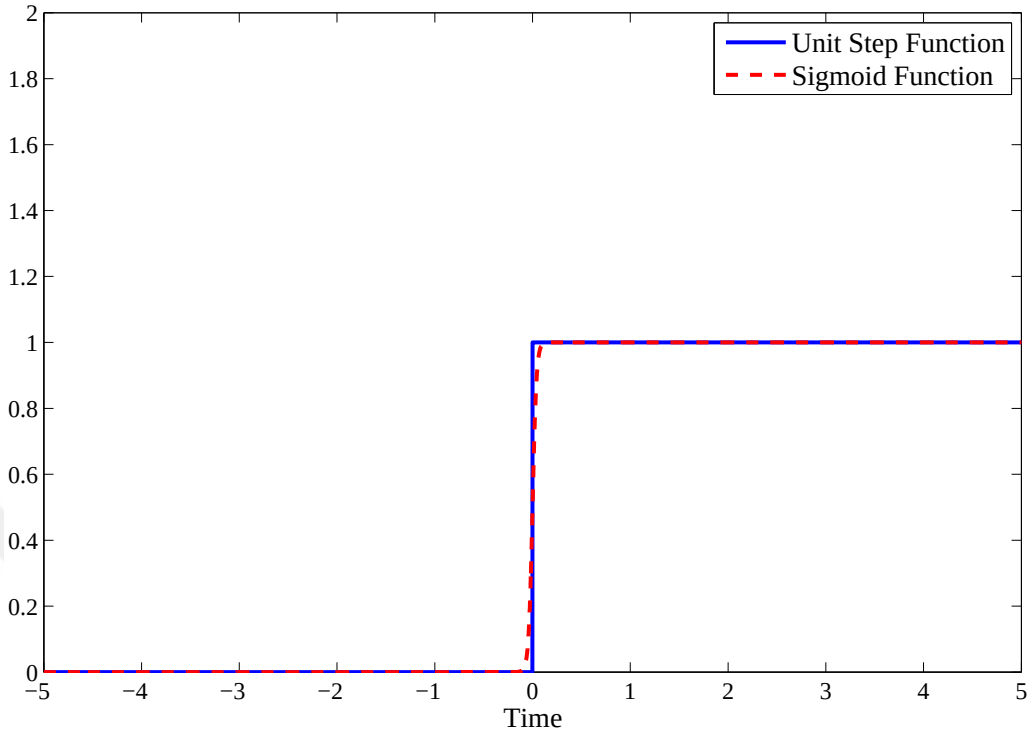

Figure 4.1. Approximation of unit step function with sigmoid function.

Similar to the previous case, $\mathbf{C}(t) = [c_{ij}]$ is the $N \times N$ matrix defined as $\mathbf{C}(t) = \mathbf{L}(t) + \mathbf{L}^T(t)$ and rest of the proof follows the same arguments. □

The problem with the analysis provided above is the discontinuities in the connection matrix. In other words we assume that $l_{ij}(t)$ values may contain unit step functions and change instantaneously. To overcome this problem, we modify our model and approximate the unit step functions with sigmoid functions as depicted in Figure 4.1. The main advantage of the sigmoid functions are that they are differentiable and by utilizing sigmoid functions the second derivative of the function can be computed which allows us to use Barbalat's Lemma. Using sigmoid functions resolves the discontinuity problem and we can use Barbalat's Lemma to show $\dot{V}(\mathbf{p}(t)) \to 0$ as $t \to \infty$, however this result does not necessarily imply convergence to a fair solution for the imperfect channel case. To guarantee the convergence to a fair solution, we require the following assumption.

Assumption 4. *The connection matrices are assumed to satisfy the following conditions:*

- $\dot{l}_{ij}(t)$ *exists and is finite for all* $i, j \in \mathcal{I}$ *and all time* $t \geq 0$.
- *There exists an infinite sequence of uniformly bounded, non-overlapping time intervals* $[t_i,\ t_{i+l})$ *for some* $\tau > 0$ *such that the union of connection matrices across each interval has a spanning tree.*

The first assumption models the time-outs in communication links with sigmoid functions and the second assumption is required to reach consensus.

Theorem 4.4. *Suppose Assumptions 2 and 4 hold. Then, the proposed algorithm described by (3.1) reaches a fair solution* $\Gamma_i = \Gamma_j$, *for all* $i, j \in \mathcal{I}$.

Proof. Reconsider (3.18) whose derivative can be computed as

$$\begin{aligned} \dot{V}(\mathbf{p}(t)) &= -\mathbf{\Gamma}(t)(\mathbf{L}(t) + \mathbf{L}^T(t))\mathbf{\Gamma}(t) \\ &= -\frac{1}{2}\sum_{(i,j)\in\mathcal{I}}^{N} c_{ij}(t)\left(\Gamma_i(t) - \Gamma_j(t)\right)^2 \end{aligned} \tag{4.8}$$

The difference is that $c_{ij}(t)$ is a continuous function and $\ddot{V}(\mathbf{p}(t))$ is bounded which allows us to conclude $\dot{V}(\mathbf{p}(t)) \to 0$ as $t \to \infty$.

Hence, at every interval $[t_k, t_{k+1})$ the candidate Lyapunov function decreases which implies that $V(\mathbf{p})$ is bounded. Furthermore, $\dot{V}(\mathbf{p})$ is equal to 0 over any time interval $[t_k, t_{k+1})$ only if $\Gamma_i(t) = \Gamma_j(t),\ \forall i, j \in \mathcal{I}$. Note that, for the imperfect connection case $\dot{V}(\mathbf{p}) = 0$ does not imply consensus is reached. However, $\dot{V}(\mathbf{p}) = 0$ over any interval defined by Assumption 4 implies consensus. Because, the union of connection matrices over the intervals contain a spanning tree $\dot{V}(\mathbf{p}) = 0$ if and only if consensus is achieved. □

The proof for the PCA-II is similar to the PCA-I case and therefore is omitted. Next, we give the result for the PCA-III algorithm.

Theorem 4.5. *If Assumption 2 and 4 holds, then the proposed algorithm (3.15) reaches a fair solution $e_i = e_j$, for all $i, j \in \mathcal{I}$.*

Proof. Reconsider the function (3.19), its derivative with time-varying setup can be represented as

$$\begin{aligned} \dot{V}(\mathbf{p}(t)) &= -\mathbf{q}(t)\mathbf{C}(t)\mathbf{q}(t) \\ &= -\frac{1}{2}\sum_{(i,j)\in\mathcal{I}}^{M} c_{ij}(t)\left(q_i(t) - q_j(t)\right)^2. \end{aligned} \tag{4.9}$$

It is straight forward to show that $\ddot{V}(\mathbf{p}(t))$ is bounded and $\dot{V}(\mathbf{p}(t)) \to 0$ as $t \to \infty$. At every interval $[t_k, t_{k+1})$ the candidate Lyapunov function decreases which implies that $V(\mathbf{p})$ is bounded. Furthermore, $\dot{V}(\mathbf{p})$ is equal to 0 over any time interval $[t_k, t_{k+1})$ only if $e_i(t) = e_j(t),\ \forall i, j \in \mathcal{I}$. Note that, for the imperfect connection case $\dot{V}(\mathbf{p}) = 0$ over any interval defined by Assumption 4 implies consensus is reached and $\dot{\mathbf{p}}(t) = 0$. □

Recall that the changes on desired SINR values is reflected via the relative error values $q_i(\mathbf{p}, t) = \Gamma_i(\mathbf{p}, t)/\gamma_i(t)$ and due to the quadratic nature of (4.7), as long as there is a minimum and maximum value for desired SINR values and $\dot{\gamma}_i(t)$ is finite, it does not effect the convergence of the proposed algorithm. This does not imply that desired SINR values have no affect on the proposed algorithm, the resulting error values are indeed affected by the values of γ_i's.

The convergence properties of the proposed algorithms presented in Chapter 3 show their ability to reach a solution for the power control problem. The analysis under imperfect channel setup reveals that the convergence properties are preserved under a setup with non-ideal links. For the problems presented in (2.8)-(2.9) and (2.16)-(2.17), we know that the proposed power algorithms converges the a solution. However, the

optimality of the solution achieved is not analyzed. The final part of the theoretical analysis contains the optimality analysis for the proposed power control algorithms and it is presented in the next section.

4.3. Optimality Analysis

In this section, the optimality of the solutions obtained by the proposed algorithms is investigated. For the problem described in (2.8)-(2.9), we show that the proposed algorithms PCA-I and PCA-II actually converges to the max-min solution defined by (2.12). Since PCA-III considers a different problem, it will be analyzed as a separate case.

Remark 4. *For mathematical tractability, an interference limited system is considered.*

For the interference limited system, SINR for user i for a given $\mathbf{p}$ is

$$\Gamma_i(\mathbf{p}, t) = \frac{p_i(t)}{\sum\limits_{j \in \mathcal{I}} z_{ij}(t) p_j(t) - p_i(t)} \tag{4.10}$$

where $z_{ij} = h_{ij}$'s are the normalized channel gains defined in (2.4) for all $i \neq j$ and $z_{ii} = 1$ for all $i \in \mathcal{I}$. Let γ^* denote the max-min solution given by

$$\gamma^* = \max\{\gamma |\ \exists\ \mathbf{p} \geq 0 : \Gamma_i \geq \gamma, \forall i\}. \tag{4.11}$$

Furthermore,

$$\gamma^* = \frac{1}{\lambda^* - 1} \tag{4.12}$$

where λ^* is the largest eigenvalue of the channel gain matrix $\mathbf{Z} = [z_{ij}]$ [90]. Note that, using bounds derived from row sums ensures $\lambda^* > 1$ [79,90]. Hence, a positive solution to the problem given in (2.8) exists.

In Sections 3.4 and 4.1, it is shown that the algorithm converges to a power vector that satisfies (2.9), which can be stated as

$$\Gamma_i(\mathbf{p}, t) = \frac{p_i(t)}{\sum\limits_{j \in \mathcal{I}} z_{ij}(t) p_j(t) - p_i(t)} = \gamma, \tag{4.13}$$

and in vector notation

$$\frac{1+\gamma}{\gamma}\mathbf{p} = \mathbf{Z}\mathbf{p}. \tag{4.14}$$

To complete the analysis, the following results from the Perron-Frobenius theorem is required:

Theorem 4.6 (see 8.3.6 in [91])**.** *For an $N \times N$ irreducible matrix $\mathbf{A} \geq 0$, each of the following is true.*

(i) $\mathbf{A}$ *has a positive real eigenvalue λ^* with algebraic multiplicity equal to* 1 *such that $\lambda^* = \max\{|\lambda_i|\}_{i=1}^N$.*

(ii) λ^* *has an associated eigenvector $\mathbf{p}^* > 0$. Furthermore, there are no nonnegative eigenvectors for* $\mathbf{A}$ *except for positive multiples of $\mathbf{p}^*$.*

The result on the optimality of the proposed algorithms is stated below.

Theorem 4.7. *If Assumption 2 holds and the algorithms (3.1) and (3.10) converge to a positive power allocation vector $\mathbf{p}^*$, then the power allocation vector $\mathbf{p}^*$ is the solution of the max-min problem (2.8) satisfying the constraint (2.9).*

Proof. Using the results from the previous section, the proposed algorithm converges to a power vector which satisfies, $\Gamma_i = \Gamma_j,\ \forall i, j \in \mathcal{I}$. By Theorem 4.6, the resulting power vector is the eigenvector (or a positive multiple of the eigenvector) associated with λ^*. For the interference limited system this is the optimal max-min solution. □

Remark 5. *For the case when noise is not ignored, increasing the power vector i.e., using a* $\alpha\mathbf{p}(t)$ *for* $\alpha > 1$*, results in a higher SINR value. The optimal power vector in this case can be obtained by using an* α *such that* $\alpha \max_{i\in\mathcal{I}} p_i = p_{max}$.

For the optimality analysis of PCA-III, an equivalent problem to the max-min problem given in (2.16)-(2.17) is introduced. Similar to the previous case, for mathematical tractability we assume thermal noise can be neglected.

An equivalent max-min problem can be defined by using q_i as determining $\mathbf{p}^*$ from

$$q(\mathbf{p}^*, t) = \max_{i\in\mathcal{I}}\min \; q_i(\mathbf{p}, t) \tag{4.15}$$

with the fairness constraint

$$\max_{i\in\mathcal{I}} \; q_i(\mathbf{p}^*, t) = \min_{i\in\mathcal{I}} \; q_i(\mathbf{p}^*, t). \tag{4.16}$$

It is clear that there exists a positive q^* which is the max-min solution defined by

$$q^* = \max\{q|\; \exists\; \mathbf{p} \geq 0 : q_i \geq q, \forall i\} \tag{4.17}$$

and a corresponding $e^* = 1 - q^*$. The equivalence of problems leads to

$$\underset{p,\; i\in\mathcal{I}}{\text{argmaxmin}} \; q_i(\mathbf{p}, t) = \underset{p,\; i\in\mathcal{I}}{\text{argminmax}} \; e_i(\mathbf{p}, t). \tag{4.18}$$

From the results of Sections 3.4 and 4.1, we deduce that the PCA-III converges to a power vector that satisfies,

$$e_i = e_j \Leftrightarrow q_i = q_j, \; \forall i, j \in \mathcal{I} \tag{4.19}$$

which can be restated in terms of SINR values as

$$\frac{p_i(t)}{\gamma_i^{des}\left(\sum\limits_{j\in\mathcal{I},j\neq i} h_{ij}(t)p_j(t)\right)} = q,\ \forall i \in \mathcal{I}. \tag{4.20}$$

In vector notation,

$$\frac{1}{q}\mathbf{p} = \mathbf{RHp}. \tag{4.21}$$

Next, the optimality result of the proposed algorithm is stated.

Theorem 4.8. *If the proposed algorithm (3.15) converges to a positive power allocation vector* $\mathbf{p}^*$*, then* $\mathbf{p}^*$ *is the solution of the max-min problem given in (2.16) satisfying the constraint (2.17).*

Proof. The proposed algorithm results in a positive power vector which satisfies $e_i = e_j,\ \forall i,j \in \mathcal{I}$, which implies $q_i = q_j,\ \forall i,j \in \mathcal{I}$. If we apply the results of Theorem 4.6 to (4.21), we can conclude that the resulting $\mathbf{p}^*$ is the eigenvector associated with the λ^* for the matrix $\mathbf{RH}$. The resulting matrix $\mathbf{RH}$ is clearly positive and will have full rank with probability one for non-degenerate cases. The λ^* is unique and also equal to $1/q^*$ corresponding to the optimal max-min solution. Using (4.18), the resulting power vector is also the max-min solution to the problem given in (2.16)-(2.17) with $e^* = \frac{\lambda^*-1}{\lambda^*}$. □

Remark 6. *Note that when* $\lambda^* > 1$, $e^* > 0$ *which implies that the system is infeasible which agrees with the analysis provided in [41], [92].*

Note that the proof relies on the convergence to a positive power vector. In the previous analysis, the proposed algorithm described in (3.15), is shown to converge to a positive power allocation vector. Hence, this condition is satisfied at all times.

4.4. Chapter Summary

This chapter concludes the theoretical analysis of this dissertation. The proposed algorithms converge to the optimal solution of the problems presented in Section 2.1. Furthermore, their ability to converge to the optimal solution is preserved under a setup with imperfect communication links. The analysis provided theoretically will be verified in the experiments and numerical results chapter. Before the numerical analysis is presented, possible future research ideas are given in the next chapter.

5. RESOURCE ALLOCATION IN HETEROGENEOUS NETWORKS

In this chapter, possible future research areas are investigated. In particular, we consider an extension of the power allocation problem and present the joint user association, frequency allocation and power control problem. A brief literature survey on the joint problem is given followed by two simple association algorithms. Then, the joint frequency power allocation problem is introduced. The joint problems are natural extensions of the power control problem and these problems will be considered as future work.

5.1. Joint User Association and Power Allocation

Efficient use of spectrum requires user association techniques to establish spectrum efficient connections. However, power control techniques along with the user association algorithms are key to achieving a good communication quality while consuming minimum system resources. The transmission powers on the links established by the user association algorithm must be adjusted in a way to maintain the required link quality without creating excessive interference on other users. The joint problem at its core is non-convex and combinatorial which makes it largely intractable [48]. On the other hand, significant gains in terms of capacity and throughput can be gained via utilizing the right combination of cell association and resource allocation [93].

One of the earliest approach to the joint user association and power allocation problem is presented in [94]. Here, base stations indicate their transmission powers in advance which allows users to compute the expected SINR level and determine the serving base station. In [95], the joint problem under fixed transmission powers is shown to be complex and methods to achieve optimal solution is proposed. In [96], user association and resource allocation problem is jointly considered and a new centralized user association scheme which favors utilizing picocells, is presented. Another user

association technique introduced in [97] uses The Jain's fairness index (JFI) [98] as a performance metric. Association is carried out based on the received signal strength plus an offset parameter which is dynamically adjusted during the association process.

In this section, we focus on user association problem along with power control problem. An important objective of the user association algorithms is to balance the load on base stations. One of the key advantages of heterogeneous networks is their ability to take the load from macrocell base station and distribute the user load to smaller cells. However, such an approach requires different metrics than received signal strength to be utilized by user association algorithms. Since macrocell base stations are capable of providing higher transmission powers compared to smaller cells, a user association algorithm should not only consider the received signal strength to accomplish load balancing [99].

Consider a system with N BSs, indexed by $j \in \mathcal{I} = \{1, \ldots, N\}$. These BSs provide service to N users, labeled by $i \in \mathcal{I} = \{1, \ldots, N\}$. Let $d_i \in \mathcal{I}$ denote the BS that user i is transmitting to and $\mathbf{d} = [d_1, \ldots, d_N]$ be the allocation vector. We assume single BS association and leave multi BS association problem for future work. Furthermore, the set of BSs that a user can transmit to is a subset of $\mathcal{I}$ due to restrictions of the network. These restrictions may be due to geometry of the network, load on BS, etc., and are irrelevant from a theoretical point. Let $W_i \subseteq \mathcal{I}$ be the set of base stations that user i is allowed to connect to and define the allocation vector for a given set as

$$\mathbf{d}(W) \equiv \{\mathbf{d} = \{d_1, \ldots, d_N\} : d_i \in W_i,\ i = 1, \ldots, N\}. \tag{5.1}$$

We use $\Gamma_i(\mathbf{p}, \mathbf{d}(W), t)$ to denote the SINR value of user i for a given association $\mathbf{d}(W)$.

The SINR value or a function of it is commonly utilized as a metric for the quality of service. Usually a logarithmic function based on the SINR value achieved by a user is utilized. This is due to the fact that the achievable data rate for user i under additive

white Gaussian noise (AWGN) model is a function of the SINR value, given by

$$r_i = Y\log(1+\Gamma_i) \tag{5.2}$$

where Y is a constant based on the bandwidth allocated.

The traditional cell association and power control problem is to find an association vector $\mathbf{d}(W)$ and power vector $\mathbf{p}$ which satisfies

$$\Gamma_i(\mathbf{p}, \mathbf{d}(W), t) \geq \gamma_i, \quad i = 1, \ldots, N \tag{5.3}$$

where γ_i is the desired SINR value for user i. Recent approaches consider different problems such as maximizing a utility function which is preferably concave and monotonically increasing component-wise. There are many approaches in literature which use the logarithmic utility function defined as $U(r_i) = log(r_i)$, [99]- [100] or a modified version of the logarithmic function [101]. A somewhat different approach considers the problem of minimizing the total of the reciprocal of SINR values [102].

The emerging applications require different data rates which results in heterogeneous QoS requirements for users. Therefore the traditional approach of maximizing the overall throughput or utility functions based on throughput values is obsolete. Providing a higher data rate than required to a user on conversational voice communication, can maximize the overall throughput of the network, while leaving a video-streaming user with insufficient signal quality. Even though the shape of the logarithmic function introduces an inherent fairness, designing an algorithm based on the heterogeneous requirements of users is essential for an effective resource allocation.

The conditions for the existence of a positive $\mathbf{p}(t)$ and $\mathbf{d}(W)$ such that (5.3) can be satisfied simultaneously are well understood in the literature. Consider the channel gain matrix defined by (2.4), the system is feasible if $\rho(\mathbf{RH})$ is less than 1 as shown in Chapter 2. This condition on eigenvalue is the necessary and the sufficient condition for

the feasibility of the power control problem. The desired SINR values along with the channel gains determines the spectral radius of the matrix **RH**. The difference in this case is that BS user association determines the **H**.

Some important properties of **RH** and its spectral radius are given below:

Property 2. $\rho(\mathbf{RH})$ *is a non-decreasing function of the number of users.*

The result follows directly from [79, Corollary 8.1.20] and implies that an infeasible system can always be managed via removing users from the system. In traditional networks removing users may be a viable solution as the links with SINR values lower than the desired SINR are considered unusable. Such an approach is not suitable for future heterogeneous networks due to the emerging applications which can operate at different data rates. Furthermore, a user or BS may access resources in different slots to attain a target data rate, where the slots may correspond to frequency and time resource. Hence, the definition of an unusable link due to not achieving a particular SINR value is obsolete.

Property 3. $\rho(\mathbf{RH})$ *is a non-decreasing function of* $\mathbf{R}$.

Since **RH** is a non-negative matrix, property 3 follows directly from [79, Corollary 8.1.18]. The result implies that an unfeasible system may be transformed into a feasible system by reducing the target SINR values. This approach is utilized in [41] to overcome feasibility problem via reducing the target SINR values of femtocells iteratively. However, such an approach may result in inferior signal quality for some of the users in the system. This is preferable compared to labeling the link as unusable and dropping the user as emerging applications are able to operate at various data rates.

In practical cellular systems, user association rules are typically based on physical layer parameters without any considerations to other performance issues such as load balancing [48, 96]. Two very simple user association algorithms that are widely utilized

in the literature is as follows:

(i) Received Signal Power: A user is associated with the base station which provides the highest signal power. To achieve this, user i computes

$$j = \underset{k \in \mathcal{I}}{\operatorname{argmax}} P_k g_{ik} \tag{5.4}$$

and connects to jth base station.

(ii) Channel Gain Based [103]: In this association setup, user i connects to the base station j, where

$$j = \underset{k \in \mathcal{I}}{\operatorname{argmax}} g_{ik}. \tag{5.5}$$

g_{ij} is the channel gain between user i and base station j.

Comparing the performance of the proposed user association algorithms with these two association approach is a common practice in the literature. Note that, the user association algorithms presented in this part are very simple to implement. However, performance metrics such as overall capacity, load balancing are not considered.

5.2. Joint Frequency-Power Allocation Problem

Another important problem is frequency-power allocation in heterogeneous networks. In OFDMA (Orthogonal Frequency Division Multiple Access)-based networks spectrum is partitioned into sub-channels which are allocated to users. Hence, the problem is also referred as the joint subchannel assignment and power control problem in the literature [61]. It is usually assumed that the interference between different subchannel can be neglected. Let $\mathcal{K} = \{1, \ldots, K\}$ be the set of all orthogonal subchannels

which are available to the users. Let o_{ik} be the decision variable defined by

$$o_{ik} = \begin{cases} 1, \text{ if subchannel } k \text{ is assigned to user } i \\ 0, \text{ otherwise} \end{cases} \tag{5.6}$$

and assume that each subchannel can be assigned to at most 1 user by its serving BS. Similar to the user association problem the SINR value achieved by a user depends on the subchannel assignment. Let $\mathbf{O} = [o_{ik}]$ be the $N \times K$ subchannel allocation matrix, then the SINR achieved by a user i over subchannel k is

$$\Gamma_i^k(\mathbf{p}^k, \mathbf{O}, t) = \frac{o_{ik} g_{ii}^k(t) p_i^k(t)}{\sum\limits_{j \in \mathcal{I}, j \neq i} o_{jk} g_{ij}^k(t) p_j^k(t) + v_i^k(t)} \tag{5.7}$$

where g_{ij}^k is the channel gain between BS j and user i over subchannel k; p_i^k is the transmission power of BS i over subchannel k; $v_i^k(t)$ is the thermal noise experienced by the user i on subchannel k. The total SINR value achieved by a user is sum of its SINR values over subchannels assigned to the user and each user aims to reach a target value,

$$\sum_{k=1}^{K} \Gamma_i^k(\mathbf{p}^k, \mathbf{O}, t) \geq \gamma_i. \tag{5.8}$$

The joint frequency-power allocation problem is determining $\mathbf{O}$ and $\mathbf{p}^k$'s such that every user achieves its target SINR requirement. Usually, the QoS requirements are given in terms of achievable data rate of users which can be computed by utilizing the SINR values in (5.2) [60,66]. The problems presented here can be considered along with power control problem which results in more complex problems compared to the stand alone allocation problems. The joint problems are a natural extension for the power control approaches presented in this thesis and are left as future work.

5.3. Chapter Summary

In this chapter, we briefly intrduced the joint user association, frequency allocation and power allocation problem. The work presented in this chapter will be considered as a part of future research direction. In the next chapter, we present the numerical analyses for the power control algorithms. For the power control approaches presented in this dissertation, we assume that the base station user association and subchannel assignment is carried out by a preceding process and we focus on the power control part of the general resource allocation problem.

6. EXPERIMENTS AND RESULTS

In this chapter, the numerical analysis for the proposed algorithms given in Chapter 3, is presented. The simulations are carried out using two different channel models. In the first model, Rayleigh fading and lognormal shadowing effects are not modeled, whereas the second model considers both slow and fast fading. A simulation setup consisting of one macrocell with radius R_c with underlaid N_f femtocells with radius R_f is utilized for the numerical analysis [41]. Each BS is assumed to serve a single user at a given slot. Extensions to MIMO systems are left as future work.

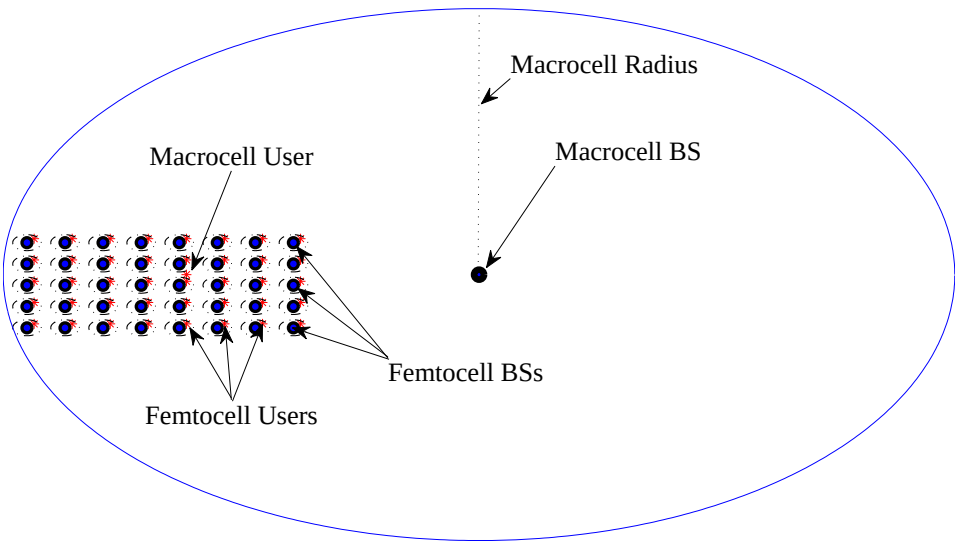

Figure 6.1. An example simulation setup with grid distribution

Figure 6.1 shows an example setup with 40 femtocell base stations [83, 85]. We used a grid based placement for femtocell BSs for comparison concerns. Such a setup allows other researchers to easily simulate and use our proposed algorithms for comparison. A random distribution of base stations is utilized in [84, 86]. An example setup with 40 randomly distributed small cell base stations is shown in Figure 6.2.

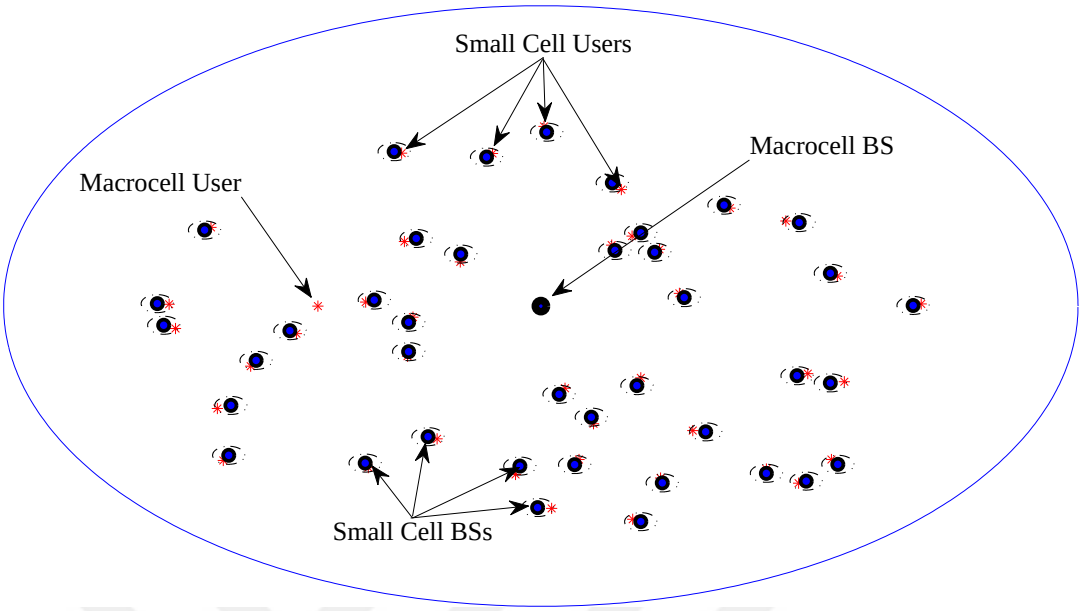

Figure 6.2. An example simulation setup with random distribution

The analysis given in Chapter 3 reveals that the convergence properties of the proposed power control algorithms are independent of the channel gains. However, the resulting SINR solution for the PCA-I and PCA-II, or the resulting error value for the PCA-III depends on channel gains.

For the simulations, the discrete time versions of the proposed power update algorithms are utilized. Algorithm 6.3 illustrates the pseudocode of the algorithm described by (3.9). The pseudocode for other algorithms is similar to the one presented with a difference in power update rule at step 5. For the simulations discrete time version of the algorithms is employed as it is not possible to utilize a continuous time power control algorithm in a real system.

6.1. Channel Models

In this section, two different channel models that are used for the simulations are introduced. The first model (referred as Setup-1) utilizes the simplified path loss model described in [104]. For all users $D_{ref} = 1$ meter is assumed. The path loss model is

1: Initialize $k \leftarrow 1$, $\mathbf{p} \leftarrow \mathbf{p}_{max}$ // Initialize initial transmission powers and iteration number.
2: **while** $k \leq$ MAXITER **do**
3: Each BS determines its neighbor set N_i.
4: Each BS exchanges its users SINR value Γ_i with its neighbors.
5: Each BS updates its transmission power according to $p_i[k+1] = p_i[k] - \beta_i \frac{\Gamma_i[k]}{p_i[k]} |N_i| [\Gamma_i[k] - \frac{1}{|N_i|} \sum_{j \in N_i} \Gamma_j[k]]$, for all $i = 1, 2, \ldots, N$.
6: $k \leftarrow k + 1$
7: **end while**

Figure 6.3. Power update algorithm example

given as

$$PL_{ij} = \begin{cases} K_c + 10\alpha_c \log(D_{ij}), & i = j = 1 \\ K_{f_i} + 10\alpha_i \log(D_{ij}), & i = j > 1 \\ K_c + \phi + 10\alpha_{f_o} \log(D_{ij}), & i = 1, \quad j > 1 \\ K_{f_o} + \phi + 10\alpha_c \log(D_{ij}), & i > 1, \quad j = 1 \\ K_{f_o} + 2\phi + 10\alpha_{f_o} \log(D_{ij}), & i \neq j, \quad i, j > 1 \end{cases}$$

where D_{ij} represents the distance between user j to BS i and PL_{ij} represents the path loss between user j and BS i. $\alpha_c, \alpha_i, \alpha_{f_o}$ denote the path loss exponents for cellular, indoor, and indoor to outdoor transmissions respectively. The first term is used to model the path loss between macrocell BS and its user. Here $K_c = 30\log_{10}(f_c) - 71\text{dB}$ is the fixed decibel propagation loss during cellular transmission to macrocell BS, where f_c is the carrier frequency in MHz. The second term represents the path loss between a small cell BS i and its user. K_{f_i} is the fixed loss between a femtocell user and its BS. The third term is the path loss between macrocell BS and a small cell user. ϕ term models wall penetration loss during indoor to outdoor (or outdoor to indoor) propagation. The fourth term is the path loss between a small cell BS and macrocell user. Here, K_{f_o} denotes the fixed loss between small cell BS i and another user. We assume $K_{f_o} = K_c$ in simulations. The final term represents the channel gain between

Table 6.1. System Parameters for Setup-1

Symbol	**Parameter**	**Value**
R_c	Macrocell Radius	1000 m
R_f	Femtocell Radius	30 m
α, α_i	Path loss exponents	4(outdoor),3(Indoor)
$P_{f,max}$	Maximum transmit power of femtocells	23dBm
$P_{m,max}$	Maximum transmit power of macrocell	43dBm
f_c	Carrier frequency	3000MHz
K_{f_i}	Indoor Loss	37 dB
ϕ	Wall Penetration Loss	3, 10 dB
N_{max}	Maximum Number of Neighbors	5
D_{max}	Maximum Connection Distance	100 m

a small cell BS and a user connected to another small cell. The path loss exponents α_c and α_{f_o} are assumed to be equal and will be referred as α in the rest of the thesis. Note that path loss exponent for indoors, α_i, is only used to model the path loss between a small cell BS and its user. Outdoor path loss exponent is used for the case of path loss between a small cell BS and a user connected to another small cell. In the simulations, it is assumed that the neighbor set of a BS consists of at most N_{max} BSs with a distance less than D_{max}. The choice of neighboring cells has no effect on the convergence properties of the proposed algorithms. However, the underlying communication graph needs to be connected. For all simulations a time step of 10ms is used (i.e., number of iterations is 1200 for a duration of 12 seconds). The rest of the simulation parameters are summarized in Table 6.1. This model is utilized in [83, 85].

The second channel model (referred as Setup-2) is utilized in [84,86]. For a transmission from a BS at position x with power P_X, the received power at location y is $P_X H_{X,Y} S_X L_{X,Y}$ [105]. H is used to model Rayleigh fading with unit average power, i.e., $H \sim exp(1)$. S_X denotes the lognormal shadowing term with standard deviation σ.

Table 6.2. System Parameters for Setup-2

Parameter	**Value**
Path loss exponent (α)	3.5
Maximum transmit power for tier-1 ($P_{1_{max}}$)	43 dBm
Maximum transmit power for tier-2 ($P_{2_{max}}$)	33 dBm
Maximum transmit power for tier-3 ($P_{3_{max}}$)	23 dBm
Lognormal standart deviation (σ)	8 dB
Carrier frequency (f_c)	2000MHz
Penetration Loss (ϕ)	10 dB
Sampling Period (T_s)	0.01s
Algorithm speed parameter (β_i)	1

Finally, $L_{X,Y} = K_c d(X,Y)^{-\alpha}$ represents the path loss with path loss exponent α and distance between X and Y is shown with $d(X,Y)$. $K_c = 30\log f_c - 71 + \phi$ dB is the constant propagation loss, f_c is the carrier frequency and ϕ is the penetration loss. The values of simulation parameters are summarized in Table 6.2. Note that, setup-2 is defined for a 3-tier heterogeneous network and maximum transmission power for only 3 different types of base stations is defined in Table 6.2. The proposed control algorithms allow the extension to multiple tiers in straight-forward manner via defining a new tier of base stations with different characteristics. The main difference between two setups is the Rayleigh fading and lognormal shadowing coefficients. These coefficients are utilized to model the fast and slow fading terms on the channel gains. Rayleigh fading models the fast changes on the channel gains whereas lognormal shadowing models the slow fading. The convergence properties of the proposed power control algorithms are independent of channel gains. However, the second model is more realistic and gives better results in the simulations.

6.2. Fairness Metrics

In this part, the fairness metrics that are used to assess the performance of the power control algorithms are introduced. Two different fairness indices, namely Jain's fairness index and Atkinson index, are utilized. The performance analysis is carried out under different spectrum allocation schemes along with varying number of users.

The Jain's fairness index (JFI) [98] is a fairness criterion that has been widely used for resource allocation [67, 106]. JFI is given by

$$JFI = \frac{\left(\sum_{i=1}^{N} \Gamma_i\right)^2}{N \sum_{i=1}^{N} \Gamma_i^2}. \tag{6.1}$$

The value of JFI changes between 1 and $1/N$ corresponding to best and worst case of fairness, respectively. For any power allocation satisfying the fairness constraint given in (2.9) or (2.17), the JFI will have a value of 1.

The Atkinson index (AI) introduced by [107] as an economical fairness metric, is another fairness index which has been used for computing the fairness performance of resource allocation algorithms [108]. AI is defined by

$$AI = \begin{cases} 1 - \frac{1}{\mu}\left[\frac{1}{N}\sum_{i=1}^{N} \Gamma_i^{1-\epsilon}\right]^{1/1-\epsilon}, & 0 \leq \epsilon \neq 1, \\ 1 - \frac{1}{\mu}\left[\prod_{i=1}^{N} \Gamma_i\right]^{1/N}, & \epsilon = 1. \end{cases} \tag{6.2}$$

Here, μ denotes the average SINR value achieved by users and N is the number of users. ϵ is a positive parameter which determines the sensitivity of the measure to higher or lower values for the given distribution. For values of ϵ around 0, the distribution of higher values have more weight in the AI value and as ϵ increases the weight of lower values increases. The best value of the AI is 0 corresponding to perfect fairness and the worst case is represented by an AI value of 1.

6.3. Simulation Results

This section includes the simulation results for the proposed algorithms. First, the numerical analysis of the PCA-I is presented, followed by the simulations for the PCA-II and PCA-III.

6.3.1. Numerical Analysis for PCA-I

The numerical analysis for the first proposed power control algorithm defined by (3.1) is presented in this section.

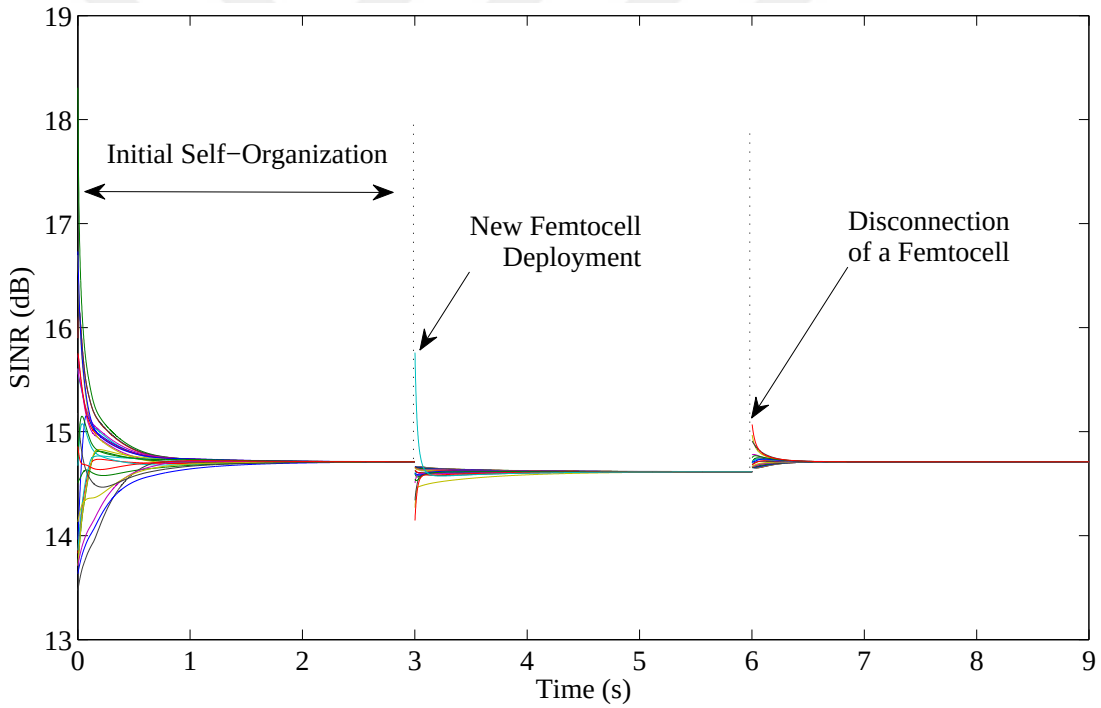

Figure 6.4. An example of SINR change under split spectrum setup

In Figure 6.4, a split spectrum setup example for a two-tier heterogeneous network with 25 femtocell users is illustrated where self-organizing properties of the power control algorithm are presented. The femtocell BSs are initialized at maximum power and by employing the power control algorithm, BSs adjust their transmission power in

a way that results in equal SINR value for each user. Note that initially, some of the users has inferior signal quality which is improved by employing the power control algorithm. After the initial self organization, a new femtocell BS is deployed with maximum transmission power which creates additional interference to existing femtocell BSs. By utilizing the SINR information from its neighboring BSs, the new deployed BS adjusts its transmission power and the system reaches consensus at a new SINR value. Note that, the adjustment period for a new femtocell deployment is shorter compared to the initial self organization period. Finally, the change of SINR values when a femtocell BS disconnects from the network is shown. As expected, the remaining femtocell BSs achieve a higher new consensus value after the disconnection of a femtocell BS.

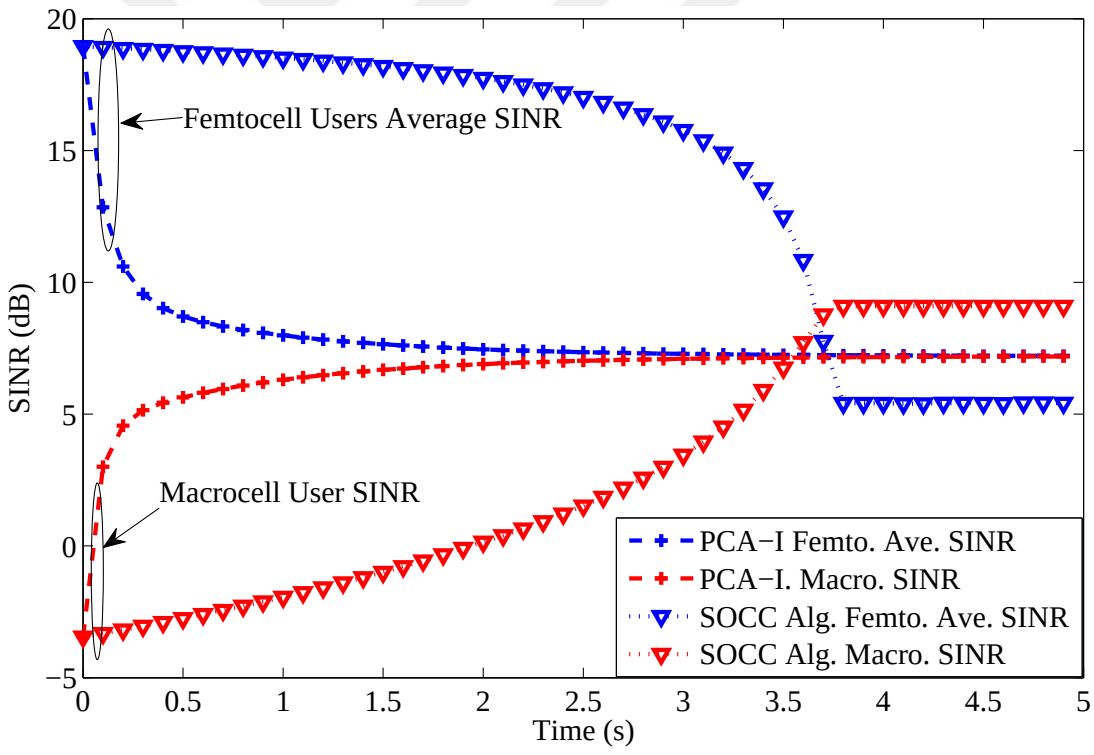

Figure 6.5. Comparison of the PCA-I with the SOCC algorithm

In Figure 6.5, comparison of the PCA-I with the SOCC algorithm under a shared spectrum setup is presented [70]. The change of the average SINR values for femto BSs and macro BS are shown for both methods. The PCA-I leads to a fair equilibrium SINR

level that is higher for the femtocell BSs than the SINR value achieved by the femto BSs using the SOCC algorithm. A predetermined threshold value $\Gamma_{th} = 5.41$dB defined in [70] is used for the SOCC algorithm. An important drawback of using a predetermined threshold is that if the threshold value is not feasible, the algorithm diverges and the test for the feasibility of a specific value requires the knowledge of channel gains. This is a drawback of the majority of the approaches in the literature, as feasibility for a given set of target SINR values are not known in a practical system. The proposed power control algorithms in this thesis are shown to converge independent of the channel gains without any feasibility concerns.

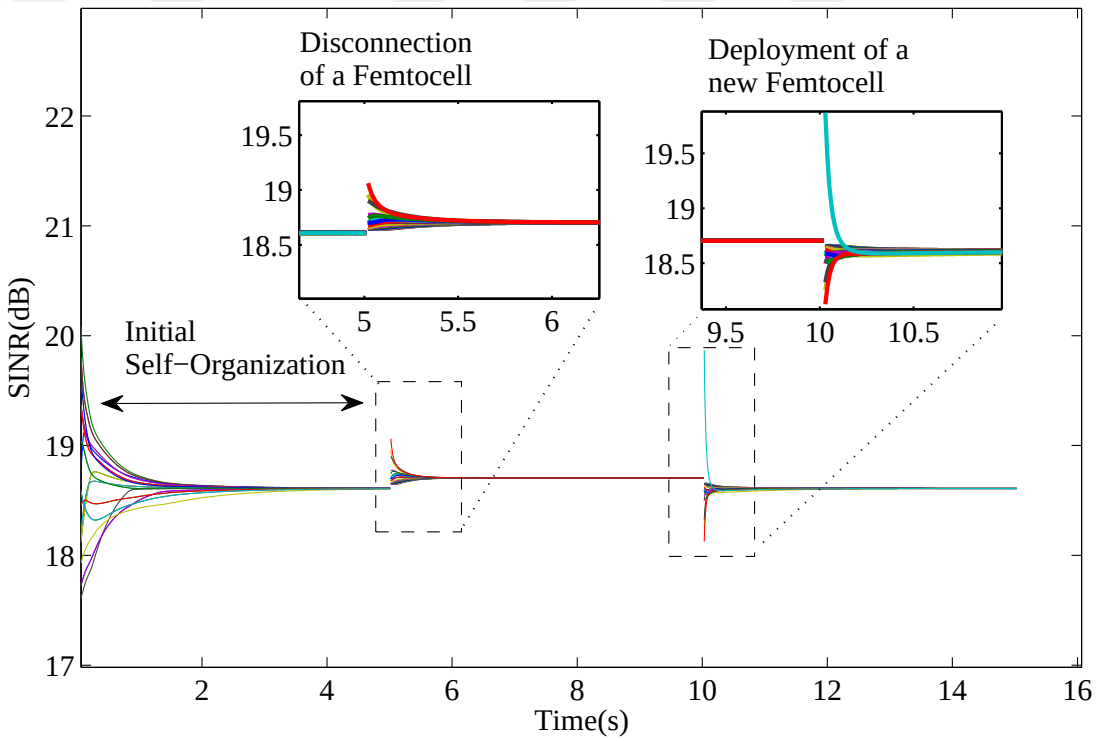

Figure 6.6. Self-organization of femtocells under split spectrum setup.

In Figure 6.6, another example which depicts the self-organizing properties of the proposed algorithm under split spectrum setup for a two-tier femtocell-macrocell network is shown. There are 27 randomly distributed femtocell users initially. All BSs are initialized with maximum power. Using the proposed algorithm, the BSs with higher SINR values compared to its neighboring users decrease their transmission powers and

vice versa, until an equal SINR value is attained. After initial self organization a femtocell is disconnected from the system, which reduces the interference created in the system. As expected, the remaining femtocells achieves consensus at a higher SINR value. An important aspect is that the adjustment period after a disconnected femtocell BS is shorter compared to initial self organization period. Finally, the change after a new femtocell BS is deployed is shown. The new femtocell starts with maximum initial power which reduces the SINR values of the existing femtocells. The newly deployed femtocell starts communicating with other femtocells and the system reaches consensus. Note that the adjustment period is faster compared to initial self-organization period again, which is crucial, because in practice a new femtocell should adjust to an existing network as quick as possible.

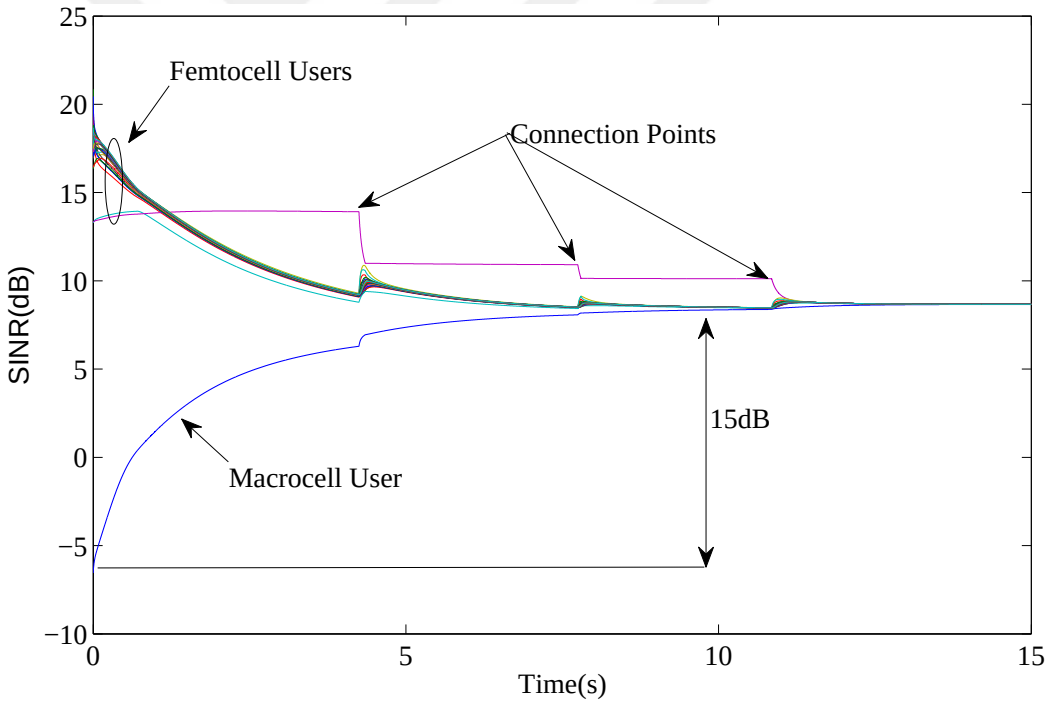

Figure 6.7. Simulation results with imperfect connections: Shared spectrum setup.

An example simulation for the PCA-I under a shared spectrum setup for a two-tier femtocell-macrocell network with imperfect communication setup is given in Figure 6.7. Note that initially the macrocell user has an inferior signal quality, despite its BS transmitting at maximum power. After employing the proposed algorithm, the powers

are adjusted such that every user achieves the same SINR value. This is especially beneficial for macrocell user as it is the user with the inferior signal quality. Furthermore, to simulate the imperfect connections, one of the femtocell BS only sends and receives information at certain intervals shown as connection points in Figure 6.7. During isolation, the transmission power is constant, which results in a slight increase in SINR value due to reduced interference. During connection intervals, the user rapidly adjusts to the system and short periods of connection results in consensus. An important point is that while one of the base station is isolated, the remaining base stations still adjusts their powers and treat the interference from the isolated base station as noise.

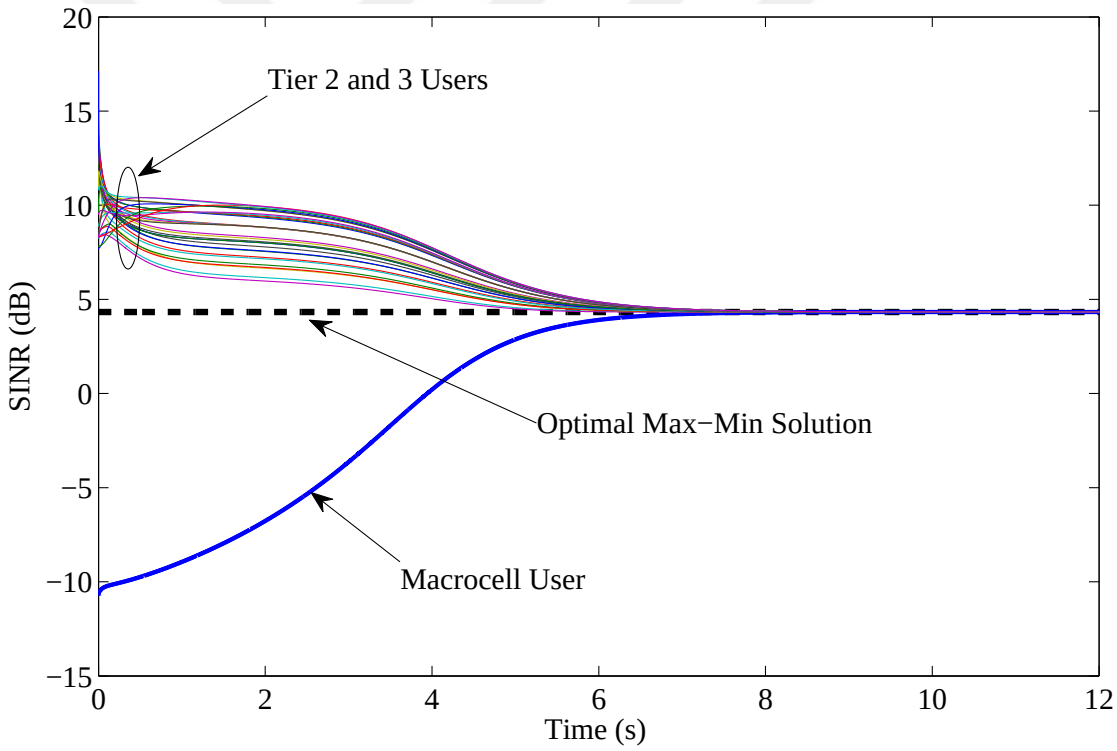

Figure 6.8. Shared spectrum example setup with 3 tiers of BSs.

To demonstrate the optimality of the PCA-I, a 3 tier setup is used as depicted in Figure 6.8. The example shows the SINR change for a total of 33 users, with 11 tier 2 and 21 tier 3 BSs with the specifications given in [109]. Initially tier 1 user (macrocell user) has inferior signal quality whereas tier 2 and 3 (picocells and femtocell) users have

higher SINR values, favoring tier 3 users. Using the proposed algorithm the SINR values converges to the optimal max-min solution obtained by (4.12). This example shows the capability of the proposed algorithm on reaching the max-min solution without any information on channel states.

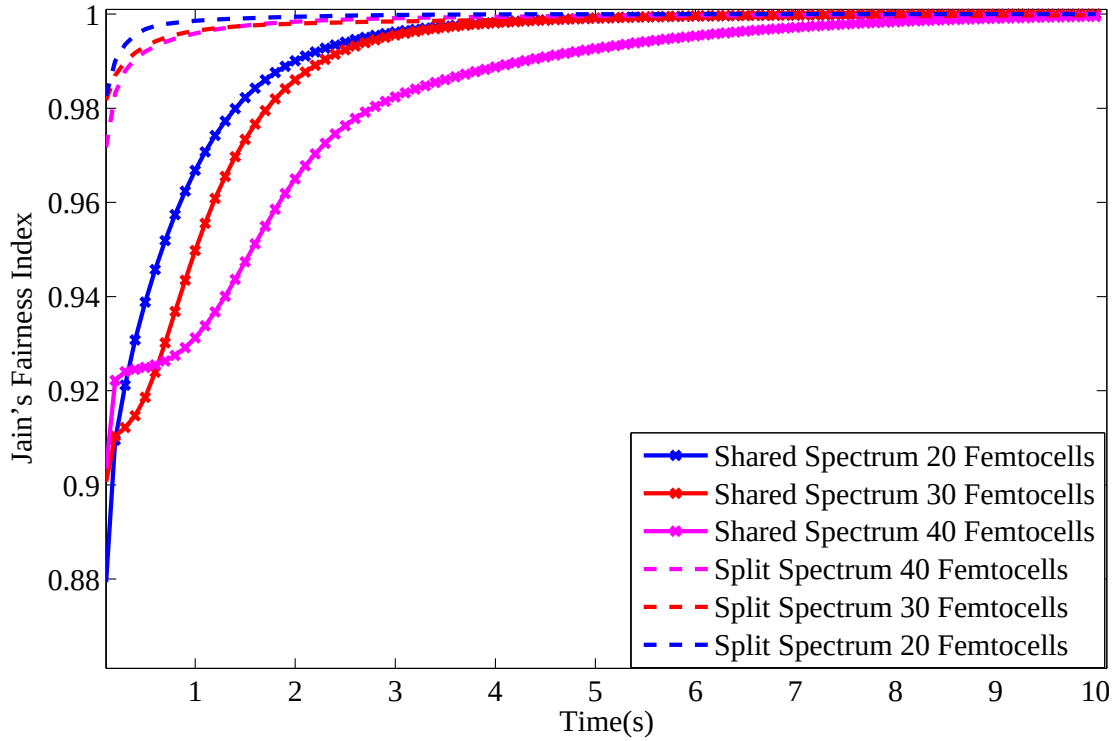

Figure 6.9. Fairness analysis of the PCA-I using Jain's Fairness Index.

The fairness performance of the PCA-I under Jain's fairness metric is depicted in Figure 6.9. The simulations are carried out split and shared spectrum setups for different number of femtocell base stations. The simulation results are in agreement with the theoretical analysis and shows the ability of the PCA-I to achieve perfect fairness. Every simulation converges to a final state where JFI is equal to 1, for both shared and split spectrum setups and independent of the number of users. However, the speed of convergence is reduced with increasing number of users and as seen in Figure 6.9, split spectrum setup converges faster compared to shared spectrum setup; this is to be expected due to the initial inferior signal quality of the macrocell user.

The simulation results for fairness analysis using Atkinson's index with two different ϵ values are illustrated in Figures 6.10 and 6.11 with $\epsilon = 1$ and $\epsilon = 0.5$, respectively. Under a shared spectrum setup, the fairness performances of the PCA-I and the SOCC algorithm are evaluated for different number of femtocell base stations. Figure 6.10 illustrates the resulting AI values with $\epsilon = 1$, The PCA-I achieves perfect fairness which concurs with the fairness performance results using Jain's Fairness Index. The SOCC algorithm gives comparable results, as it utilizes the same target SINR value for all the small cell base stations. However, due to macrocell user the SOCC fails to achieve perfect fairness. Another important advantage of the PCA-I is the convergence rate which is shown to be exponential.

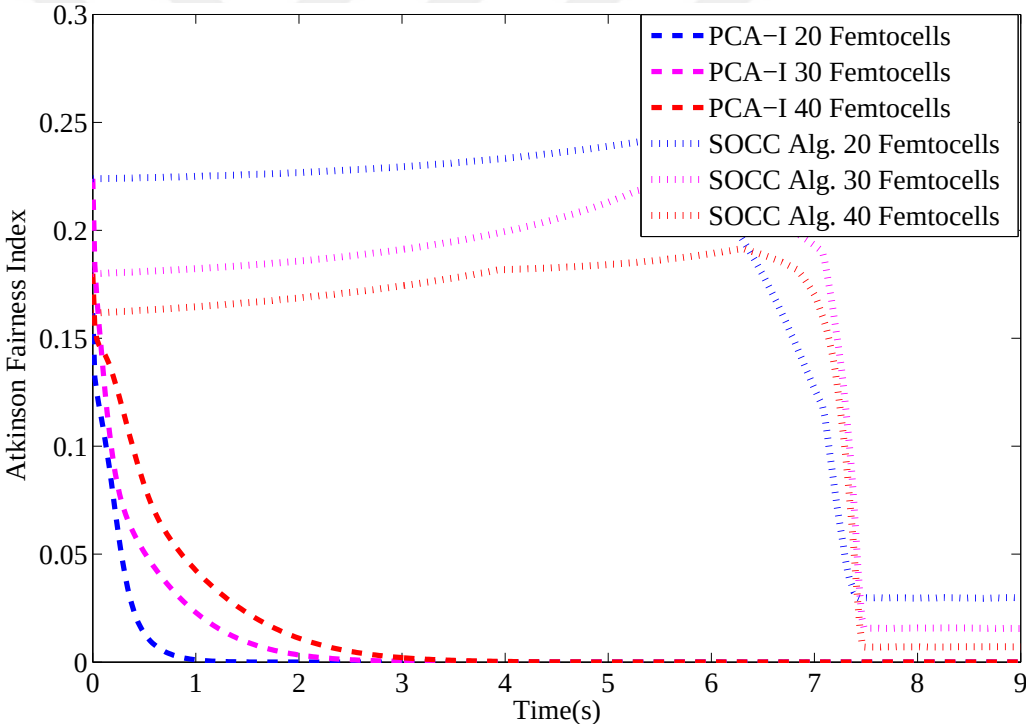

Figure 6.10. Evaluation of fairness based on Atkinson Index ($\epsilon = 1$).

The fairness performance results utilizing Atkinson's Index with $\epsilon = 0.5$ is depicted in Figure 6.11. The resulting performance of both the PCA-I and SOCC algorithms are similar to the case with $\epsilon = 1$. The performance difference between two algorithms lessens ϵ decreases as a result of giving less weight to lower SINR values.

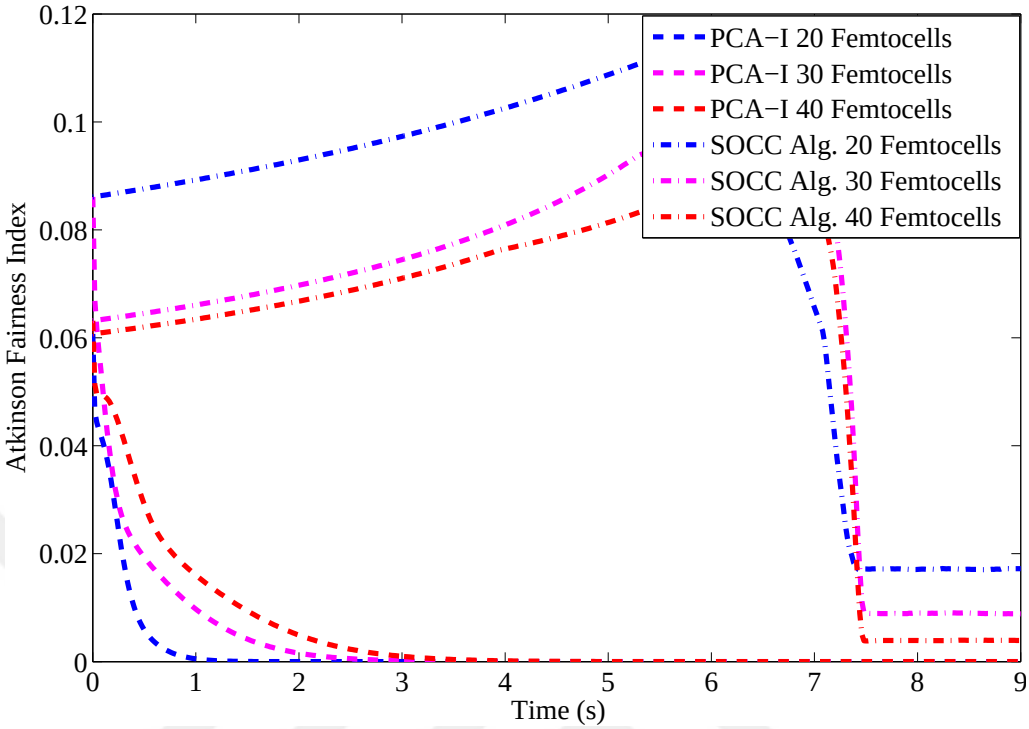

Figure 6.11. Evaluation of fairness based on Atkinson Index ($\epsilon = 0.5$).

The numerical analysis presented for the PCA-I shows the algorithms ability to reach the optimal solution of the problem presented in (2.8)-(2.9) under imperfect channel conditions. Furthermore, the self-organizing properties along with its ability to reach perfect fairness are exhibited. Next, we analyze the effect of two important parameters, namely D_{max} and N_{max} on the convergence of the PCA-I. N_{max} parameter is an upper limit on the maximum number of users that can be in the neighbor set of a user and D_{max} determines the maximum distance between two users to be considered as neighbors.

The change on SINR values with different N_{max} values is depicted in Figure 6.12. An important point is that the convergence of the algorithm is not effected by the N_{max} value, however the speed of convergence is. Using a larger value of N_{max} results in a slower convergence rate as for the fixed D_{max} value the number of neighbors that can send information is fixed, and with a large N_{max} these values are utilized with a

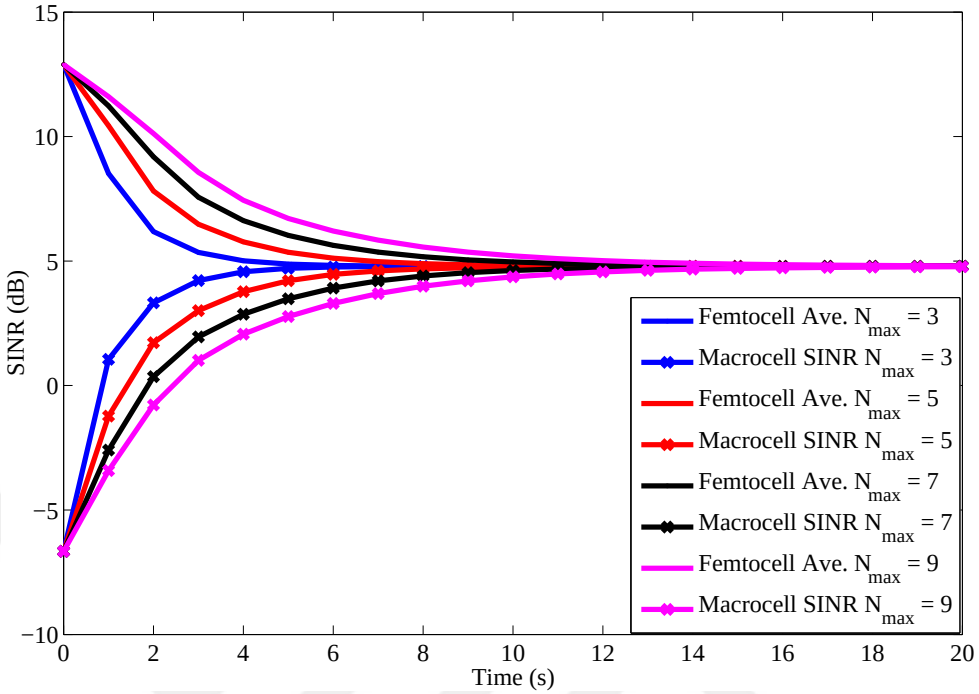

Figure 6.12. The effect of N_{max}.

smaller scaling term which results in a slower convergence rate. The numerical analysis shows that utilizing higher weights for the information received from other users results in a faster convergence. Note that, the numerical analysis agrees with the theoretical analysis provided in Section 3.4.1.1. The solution converged by the PCA-I is independent of the N_{max} value which is to be expected as the PCA-I is shown to achieve the optimal max-min solution.

Figure 6.13 illustrates the effect of changing D_{max} values under a fixed N_{max} value of 8. Similar to the previous case, the value of D_{max} does not change the convergence properties of the algorithm nor the solution obtained, but it effects the convergence rate. The convergence speed of the algorithm increases with increasing D_{max}, which indicates the significance of utilizing the available SINR values. As users are able to communicate with more users and obtain more information on SINR values, the convergence rate increases. The analysis given in Section 3.4.1.1 shows that the convergence rate scales with algebraic connectivity, i.e., second smallest eigenvalue of the connection

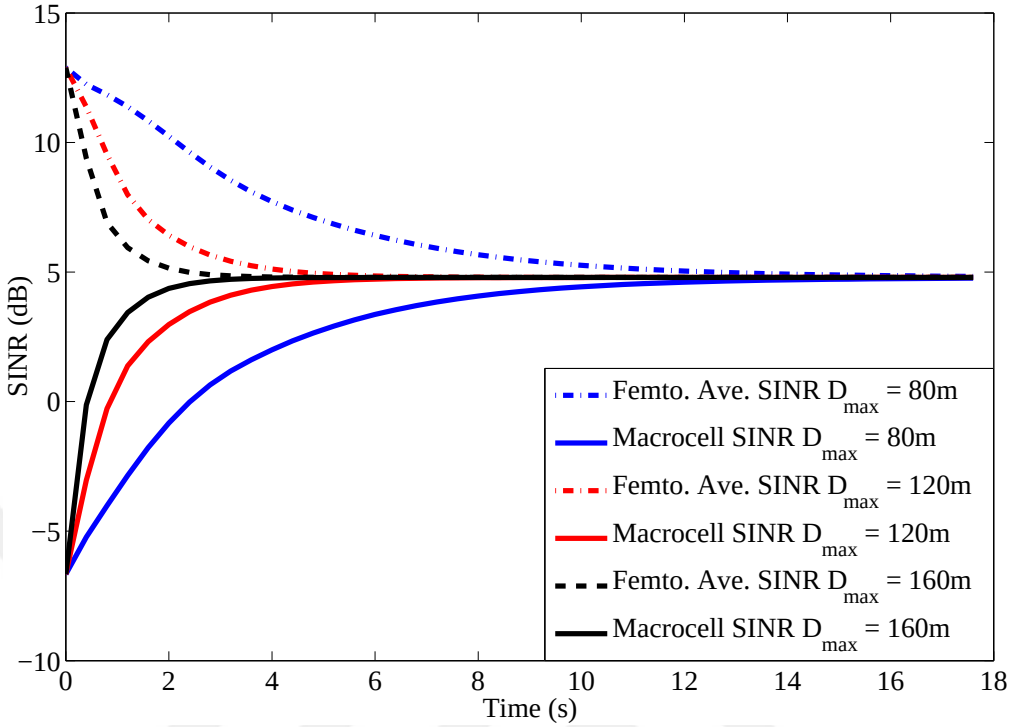

Figure 6.13. The effect of D_{max}.

matrix. Hence, a greater D_{max} results in a more connected graph which in turn increases the convergence rate of the proposed algorithm.

6.3.2. Numerical Analysis for PCA-II

The simulations for the PCA-II algorithm is carried out using the parameters given in Table 6.1. The discrete-time algorithm described by (3.13) is utilized for the simulations.

The change on SINR values in a two-tier system after employing the PCA-II is depicted in Figure 6.14 which also shows the self organizing nature of the proposed algorithm. After consensus is achieved, 5 more femtocell BSs are activated with maximum power. The activation of new BSs reduce the signal quality of other users in the system; the effect is especially apparent for the macrocell user. After the new femtocell BSs connect to the underlying network and apply the proposed algorithm, consensus

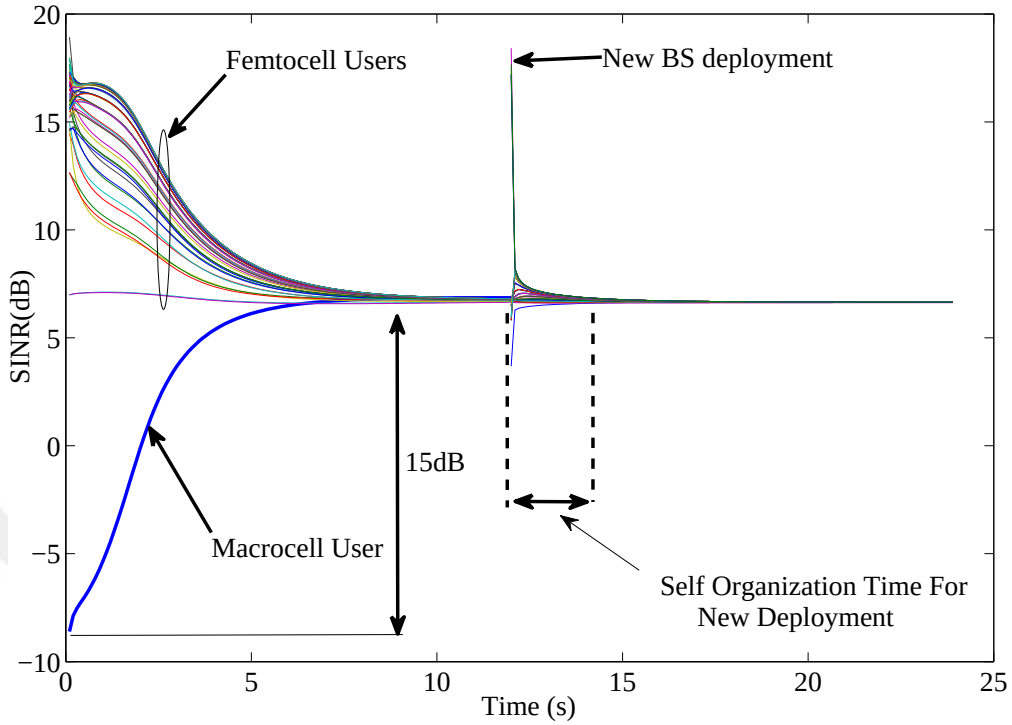

Figure 6.14. SINR change under new femtocell deployment for the PCA-II.

is achieved again. Note that the self organization of new deployments into the existing network is faster compared to the initial adjustment period.

To demonstrate the short-comings of using a fixed target SINR, the SOCC algorithm [70] and the PCA-II are compared. Since SOCC algorithm has been proposed to adjust the transmission powers of only femtocell BSs, the power of macrocell user is adjusted to achieve maximum feasible SINR value in simulations. In [70], a pre-defined threshold value Γ_{th} is provided based on wall penetration loss. For a better comparison, different Γ_{th} values are used for simulations and the results are depicted in Figure 6.8. Like any other fixed threshold algorithm, as long as the given target SINR is feasible, the SOCC algorithm converges. However, for the case where the target SINR values are not feasible the algorithm diverges. For example, the case where we choose $\Gamma_{th} = 10$dB, some of the femtocell users are not able to reach this target SINR value and without a constraint on maximum transmission power levels, power levels will diverge in such a case. Even for this scenario the PCA-II leads to self-organization

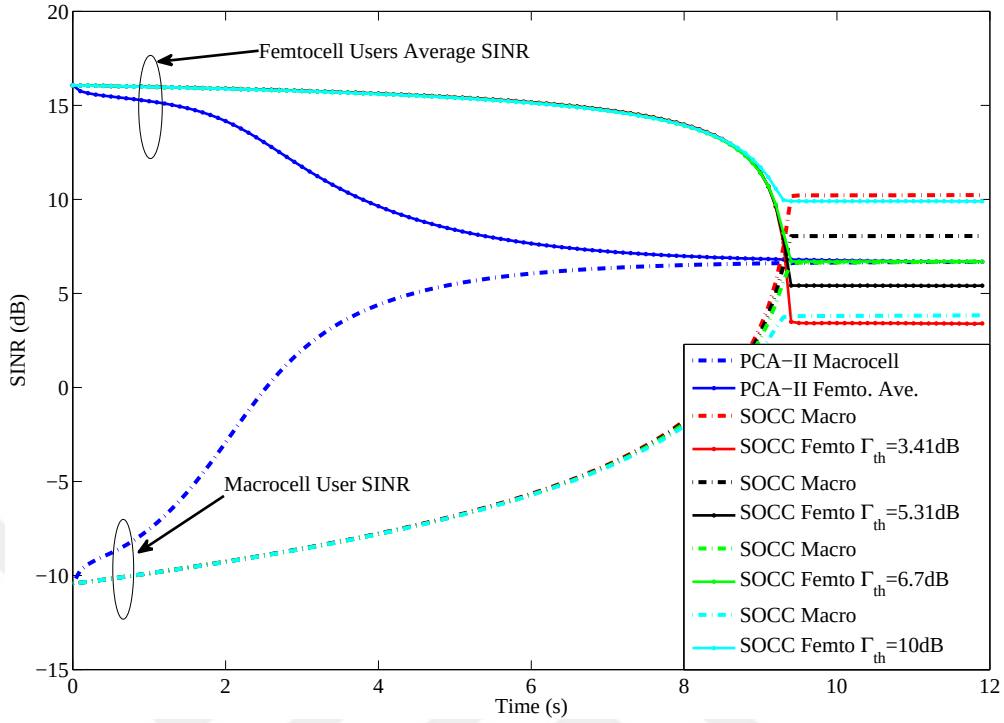

Figure 6.15. Comparison of the PCA-II with SOCC.

of BSs and achieves fairness without any predefined SINR value.

Figure 6.16 depicts the comparison of the proposed algorithm with link quality protection (LQP) algorithm [41]. Simulations are carried out with 20 femtocell users and a single macrocell user in a shared spectrum setup. The proposed algorithm adjusts power levels such that every user can achieve an SINR value of 7.5 dB at consensus. This value is given as the target SINR value for the LQP algorithm. However, the LQP algorithm converges to a value that is higher for macrocell user and lower for femtocell users. This is due to the fact that initially the macrocell user is not able to achieve the target SINR value which leads to a decreased target SINR value for femtocell users. Also note that the channel gains between macrocell user and femtocell BSs are assumed to be available at each iteration for the LQP. This information is utilized at macrocell BS to create the feedbacks for the power adjustment of femtocell BS whereas The PCA-II does not require any information on channel gains.

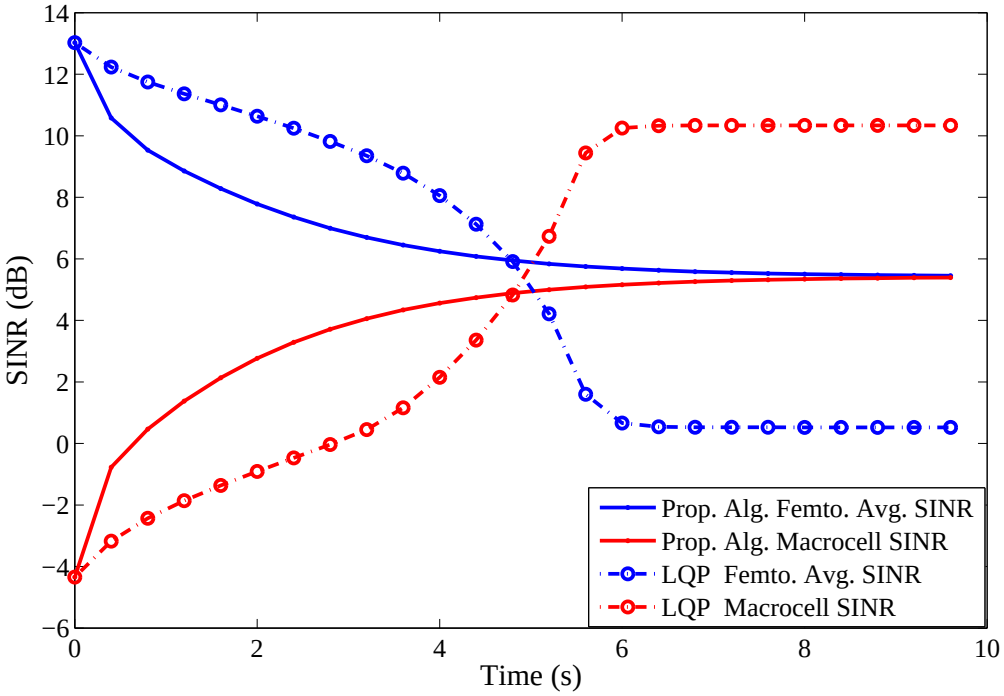

Figure 6.16. Comparison of the PCA-II with the LQP.

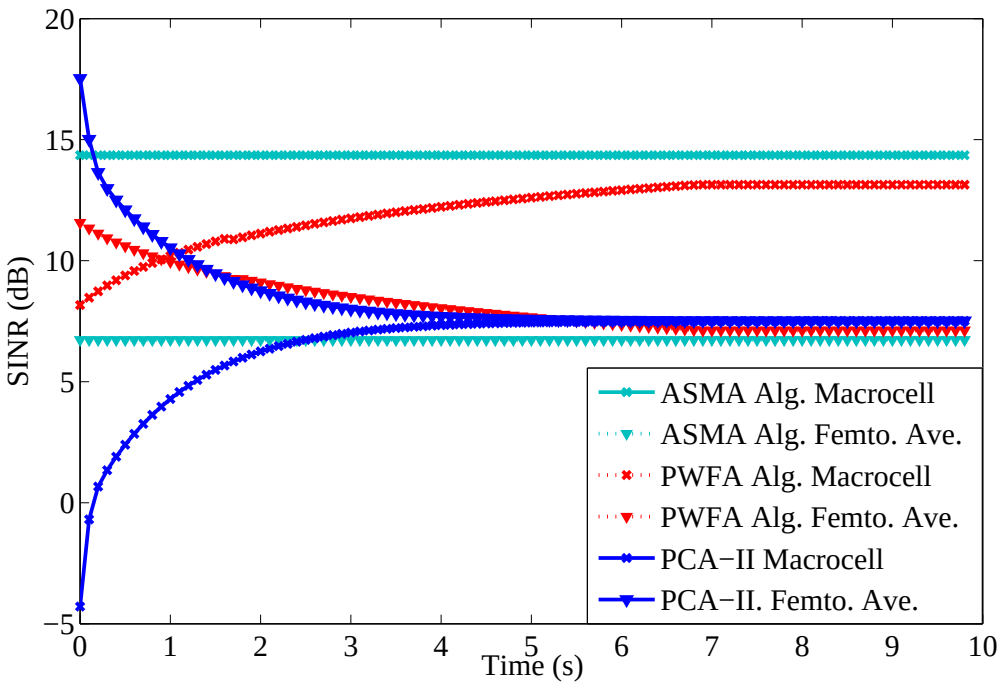

Figure 6.17. Comparison of the PCA-II with the ASMA and PWFA.

Figure 6.17 depicts the comparison of the proposed algorithm with ASMA and PWFA algorithms [40]. Similar to LQP case, the PCA-II adjusts power levels such that every user can achieve an SINR value of 7.5 dB at consensus. The interference experienced by the macrocell user after consensus is used as the maximum tolerable interference value (I_m) for PWFA and ASMA algorithms. Figure 6.17 shows the change on macrocell and average femtocell SINR values. ASMA algorithm achieves the highest SINR value for macrocell user and a slightly lower average femtocell SINR value than the proposed algorithm. There is no change on SINR values because the feedbacks created in ASMA depends on I_m, number of interfering femtocells and the channel gains. After initial adjustment the power levels do not change. PWFA algorithm gives similar results with a high macrocell user SINR and a lower average femtocell SINR value compared to the proposed algorithm. Unlike ASMA, the feedbacks from macrocell changes based on the interference experienced. However, a crucial drawback of ASMA and PWFA algorithms is that, in both cases %20 of femtocell users have SINR values less than 0dB. Note that all of the three algorithms (LQP, PWFA, ASMA) requires the information on the channel gains in addition to a predefined target parameters which may or may not be feasible. Only for the LQP case the feasibility problem is solved by iteratively reducing the target SINR value for femtocell users. Similar to the case shown in Figure 6.15, different results can be obtained via changing the target values or maximum tolerable interference values.

The simulation results of the fairness performance utilizing Jain's fairness index is shown in Figure 6.18. The PCA-II is compared with 4 different power adjustment algorithms. For the PFWA and ASMA algorithms the resulting JFI value is lower, since these algorithms converge to SINR values where %20 of users have lower than 0dB SINR. Furthermore %50 of users have less than 3dB which results in a low JFI value. This is expected as both the PWFA and ASMA algorithms suppresses the interfering small cell users in order to protect the macrocell user. LQP and SOCC algorithms achieve results comparable to the proposed algorithm which achieves an JFI value of 1 corresponding to perfect fairness.

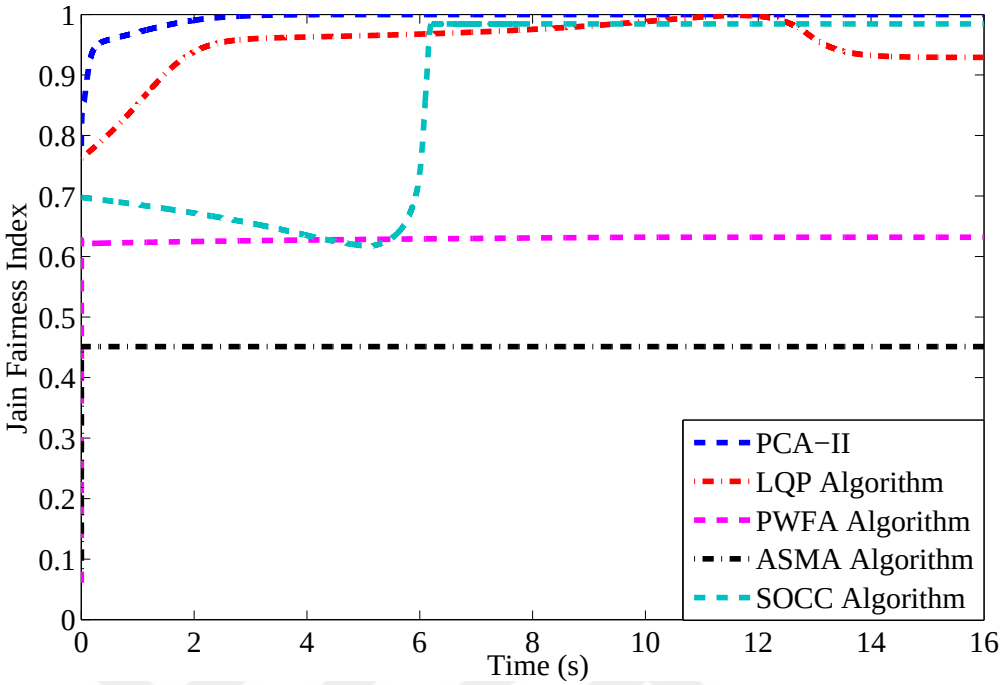

Figure 6.18. Evaluation of fairness based on Jain's Index.

Figures 6.19 and 6.20 depict the simulation results using AI for $\epsilon = 0.5$ and $\epsilon = 1$. Similar to JFI results, the PCA-II achieves the best fairness possible whereas LQP and SOCC algorithms achieve comparable results. ASMA and PWFA algorithms have worse performances similar to the previous case especially when $\epsilon = 1$. However, as ϵ decreases, i.e. as lower SINR values become less important, the difference in fairness performance decreases.

The simulations show that the PCA-II achieves the optimal solution to the problem presented in (2.8)-(2.9). The comparison with other approaches reveals some desired properties of the PCA-II such as self-organization, perfect fairness, optimality. A crucial advantage of the PCA-II is that during the power adjustment process, the channel gains are not utilized. Similar to the other proposed algorithms perfect fairness is achieved without any explicit effort. Further numerical analysis on the PCA-2 is given in [85, 110].

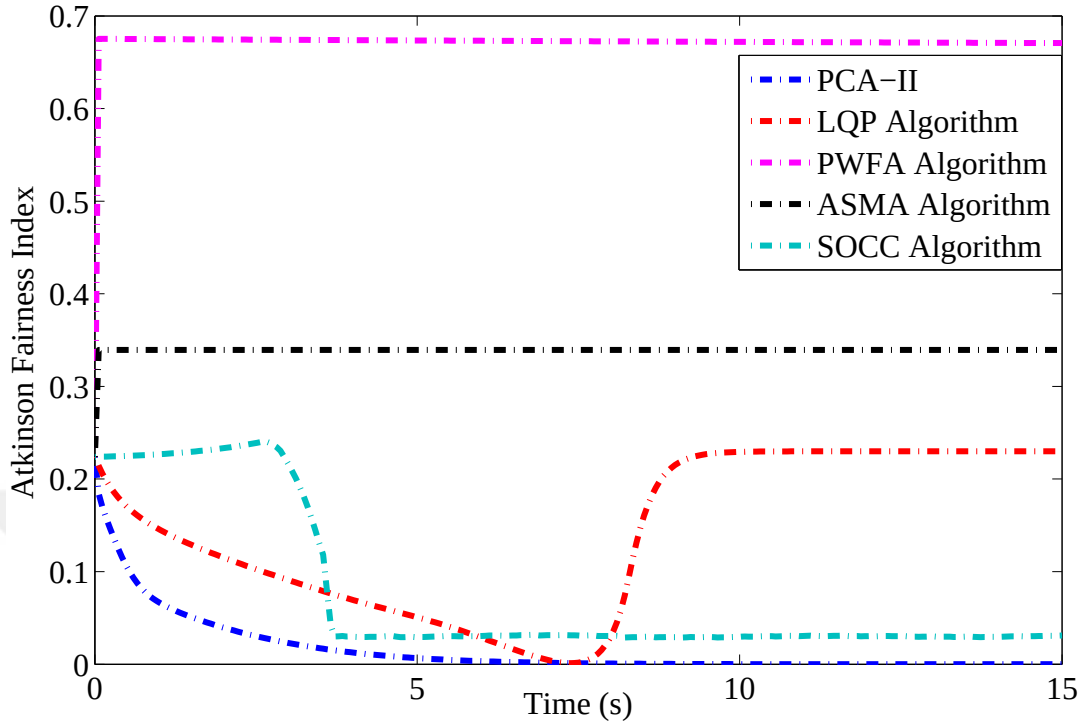

Figure 6.19. Evaluation of fairness based on Atkinson Index ($\epsilon = 1$).

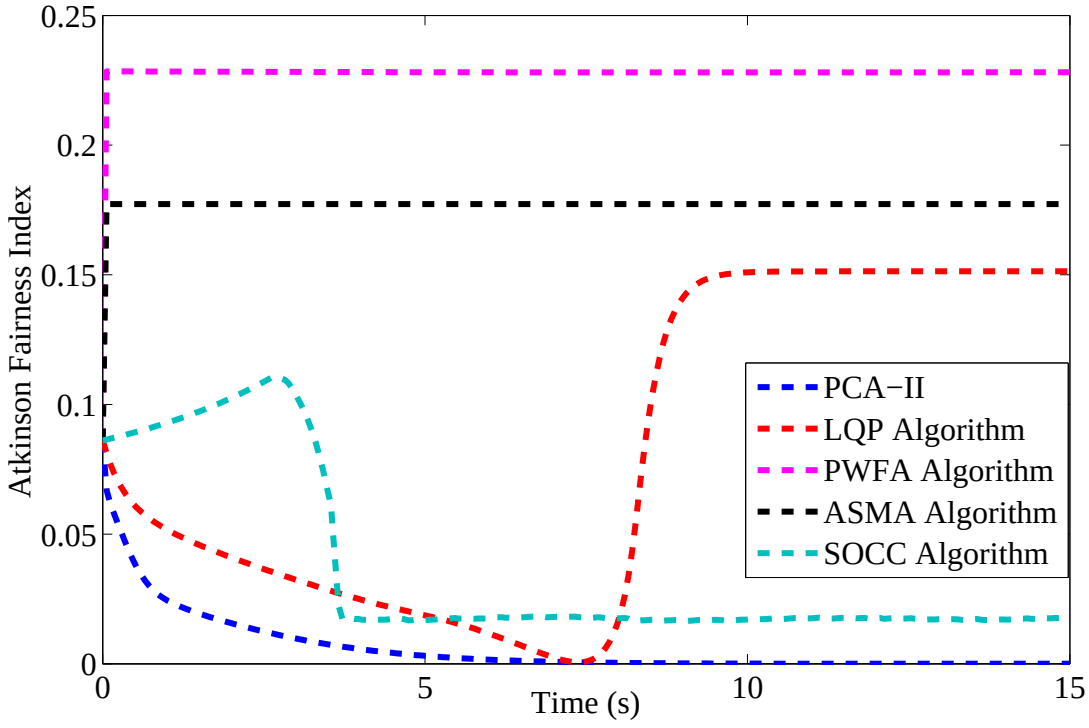

Figure 6.20. Evaluation of fairness based on Atkinson Index ($\epsilon = 0.5$).

6.3.3. Comparison of PCA-I and PCA-II

In this dissertation, there are two different proposed power control algorithms which consider the problem defined by (2.8)-(2.9), namely PCA-I and PCA-II. In this section, the comparison of PCA-I and PCA-II is presented.

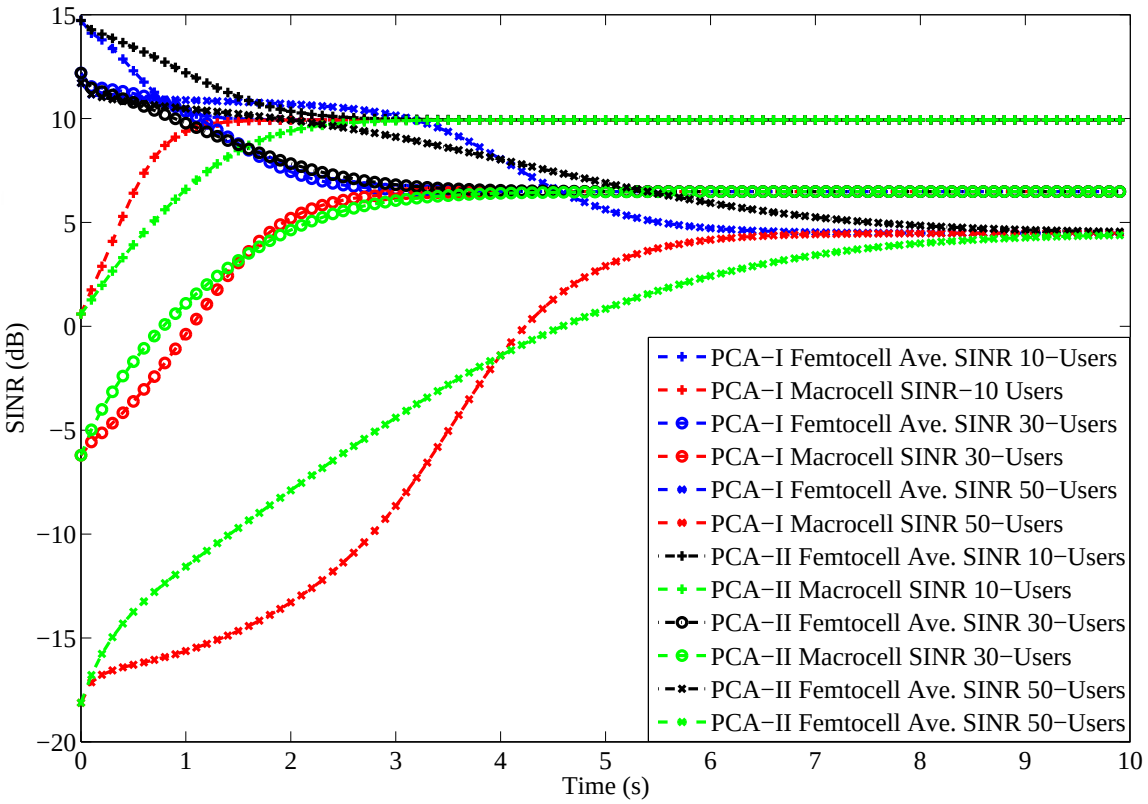

Figure 6.21. Comparison of PCA-I and PCA-II.

The PCA-I and PCA-II considers the same problem and we compare their performances for various number of users in Figure 6.21. Both of the algorithms converge to the same solution which is shown to be optimal, at each case. We see that as the number of users increases, the time required for the convergence increases and the algorithms converge to a lower SINR value. The convergence rate is faster for the PCA-I algorithm and the difference increases with increasing number of users.

6.3.4. Numerical Analysis for PCA-III

In this section, the numerical analysis for the PCA-III described by (3.15) is presented. The simulations presented in this section are carried out under the second channel model.

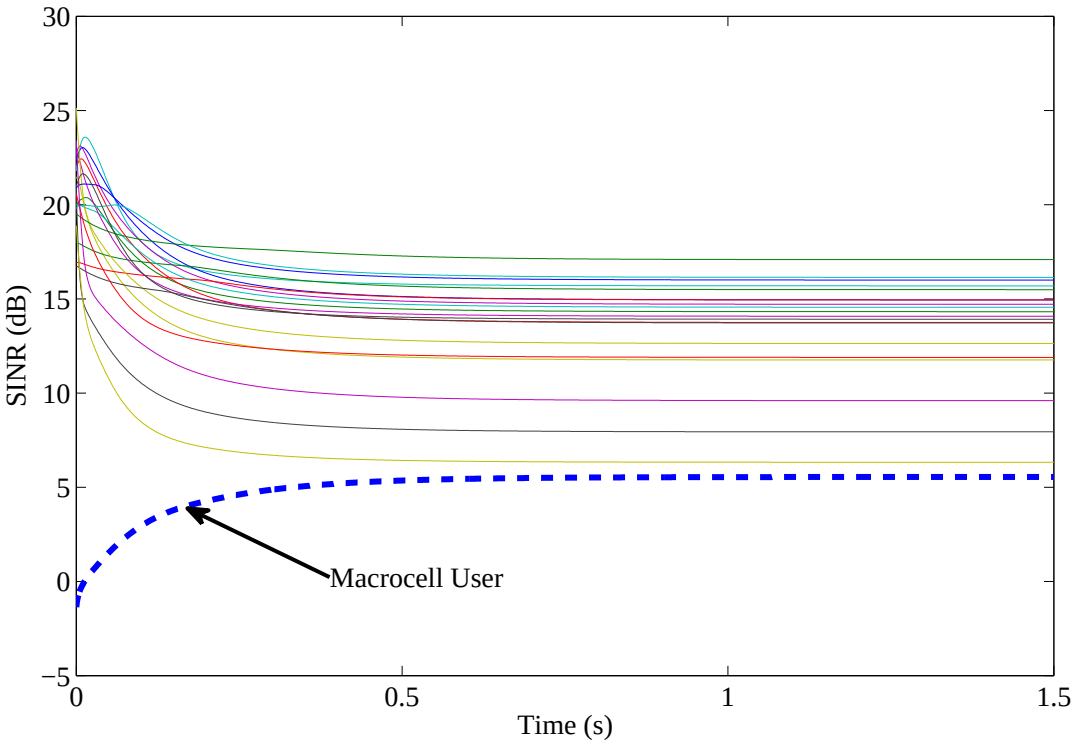

Figure 6.22. SINR adjustment example for the PCA-3 under a 2-tier setup.

An example power adjustment with 25 users consisting of 1 macrocell and 24 femtocell user is depicted in Figures 6.22 and 6.23. Target SINR values are randomly chosen between $[5, 20]$ for femtocells whereas macrocell user's target SINR value is 5 for this particular example. Initially despite transmitting at maximum power, macrocell BS is not able to provide the target SINR for its user. Using the proposed algorithm, BSs adjust their transmission power in a way that every user has the same error based on their target SINR value. The change for the error values depicted in Figure 6.23 shows consensus at a value of -0.05 implying that every user reaches an SINR value 5% higher than their target SINRs. Note that, initially the macrocell user is not able

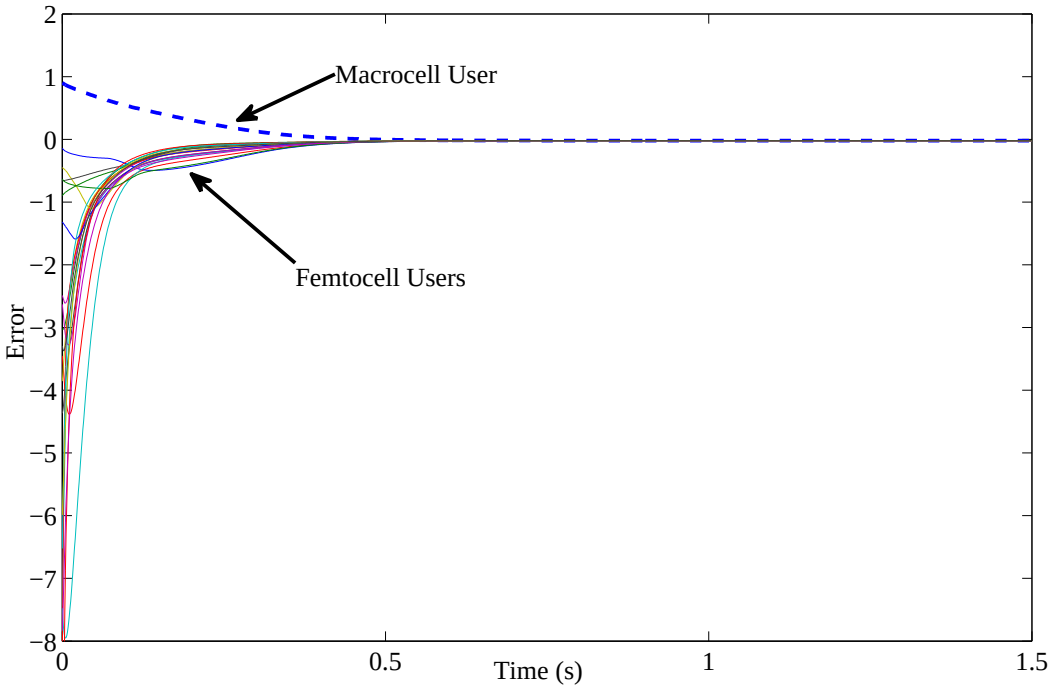

Figure 6.23. Error change example for the PCA-3 under a 2-tier setup.

to reach even 50% of its target SINR value, whereas some of the femtocell users achieve SINR values that are 8 times higher than their target SINR value.

Figure 6.24 illustrates the performance of the PCA-III with non-ideal communication links. In the example, one of the users is not able to communicate with the rest of the BSs, while the rest of the BSs communicate and adjust their transmission powers using the PCA-III. The isolated BS is only able to communicate at the connection points and is still able to adjust its power to some degree with the limited information it receives. Note that, the rest of the BS considers the isolated BS as a noise and is still able to adjust their power despite the lack of communication with the isolated BS.

The optimum error e^* and the resulting error value of the proposed algorithm is illustrated in Figure 6.25. For this particular example, the system is not feasible and $\rho(\mathbf{RG}) = 2.049$. The corresponding $q^* = 0.488$ and $e^* = 0.512$ is achieved by the PCA-III which agrees with the results provided in Theorem 4.8.

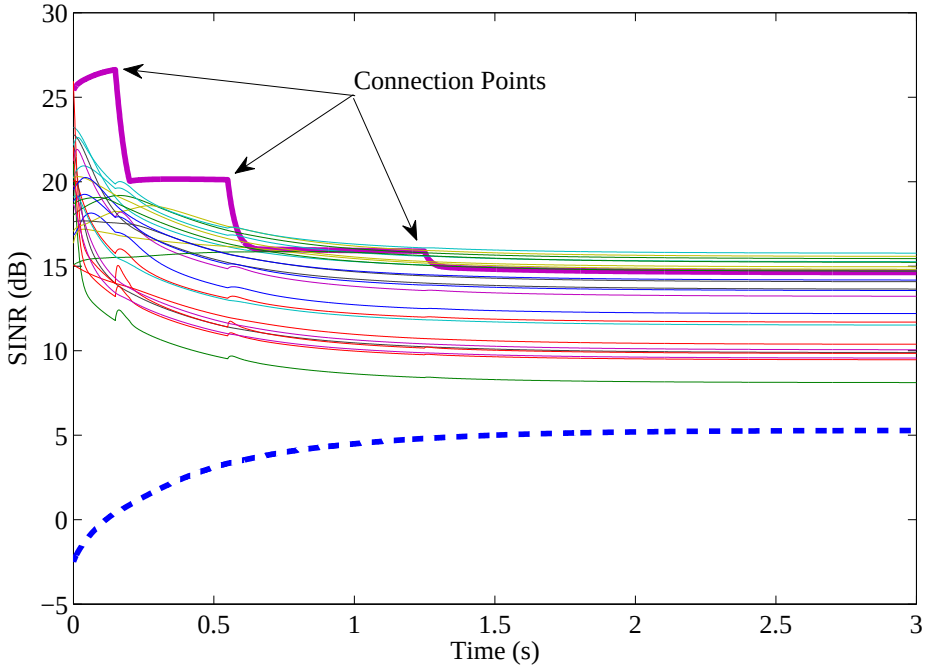

Figure 6.24. SINR change example for the PCA-3 under a 2-tier setup with imperfect communication links.

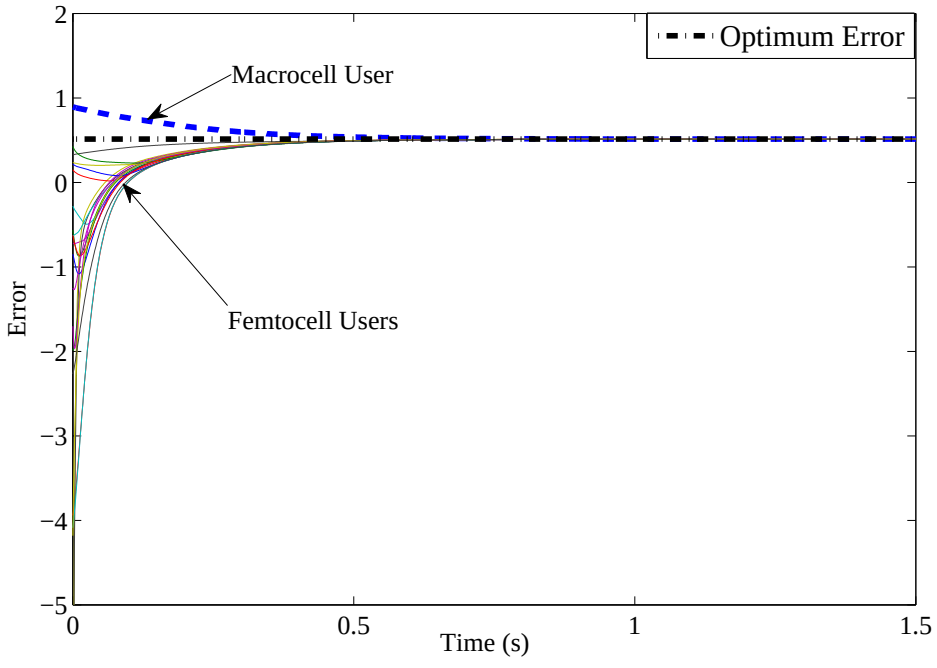

Figure 6.25. Optimum solution and error change for an infeasible example.

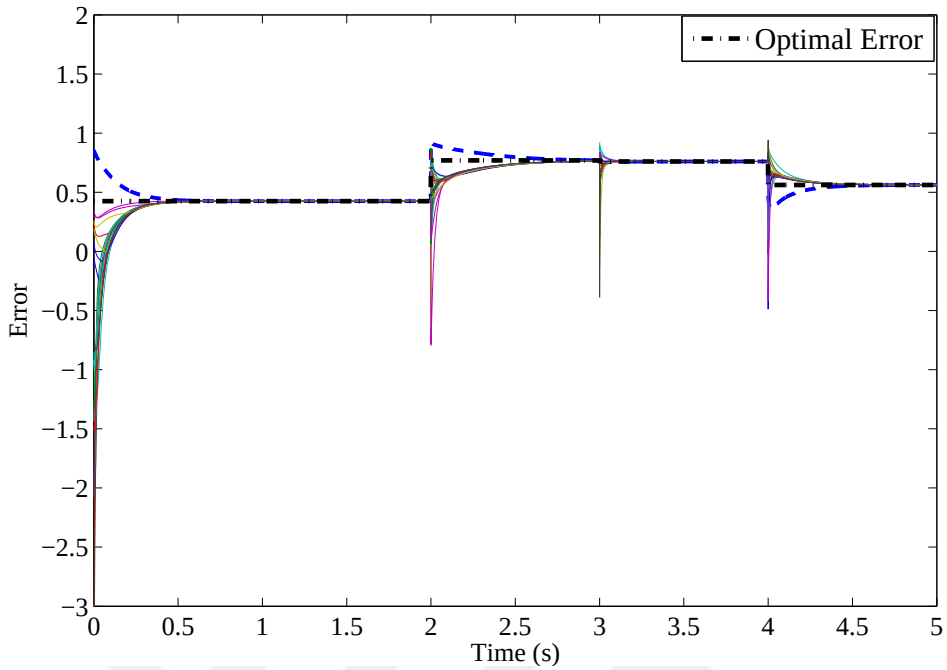

Figure 6.26. Optimum solution and error change example with dynamic desired SINR values.

To demonstrate the self-organizing properties of the PCA-III, a setup where desired SINR values change during adjustment is depicted in Figure 6.26. Here, the system is infeasible and resulting consensus error value is greater than 0 at all times. The desired SINR values change randomly at 3 separate instances after the initial convergence. The resulting convergence values along with the optimum error values are depicted. This example shows the ability of the proposed algorithm to converge to optimum error value under a highly dynamic system.

In Figure 6.27, JFI values obtained by the PCA-III are depicted for different number of femtocells. To compute JFI values relative QoS parameter is utilized. The proposed algorithm achieves perfect fairness in terms of relative QoS at each case. Note that, the perfect fairness in terms of relative QoS implies the perfect fairness in terms of error values. An important observation is the change on the speed of convergence which slightly slows down with the increased number of users. It can be concluded that the performance of the PCA-III in terms of fairness is independent of the number

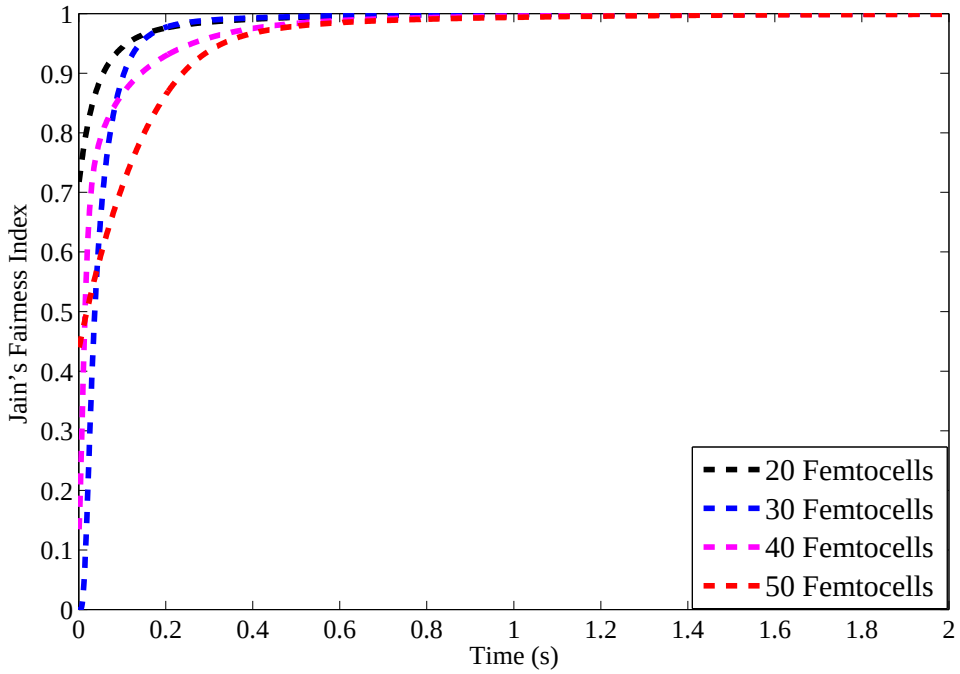

Figure 6.27. Fairness analysis based on relative QoS values using Jain's Fairness Index.

of BSs in the system.

6.3.5. Numerical Analysis on Transmission Powers

The numerical analyses presented in the previous sections focused on the change of SINR values for the PCA-I and PCA-II or relative error values for the PCA-III. However, the change of transmission powers is neglected so far. In this section, we focus on the change of transmission powers using the proposed power control algorithms.

In order to understand the change of power values, we utilize tools from Monte-Carlo analysis. The setup used for Monte-Carlo simulations is summarized below.

(i) There is a single macrocell BS with 40 small cell BSs and their associated users, with a total of 41 users in the system.

(ii) At each iteration, users and BSs are randomly distributed as shown in Figure 6.2.

(iii) For the given setup power adjustment algorithms PCA-I and PCA-II is initialized with random initial transmission powers.

(iv) The power adjustment is carried out until maximum number of iterations is reached. We consider a 15 second duration with 10ms sampling period for the power adjustment process.

(v) The process is repeated for 1000 times.

For the simulations, there are no power constraints during the adjustment process. There are no predefined maximum or minimum power transmission power levels. The obtained data allows us to obtain the histogram and empirical cumulative distribution function of the transmission powers.

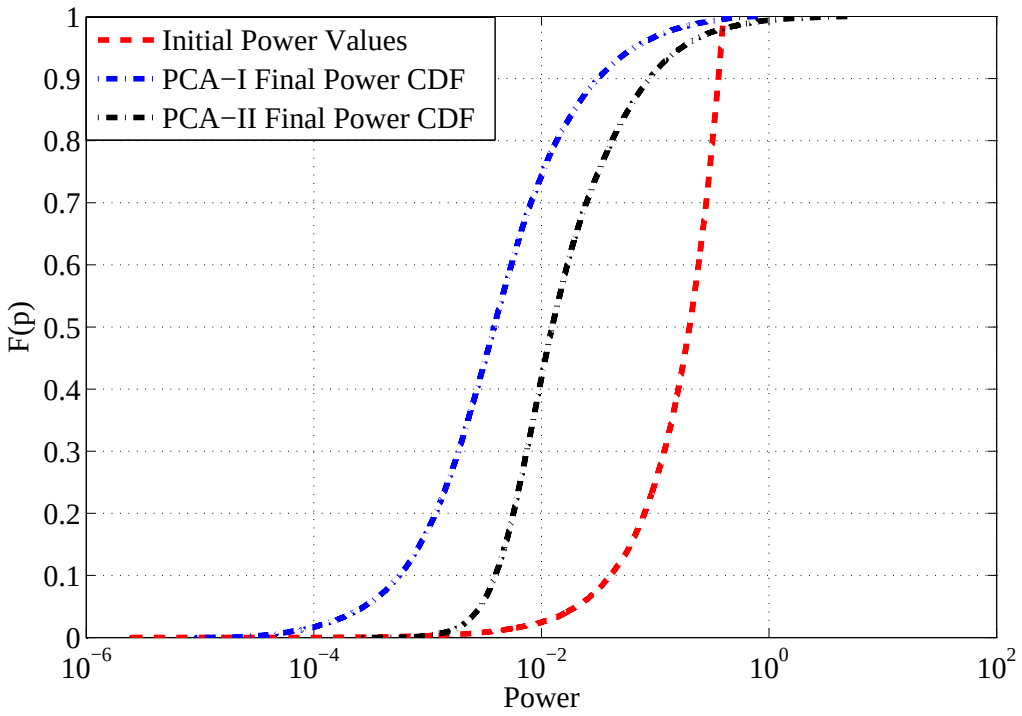

Figure 6.28. Empirical CDF of the transmission powers for the PCA-I and PCA-II.

Figure 6.28 illustrate the empirical cumulative distribution function obtained from the transmission power values of the proposed power control algorithms. Both of

the algorithms converge to final transmission values which is lower compared to the initial transmission power values. This effect of the decrease in transmission powers is reflected in the CDF function. This does not necessarily mean that every BS ends up with a lower transmission power value, but the total transmission value is lower than the initial total power value. Compared to the PCA-II, the PCA-I results in lower transmission values which is a desired property in heterogeneous networks as the energy consumption is a crucial problem.

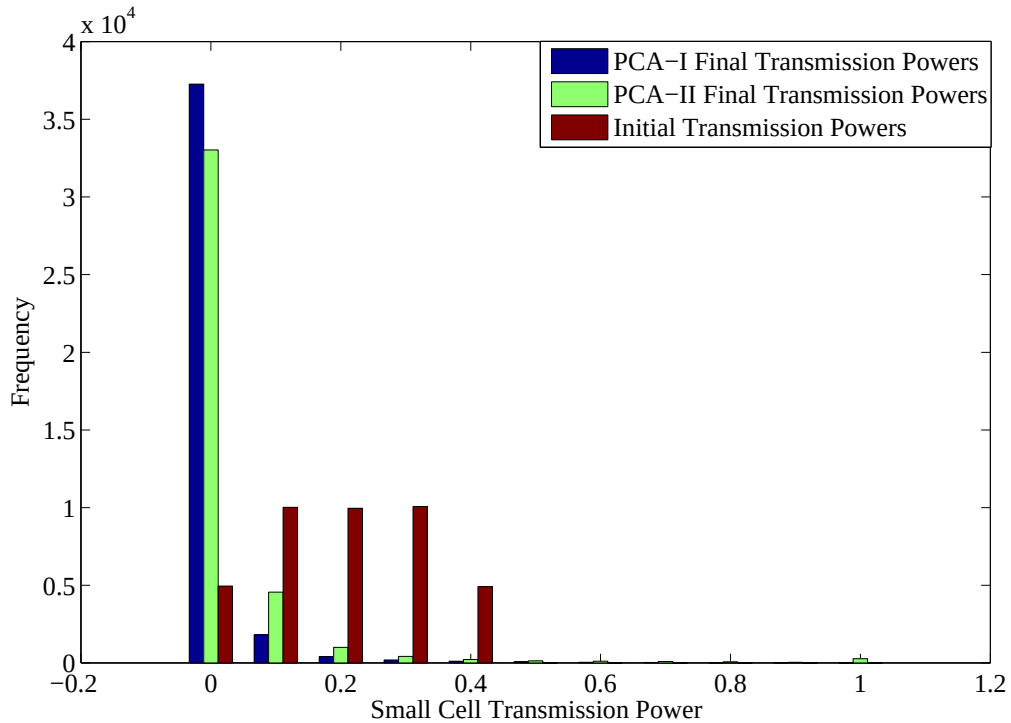

Figure 6.29. Histogram of the transmission powers for the PCA-I and PCA-II along with the initial power levels.

The histogram of the transmission powers is illustrated in Figure 6.29. The initial transmission powers are distributed uniformly which is reflected in their histograms. The histogram data reveals the difference between PCA-I and PCA-II more clearly. PCA-I converges to lower transmission values. However, the difference is small between the final transmission power levels between the PCA-I and PCA-II.

The fairness performance of the algorithms are compared by using the Jain's fairness index on the resulting SINR values. The results are depicted in Figure 6.30. It may be concluded that the PCA-I algorithm has a slight edge compared to the PCA-II algorithm in terms of fairness performance.

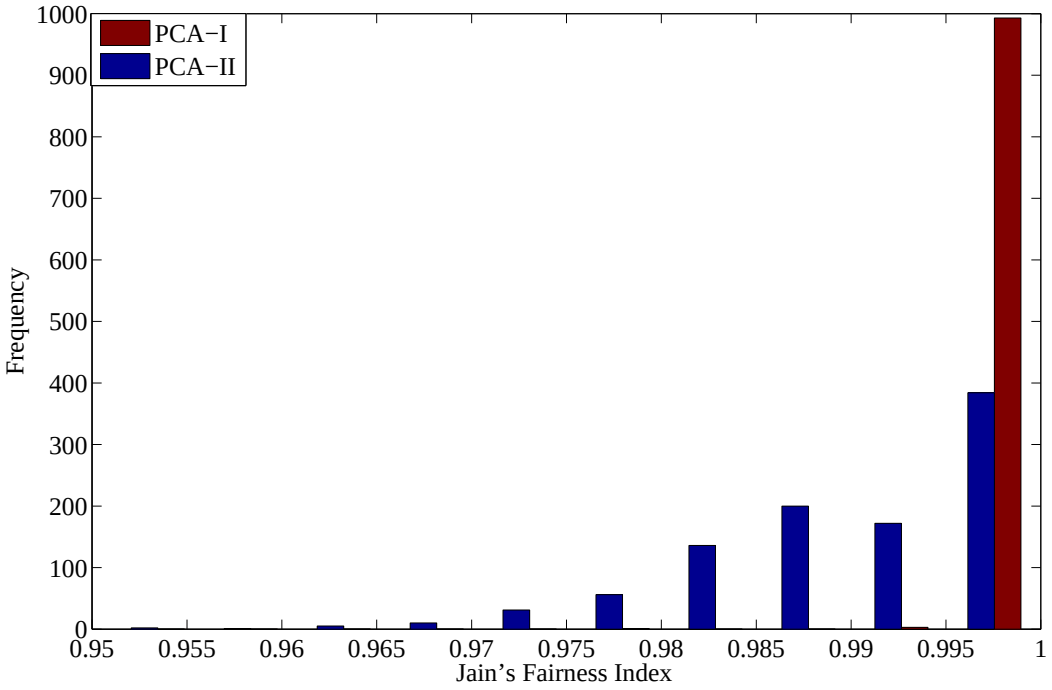

Figure 6.30. Histogram of the resulting Jain's Fairness Index values for the PCA-I and PCA-II.

6.4. Chapter Summary

In this chapter, the numerical analysis for the proposed algorithms is presented. The simulations are in-agreement with the theoretical results provided in Chapter 3 and 4. PCA-I and PCA-II reach the optimal solution for the problem described by (2.8) - (2.9) whereas PCA-III provides the solution for the problem given in (2.16) - (2.17). Furthermore, the fairness analysis reveals that the proposed algorithms achieve perfect fairness in terms of SINR (PCA-I and PCA-II) and relative QoS (PCA-III).

7. CONCLUSION

This dissertation is concerned with power allocation problem in heterogeneous networks. In the first part of the thesis, the proposed power control algorithms are introduced and the theoretical properties of the consensus inspired algorithms are investigated. An important contribution of this dissertation is that the optimal solution for the power control problem with fairness constraint, can be achieved by the proposed algorithms in a distributed manner. A realistic setup with non-ideal communication links which is utilized to model the information exchange between base stations, is introduced. The analysis under this non-ideal setup reveals that the convergence properties of the proposed algorithms are preserved. The extensive numerical analysis verifies the results of the theoretical analysis.

An important contribution of this thesis is to demonstrate how to modify consensus algorithms in way to achieve power allocation in heterogeneous networks. By exploiting the inherent nature of consensus algorithms, fairness constraint is satisfied without any explicit effort. Furthermore, a compelling obstacle for the resource allocation algorithms, obtaining channel state information, is avoided with ease by the proposed algorithms. Note that, SINR values actually contain the channel state information and by efficiently using the SINR values, explicit information on channel states is not required during the allocation process.

PCA-III shows how multi-rate requirement of users may be considered by a consensus algorithm. The algorithm is designed to adjust transmission powers of base stations under heterogeneous QoS provisions. Our approach demonstrates that consensus based algorithms are not limited to only provide fairness in terms of SINR values. Such an approach is also suitable for load balancing and frequency allocation problems.

REFERENCES

1. Nakamura, T., S. Nagata, A. Benjebbour, Y. Kishiyama, T. Hai, S. Xiaodong, Y. Ning and L. Nan, "Trends in Small Cell Enhancements in LTE Advanced", *IEEE Communications Magazine*, Vol. 51, No. 2, pp. 98–105, 2013.

2. Hoydis, J., M. Kobayashi and M. Debbah, "Green Smallcell Networks", *IEEE Vehicular Technology Magazine*, Vol. 6, No. 1, pp. 37–43, 2011.

3. Zhang, J. and G. De la Roche, *Femtocells: Technologies and Deployment*, Wiley Online Library, 2010.

4. Andrews, J. G., "Seven Ways that HetNets are a Cellular Paradigm Shift", *IEEE Communications Magazine*, Vol. 51, No. 3, pp. 136–144, 2013.

5. Malladi, D., "Heterogeneous Networks in 3G and 4G", *Proceedings of IEEE Communication Theory Workshop*, 2012.

6. Jo, H. S., P. Xia and J. G. Andrews, "Open, Closed, and Shared Access Femtocells in the Downlink", *EURASIP Journal on Wireless Communications and Networking*, Vol. 2012, No. 1, pp. 1–16, 2012.

7. Chin, W. H., Z. Fan and R. Haines, "Emerging Technologies and Research Challenges for 5G Wireless Networks", *IEEE Wireless Communications*, Vol. 21, No. 2, pp. 106–112, 2014.

8. Chandrasekhar, V., J. G. Andrews and A. Gatherer, "Femtocell Networks: A Survey", *IEEE Communications Magazine*, Vol. 46, No. 9, pp. 59–67, 2008.

9. Grandhi, S. A., R. Vijavan, D. J. Goodman and J. Zander, "Centralized Power Control in Cellular Radio Systems", *IEEE Transactions on Vehicular Technology*, Vol. 42, No. 4, pp. 466–468, 1993.

10. Zander, J., "Distributed Cochannel Interference Control in Cellular Radio Systems", *IEEE Transactions on Vehicular Technology*, Vol. 41, No. 3, pp. 305–311, 1992.

11. Grandhi, S. A., R. Vijayan and D. J. Goodman, "Distributed Power Control in Cellular Radio Systems", *IEEE Transactions on Communications*, Vol. 42, No. 234, pp. 226–228, 1994.

12. Sung, C. W. and W. S. Wong, "The Convergence of an Asynchronous Cooperative Algorithm for Distributed Power Control in Cellular Systems", *IEEE Transactions on Vehicular Technology*, Vol. 48, No. 2, pp. 563–570, 1999.

13. Lee, C. Y. and T. Park, "A Parametric Power Control with Fast Convergence in Cellular Radio Systems", *IEEE Transactions on Vehicular Technology*, Vol. 47, No. 2, pp. 440–449, 1998.

14. Foschini, G. J. and Z. Miljanic, "A Simple Distributed Autonomous Power Control Algorithm and its Convergence", *IEEE Transactions on Vehicular Technology*, Vol. 42, No. 4, pp. 641–646, 1993.

15. Jantti, R. and S. L. Kim, "Second-order Power Control with Asymptotically Fast Convergence", *IEEE Journal on Selected Areas in Communications*, Vol. 18, No. 3, pp. 447–457, 2000.

16. Hanly, S. V., "An Algorithm for Combined Cell-site Selection and Power Control to Maximize Cellular Spread Spectrum Capacity", *IEEE Journal on Selected Areas in Communications*, Vol. 13, No. 7, pp. 1332–1340, 1995.

17. Yates, R. D. and C. Y. Huang, "Integrated Power Control and Base Station Assignment", *IEEE Transactions on Vehicular Technology*, Vol. 44, No. 3, pp. 638–644, 1995.

18. Kim, Y., S. Lee and D. Hong, "Performance Analysis of Two-tier Femtocell Net-

works with Outage Constraints", *IEEE Transactions on Wireless Communications*, Vol. 9, No. 9, pp. 2695–2700, 2010.

19. Togo, T., I. Yoshii and R. Kohno, "Dynamic Cell-Size Control According to Geographical Mobile Distribution in a DS/CDMA Cellular System", *Proceedings of the Ninth IEEE Symposium on Personal, Indoor and Mobile Radio Communications*, Vol. 2, pp. 677–681, 1998.

20. Shin, S. H. and K. S. Kwak, "Power Control for CDMA Macro-Micro Cellular System", *Proceedings of the 51st IEEE Vehicular Technology Conference*, Vol. 3, pp. 2133–2136, 2000.

21. Hasan, Z., H. Boostanimehr and V. K. Bhargava, "Green Cellular Networks: A Survey, some Research Issues and Challenges", *IEEE Communications Surveys and Tutorials*, Vol. 13, No. 4, pp. 524–540, 2011.

22. Zhang, R. and J. M. Cioffi, "Iterative Spectrum Shaping with Opportunistic Multiuser Detection", *IEEE Transactions on Communications*, Vol. 60, No. 6, pp. 1680–1691, 2012.

23. Song, L., Z. Han, Z. Zhang and B. Jiao, "Non-cooperative Feedback-rate Control Game for Channel State Information in Wireless Networks", *IEEE Journal on Selected Areas in Communications*, Vol. 30, No. 1, pp. 188–197, 2012.

24. Xiao, Y., J. Park and M. van der Schaar, "Intervention in Power Control Games with Selfish Users", *IEEE Journal on Selected Topics in Signal Processing*, Vol. 6, No. 2, pp. 165–179, 2012.

25. Saquib, N., E. Hossain, L. B. Le and D. I. Kim, "Interference Management in OFDMA Femtocell Networks: Issues and Approaches", *IEEE Wireless Communications*, Vol. 19, No. 3, pp. 86–95, 2012.

26. Huang, K., J. G. Andrews, D. Guo, R. W. Heath and R. A. Berry, "Spatial In-

terference Cancellation for Multiantenna Mobile ad hoc Networks", *IEEE Transactions on Information Theory*, Vol. 58, No. 3, pp. 1660–1676, 2012.

27. Vaze, R. and R. W. Heath, "Transmission Capacity of ad-hoc Networks with Multiple Antennas Using Transmit Stream Adaptation and Interference Cancellation", *IEEE Transactions on Information Theory*, Vol. 58, No. 2, pp. 780–792, 2012.

28. Irmer, R., H. Droste, P. Marsch, M. Grieger, G. Fettweis, S. Brueck, H. P. Mayer, L. Thiele and V. Jungnickel, "Coordinated Multipoint: Concepts, Performance, and Field Trial Results", *IEEE Communications Magazine*, Vol. 49, No. 2, pp. 102–111, 2011.

29. Lee, D., H. Seo, B. Clerckx, E. Hardouin, D. Mazzarese, S. Nagata and K. Sayana, "Coordinated Multipoint Transmission and Reception in LTE-advanced: Deployment Scenarios and Operational Challenges", *IEEE Communications Magazine*, Vol. 50, No. 2, pp. 148–155, 2012.

30. Zhang, X. and M. Haenggi, "The Performance of Successive Interference Cancellation in Random Wireless Networks", *IEEE Transactions on Information Theory*, Vol. 60, No. 10, pp. 6368–6388, 2014.

31. Kaufman, B., E. Erkip, J. Lilleberg and B. Aazhang, "Femtocells in Cellular Radio Networks with Successive Interference Cancellation", *IEEE International Conference on Communications Workshops*, pp. 1–5, 2011.

32. Lee, J. Y., S. J. Bae, Y. M. Kwon and M. Y. Chung, "Interference Analysis for Femtocell Deployment in OFDMA Systems based on Fractional Frequency Reuse", *IEEE Communications Letters*, Vol. 15, No. 4, pp. 425–427, 2011.

33. Nguyen, T. M. and L. B. Le, "Opportunistic Spectrum Sharing in Poisson Femtocell Networks", *IEEE Wireless Communications and Networking Conference*, pp. 1467–1472, 2014.

34. Novlan, T. D., R. K. Ganti, A. Ghosh and J. G. Andrews, "Analytical Evaluation of Fractional Frequency Reuse for OFDMA Cellular Networks", *IEEE Transactions on Wireless Communications*, Vol. 10, No. 12, pp. 4294–4305, 2011.

35. Novlan, T. D., R. K. Ganti, A. Ghosh and J. G. Andrews, "Analytical Evaluation of Fractional Frequency Reuse for Heterogeneous Cellular Networks", *IEEE Transactions on Communications*, Vol. 60, No. 7, pp. 2029–2039, 2012.

36. Hatoum, A., R. Langar, N. Aitsaadi, R. Boutaba and G. Pujolle, "Cluster-based Resource Management in OFDMA Femtocell Networks with QoS Guarantees", *IEEE Transactions on Vehicular Technology*, Vol. 63, No. 5, pp. 2378–2391, 2014.

37. Andrews, J. G., H. Claussen, M. Dohler, S. Rangan and M. C. Reed, "Femtocells: Past, Present, and Future", *IEEE Journal on Selected Areas in Communications*, Vol. 30, No. 3, pp. 497–508, 2012.

38. Yun, J. H. and K. G. Shin, "Adaptive Interference Management of OFDMA Femtocells for Co-channel Deployment", *IEEE Journal on Selected Areas in Communications*, Vol. 29, No. 6, pp. 1225–1241, 2011.

39. Guan, X., Q. Han, K. Ma and Z. Liu, "Price-based Interference Control for Two-tier Femtocell Networks", *Physical Communication*, Vol. 7, pp. 122–133, 2013.

40. Shen, S. and T. M. Lok, "Dynamic Power Allocation for Downlink Interference Management in a Two-tier OFDMA Network", *IEEE Transactions on Vehicular Technology*, Vol. 62, No. 8, pp. 4120–4125, 2013.

41. Chandrasekhar, V., J. G. Andrews, T. Muharemovic, Z. Shen and A. Gatherer, "Power control in Two-tier Femtocell Networks", *IEEE Transactions on Wireless Communications*, Vol. 8, No. 8, pp. 4316–4328, 2009.

42. Zheng, W., T. Su, H. Zhang, W. Li, X. Chu and X. Wen, "Distributed Power Optimization for Spectrum-sharing Femtocell Networks: A Fictitious Game Ap-

proach", *Journal of Network and Computer Applications*, Vol. 37, pp. 315–322, 2014.

43. Zhang, H., C. Jiang, J. Cheng and V. C. Leung, "Cooperative Interference Mitigation and Handover Management for Heterogeneous Cloud Small Cell Networks", *IEEE Wireless Communications*, Vol. 22, No. 3, pp. 92–99, 2015.

44. He, S., Y. Huang, S. Jin and L. Yang, "Coordinated Beamforming for Energy Efficient Transmission in Multicell Multiuser Systems", *IEEE Transactions on Communications*, Vol. 61, No. 12, pp. 4961–4971, 2013.

45. Xia, P., C. H. Liu and J. G. Andrews, "Downlink Coordinated Multi-point with Overhead Modeling in Heterogeneous Cellular Networks", *IEEE Transactions on Wireless Communications*, Vol. 12, No. 8, pp. 4025–4037, 2013.

46. Cadambe, V. R. and S. A. Jafar, "Interference Alignment and Degrees of Freedom of the User Interference Channel", *IEEE Transactions on Information Theory*, Vol. 54, No. 8, pp. 3425–3441, 2008.

47. Ntranos, V., M. A. Maddah-Ali and G. Caire, "Cellular Interference Alignment", *IEEE Transactions on Information Theory*, Vol. 61, No. 3, pp. 1194–1217, 2015.

48. Peng, M., C. Wang, J. Li, H. Xiang and V. Lau, "Recent Advances in Underlay Heterogeneous Networks: Interference Control, Resource Allocation, and Self-organization", *IEEE Communications Surveys and Tutorials*, Vol. 17, No. 2, pp. 700–729, 2015.

49. Thomas, R. W., R. S. Komali, A. B. MacKenzie and L. A. DaSilva, "Joint Power and Channel Minimization in Topology Control: A Cognitive Network Approach", *IEEE International Conference on Communications*, pp. 6538–6543, 2007.

50. Bejerano, Y. and S. J. Han, "Cell Breathing Techniques for Load Balancing in Wireless LANs", *IEEE Transactions on Mobile Computing*, Vol. 8, No. 6, pp.

735–749, 2009.

51. Huang, Z., Z. Zeng, H. Xia and J. Shi, "Power control in Two-tier OFDMA Femtocell Networks with Particle Swarm Optimization", *Proceedings of the 73rd IEEE Vehicular Technology Conference*, pp. 1–5, 2011.

52. Huang, Z., Z. Zeng and H. Xia, "Interference Mitigation in Two-tier OFDMA Femtocell Networks with Differential Evolution", *Proceedings of the IEEE Global Telecommunications Conference*, pp. 1–6, 2011.

53. Patra, S. S. M., K. Roy, S. Banerjee and D. P. Vidyarthi, "Improved Genetic Algorithm for Channel Allocation with Channel Borrowing in Mobile Computing", *IEEE Transactions on Mobile Computing*, Vol. 5, No. 7, pp. 884–892, 2006.

54. Bu, S., F. R. Yu and H. Yanikomeroglu, "Interference-aware Energy-efficient Resource Allocation for OFDMA-based Heterogeneous Networks with Incomplete Channel State Information", *IEEE Transactions on Vehicular Technology*, Vol. 64, No. 3, pp. 1036–1050, 2015.

55. Bu, S. and F. R. Yu, "Green Cognitive Mobile Networks with Small Cells for Multimedia Communications in the Smart Grid Environment", *IEEE Transactions on Vehicular Technology*, Vol. 63, No. 5, pp. 2115–2126, 2014.

56. Zhang, H., C. Jiang, N. C. Beaulieu, X. Chu, X. Wang and T. Q. Quek, "Resource Allocation for Cognitive Smallcell Networks: A Cooperative Bargaining Game Theoretic Approach", *IEEE Transactions on Wireless Communications*, Vol. 14, No. 6, pp. 3481–3493, 2015.

57. Zhu, K., E. Hossain and A. Anpalagan, "Downlink Power Control in Two-tier Cellular OFDMA Networks under Uncertainties: A Robust Stackelberg Game", *IEEE Transactions on Communications*, Vol. 63, No. 2, pp. 520–535, 2015.

58. Semasinghe, P., E. Hossain and K. Zhu, "An Evolutionary Game for Distributed

Resource Allocation in Self-organizing Small Cells", *IEEE Transactions on Mobile Computing*, Vol. 14, No. 2, pp. 274–287, 2015.

59. Abdelnasser, A., E. Hossain and D. I. Kim, "Tier-aware Resource Allocation in OFDMA Macrocell-Small Cell Networks", *IEEE Transactions on Communications*, Vol. 63, No. 3, pp. 695–710, 2015.

60. Ha, V. N. and L. B. Le, "Fair Resource Allocation for OFDMA Femtocell Networks with Macrocell Protection", *IEEE Transactions on Vehicular Technology*, Vol. 63, No. 3, pp. 1388–1401, 2014.

61. Ngo, D. T., S. Khakurel and T. Le-Ngoc, "Joint Subchannel Assignment and Power Allocation for OFDMA Femtocell Networks", *IEEE Transactions on Wireless Communications*, Vol. 13, No. 1, pp. 342–355, 2014.

62. Han, B., M. Peng, Z. Zhao and W. Wang, "A Multidimensional Resource Allocation Optimization Algorithm for the Network Coding based Multiple Access Relay Channels in OFDM Systems", *IEEE Transactions on Vehicular Technology*, Vol. 62, No. 8, pp. 4069–4078, 2013.

63. Soret, B., K. I. Pedersen, N. T. Jørgensen and V. Fernández-López, "Interference Coordination for Dense Wireless Networks", *IEEE Communications Magazine*, Vol. 53, No. 1, pp. 102–109, 2015.

64. Aristomenopoulos, G., T. Kastrinogiannis, S. Lamprinakou and S. Papavassiliou, "Optimal Power Control and Coverage Management in Two-tier Femtocell Networks", *EURASIP Journal on Wireless Communications and Networking*, Vol. 2012, No. 1, pp. 1–13, 2012.

65. Ha, V. N. and L. B. Le, "Distributed Base Station Association and Power Control for Heterogeneous Cellular Networks", *IEEE Transactions on Vehicular Technology*, Vol. 63, No. 1, pp. 282–296, 2014.

66. Zhang, H., C. Jiang, N. C. Beaulieu, X. Chu, X. Wen and M. Tao, "Resource Allocation in Spectrum-sharing OFDMA Femtocells with Heterogeneous Services", *IEEE Transactions on Communications*, Vol. 62, No. 7, pp. 2366–2377, 2014.

67. Langar, R., S. Secci, R. Boutaba and G. Pujolle, "An Operations Research Game Approach for Resource and Power Allocation in Cooperative Femtocell Networks", *IEEE Transactions on Mobile Computing*, Vol. 14, No. 4, pp. 675–687, 2015.

68. Zarakovitis, C. C., Q. Ni, D. E. Skordoulis and M. G. Hadjinicolaou, "Power-efficient Cross-layer Design for OFDMA Systems with Heterogeneous QoS, Imperfect CSI, and Outage Considerations", *IEEE Transactions on Vehicular Technology*, Vol. 61, No. 2, pp. 781–798, 2012.

69. Zander, J., S.-L. Kim, M. Almgren and O. Queseth, *Radio Resource Management for Wireless Networks*, Artech House, Inc., 2001.

70. Jo, H. S., C. Mun, J. Moon and J. G. Yook, "Self-optimized Coverage Coordination in Femtocell Networks", *IEEE Transactions on Wireless Communications*, Vol. 9, No. 10, pp. 2977–2982, 2010.

71. DeGroot, M. H., "Reaching a Consensus", *Journal of the American Statistical Association*, Vol. 69, No. 345, pp. 118–121, 1974.

72. Fax, J. A. and R. M. Murray, "Information Flow and Cooperative Control of Vehicle Formations", *IEEE Transactions on Automatic Control*, Vol. 49, No. 9, pp. 1465–1476, 2004.

73. Olfati-Saber, R. and R. M. Murray, "Consensus Problems in Networks of Agents with Switching Topology and Time-delays", *IEEE Transactions on Automatic Control*, Vol. 49, No. 9, pp. 1520–1533, 2004.

74. Olfati-Saber, R., J. A. Fax and R. M. Murray, "Consensus and Cooperation in Networked Multiagent Systems", *Proceedings of the IEEE*, Vol. 95, No. 1, pp.

215–233, 2007.

75. Godsil, C. and G. F. Royle, *Algebraic Graph Theory*, Vol. 207, Springer Science and Business Media, 2013.

76. Ostrowski, A., "Über die Determinanten mit überwiegender Hauptdiagonale", *Commentarii Mathematici Helvetici*, Vol. 10, No. 1, pp. 69–96, 1937.

77. Berman, A. and R. J. Plemmons, "Nonnegative Matrices", *The Mathematical Sciences, Classics in Applied Mathematics,*, Vol. 9, 1979.

78. Poole, G. and T. Boullion, "A Survey on M-matrices", *SIAM review*, Vol. 16, No. 4, pp. 419–427, 1974.

79. Horn, R. A. and C. R. Johnson, *Matrix Analysis*, Cambridge university press, 2012.

80. Schneider, H., "An Inequality for Latent Roots Applied to Determinants with Dominant Principal Diagonal", *Journal of the London Mathematical Society*, Vol. 1, No. 1, pp. 8–20, 1953.

81. Ren, W., R. W. Beard and E. M. Atkins, "Information Consensus in Multivehicle Cooperative Control", *IEEE Control Systems*, Vol. 27, No. 2, pp. 71–82, 2007.

82. Merris, R., "Laplacian Matrices of Graphs: A Survey", *Linear Algebra and its Applications*, Vol. 197, pp. 143–176, 1994.

83. Şenel, K. and M. Akar, "A Consensus-Based Coverage Algorithm for Self-Organizing Femtocell Networks", *IEEE Communications Letters*, Vol. 20, No. 1, pp. 141–144, 2016.

84. Şenel, K. and M. Akar, "Fair Resource Allocation in Self-Organizing Heterogeneous Networks with Imperfect Connections", *IEEE Transactions on Vehicular Technology, manuscript submitted*, 2016.

85. Şenel, K. and M. Akar, "A Distributed Coverage Adjustment Algorithm for Femtocell Networks", *IEEE Transactions on Vehicular Technology, accepted for publication*, 2016.

86. Şenel, K. and M. Akar, "A Power Allocation Algorithm for Multi-tier Cellular Networks with Heterogeneous QoS and Imperfect Channel Considerations", *IEEE Transactions on Wireless Communications, manuscript submitted*.

87. Slotine, J.-J. E., W. Li *et al.*, *Applied Nonlinear Control*, Vol. 199, Prentice-Hall Englewood Cliffs, NJ, 1991.

88. Fiedler, M., "Laplacian of Graphs and Algebraic Connectivity", *Banach Center Publications*, Vol. 25, No. 1, pp. 57–70, 1989.

89. Branicky, M. S., "Multiple Lyapunov Functions and other Analysis Tools for Switched and Hybrid Systems", *IEEE Transactions on Automatic Control*, Vol. 43, No. 4, pp. 475–482, 1998.

90. Zander, J., "Performance of Optimum Transmitter Power Control in Cellular Radio Systems", *IEEE Transactions on Vehicular Technology*, Vol. 41, No. 1, pp. 57–62, 1992.

91. Meyer, C. D., *Matrix Analysis and Applied Linear Algebra*, Vol. 2, Siam, 2000.

92. Grandhi, S. A. and J. Zander, "Constrained Power Control in Cellular Radio Systems", *Proceedings of the 44th IEEE Vehicular Technology Conference*, pp. 824–828, 1994.

93. Qian, L. P., Y. J. A. Zhang, Y. Wu and J. Chen, "Joint Base Station Association and Power Control via Benders' Decomposition", *IEEE Transactions on Wireless Communications*, Vol. 12, No. 4, pp. 1651–1665, 2013.

94. Madan, R., J. Borran, A. Sampath, N. Bhushan, A. Khandekar and T. Ji, "Cell

Association and Interference Coordination in Heterogeneous LTE-A Cellular Networks", *IEEE Journal on Selected Areas in Communications*, Vol. 28, No. 9, pp. 1479–1489, 2010.

95. Madan, R., S. P. Boyd and S. Lall, "Fast Algorithms for Resource Allocation in Wireless Cellular Networks", *IEEE/ACM Transactions on Networking*, Vol. 18, No. 3, pp. 973–984, 2010.

96. Fooladivanda, D. and C. Rosenberg, "Joint Resource Allocation and User Association for Heterogeneous Wireless Cellular Networks", *IEEE Transactions on Wireless Communications*, Vol. 12, No. 1, pp. 248–257, 2013.

97. Siomina, I. and D. Yuan, "Load Balancing in Heterogeneous LTE: Range Optimization via Cell Offset and Load-coupling Characterization", *Proceedings of the IEEE International Conference on Communications*, pp. 1357–1361, 2012.

98. Jain, R., D.-M. Chiu and W. R. Hawe, *A Quantitative Measure of Fairness and Discrimination for Resource Allocation in Shared Computer System*, Vol. 38, Eastern Research Laboratory, Digital Equipment Corporation Hudson, MA, 1984.

99. Ye, Q., B. Rong, Y. Chen, M. Al-Shalash, C. Caramanis and J. G. Andrews, "User Association for Load Balancing in Heterogeneous Cellular Networks", *IEEE Transactions on Wireless Communications*, Vol. 12, No. 6, pp. 2706–2716, 2013.

100. Shen, K. and W. Yu, "Distributed Pricing based User Association for Downlink Heterogeneous Cellular Networks", *IEEE Journal on Selected Areas in Communications*, Vol. 32, No. 6, pp. 1100–1113, 2014.

101. Bethanabhotla, D., O. Y. Bursalioglu, H. C. Papadopoulos and G. Caire, "Optimal User-cell Association for Massive MIMO Wireless Networks", *IEEE Transactions on Wireless Communications*, Vol. 15, No. 3, pp. 1835–1850, 2016.

102. Chen, C. S. and F. Baccelli, "Self-optimization in Mobile Cellular Networks:

Power Control and User Association", *Proceedings of the IEEE International Conference on Communications*, pp. 1–6, IEEE, 2010.

103. Khandekar, A., N. Bhushan, J. Tingfang and V. Vanghi, "LTE-advanced: Heterogeneous Networks", *Proceedings of the IEEE European Wireless Conference*, pp. 978–982, 2010.

104. Recommendation M.1225, I. T. U., "Guidelines for Evaluation of Radio Transmission Technologies for IMT-2000", *International Telecommunication Union*, 1997.

105. Singh, S., X. Zhang and J. G. Andrews, "Joint Rate and SINR Coverage Analysis for Decoupled Uplink Downlink Biased Cell Associations in HetNets", *IEEE Transactions on Wireless Communications*, Vol. 14, No. 10, pp. 5360–5373, 2015.

106. Ertürk, M. C., I. Güvenç, S. Mukherjee and H. Arslan, "Fair and QoS-oriented Resource Management in Heterogeneous Networks", *EURASIP Journal on Wireless Communications and Networking*, Vol. 2013, No. 1, pp. 1–14, 2013.

107. Atkinson, A. B., "On the Measurement of Inequality", *Journal of Economic Theory*, Vol. 2, No. 3, pp. 244–263, 1970.

108. Lan, T. and M. Chiang, "Measuring Fairness: Axioms and Applications", *Proceedings of the 49th IEEE Annual Allerton Conference on Communication, Control, and Computing*, pp. 156–163, 2011.

109. Lopez Perez, D., I. Guvenc, G. De la Roche, M. Kountouris, T. Q. Quek and J. Zhang, "Enhanced Intercell Interference Coordination Challenges in Heterogeneous Networks", *IEEE Wireless Communications*, Vol. 18, No. 3, pp. 22–30, 2011.

110. Şenel, K. and M. Akar, "Coverage Coordination in Self-organizing Femtocell Networks", *Proceedings of the 24th IEEE Mediterranean Conference on Control and Automation*, pp. 761–766, 2016.